

DISSERTATION

# Partial Frequency Reuse for Long Term Evolution

ausgeführt zum Zwecke der Erlangung des akademischen Grades eines  
Doktors der technischen Wissenschaften

unter der Leitung von  
Prof. Christoph F. Mecklenbräuer  
Institute of Telecommunications

eingereicht an der Technischen Universität Wien  
Fakultät für Elektrotechnik

von  
Bujar Krasniqi

Wien, im December 2011

---



Die Begutachtung dieser Arbeit erfolgte durch:

1. Prof. Christoph F. Mecklenbräuer

Institute of Telecommunications  
Technische Universität Wien

2. Prof. Erik G. Ström

Department of Signals and Systems  
Chalmers University



————— *to my family* —————



# Abstract

---

In this thesis, I propose, develop, and analyze novel optimization techniques which solve resource allocation problems in partial frequency reuse (PFR) networks. In long term evolution (LTE), multiple access in the downlink is established by Orthogonal Frequency Division Multiple Access (OFDMA). As a consequence, the cell edge users suffer from strong inter cell interference (ICI). This effect becomes even more severe, due to the low signal power which the cell edge users receive from the base station. Therefore, in this work, we have formulated algorithms that mitigate the ICI by optimizing the Radio Resource Allocation (RRA).

An efficient use of radio resources (bandwidth and transmit power) is indispensable, since they are expensive and limited by spectrum licenses. For Inter Cell Interference (ICI) reduction, we define Partial Frequency Reuse (PFR) such that frequency reuse-1 is allocated to center-cell users and frequency reuse-3 is allocated to cell-edge users. Near the cell edges, the Orthogonal Frequency Division Multiplexing (OFDM) sub-carriers are allocated such that the users within do not use the same frequencies simultaneously (frequency reuse-3). We note that some bandwidth remains unused if the users spatial distribution is inhomogeneous in the cell. In this case, such a PFR scheme does not lead to an efficient utilization of radio resources. To mitigate this apparent inefficiency, I propose a novel bandwidth re-allocation scheme by maximizing the cell capacity density (i.e. achievable data rate per bandwidth per unit area). The proposed scheme re-allocates bandwidth from the cell edge to the center of the cell. The cell capacity density is a metric that represents the expected capacity per unit area for a randomly positioned user (uniformly distributed) in the cell. The network operators are interested in the achievable transmission rate per user. Therefore, we formulate the optimization problem as a maximization of the sum-rate under power and bandwidth constraints. We proved that this sum-rate maximization problem becomes *convex* for a fixed PFR bandwidth allocation scheme under a suitable additional power equality constraint. Using the Lagrangian, the analytical solutions are derived for the optimal power allocation, in a manner which is closely related to water-filling. Furthermore, we formulated two specific problems for the joint optimization of power and bandwidth allocation as convex geometric programs, i.e. the maximization of the minimum rate and the sum-power minimization, respectively.

In PFR, a fundamental issue is to classify the users to the cell edge and center-cell regions. Two user classification schemes are investigated in this thesis in detail: The first classification scheme is based on the distance between the user and its serving base station. The second classification scheme is based on the users Large-Scale Path-Loss Attenuation (LSPLA). Compared to the first classification scheme, the LSPLA scheme is proved to enhance the achievable user-rates. We have shown that the LSPLA classification scheme is successfully applicable to all discussed problems. Finally, we conclude that the LSPLA scheme allows us to formulate spectrally efficient RRA algorithms in a form which can be implemented with fairly low numerical complexity.



# Kurzfassung

---

In dieser Arbeit präsentiere ich die Entwicklung und Analyse neuer Optimierungstechniken, mit deren Hilfe das Problem der Aufteilung begrenzter Betriebsmittel in zellulären Kommunikationsnetzen mit teilweiser Frequenz-Wiederverwendung (engl. partial frequency reuse (PFR)) gelöst werden kann. Gemäß dem Mobilfunkstandard der vierten Generation (4G), bekannt unter dem Akronym LTE (long term evolution), wird der Vielfachzugriff auf den Funkkanal in der Abwärtsstrecke durch das Verfahren des orthogonalen Frequenzmultiplexzugriffs (engl. orthogonal frequency division multiple (OFDM) access (OFDMA)) realisiert. Dies hat zur Folge, dass die Empfangsqualität in den Geräten der Netzteilnehmer nahe der Zellgrenzen stark durch die von den Nachbarzellen verursachten Interferenzen (engl. inter cell interference (ICI)) beeinträchtigt wird. Aus dieser Motivation heraus formulieren wir in dieser Arbeit Algorithmen zur Optimierung der Funkbetriebsmittelzuweisung (engl. radio resource allocation (RRA)), die es erlauben den negativen Einfluss durch ICI wesentlich zu reduzieren.

Spektrumslizenzen und Energiekosten machen die effiziente Nutzung der Betriebsmittel (spektrale Bandbreite und Sendeleistung) in drahtlosen Kommunikationsnetzen unabdingbar. Mit dem Ziel der Reduktion von ICI definieren wir PFR so, dass den Netzteilnehmern in den Kerngebieten aller Zellen die gleichen Frequenzbänder zur Verfügung stehen. In den Bereichen nahe der Zellgrenzen werden die zuweisbaren OFDM Teilträger hingegen so eingeschränkt, dass Netzteilnehmer benachbarter Zellen unter keinen Umständen die gleichen Frequenzen benutzen können. Die in den Kerngebieten genutzte Frequenzaufteilungsstrategie wird in der Literatur häufig mit frequency reuse-1 (deu. Frequenz Wiederverwendung-1) bezeichnet, jene für die Bereiche nahe der Zellgrenzen mit frequency reuse-3 (deu. Frequenz Wiederverwendung-3). An dieser Stelle sei darauf hingewiesen, dass die hier gewählte PFR Methode keine optimale Nutzung der spektralen Ressourcen erlaubt, wenn die räumliche Verteilung der Netzteilnehmer in den Zellen ungleichmäßig ist. Um dieser offensichtlichen Ineffizienz zu begegnen, führe ich ein neues Verfahren ein, das es in jeder Zelle erlaubt Teilbänder je nach Bedarf entweder dem Kerngebiet oder dem grenznahen Bereich zuzuordnen. Auf diese Weise kann die Dichte der Zellkapazität, die ein flächenbezogenes Maß für die erwartete Kapazität eines im gesamten Zellgebiet gleichermaßen wahrscheinlich positionierten Netzteilnehmers ist, maximiert werden. Die

Netzbetreiber sind an der erzielbaren Übertragungsrate pro Netzteilnehmer interessiert. Aus diesem Grund entwickeln wir die hier präsentierten Verfahren durch die Formulierung von Optimierungsproblemen, die die Gesamtübertragungsrate aller Netzteilnehmer maximieren und zusätzlich erlauben die Begrenztheit von Bandbreite und Sendeleistung in Form von Nebenbedingungen zu berücksichtigen. Für PFR mit fixer Bandbreitenzuweisung und unter der Annahme gleicher Gesamtsendeleistung aller Zellen, konnten wir zeigen, dass das entsprechende Optimierungsproblem konvex ist. Mit Hilfe der Lagrangefunktion gelingt es uns, für dieses Problem eine geschlossene Lösung anzugeben, die der Methode des Water-Filling ähnelt und eine optimale Leistungsaufteilung garantiert. Darüber hinaus formulieren wir das Problem der gemeinsamen Optimierung von Sendeleistung und Bandbreitenzuweisung für zwei spezielle Fälle. Im einen Fall wird die minimale Übertragungsrate maximiert, im anderen Fall wird die Gesamtsendeleistung minimiert. Beide Varianten lassen sich in Optimierungsprobleme der bekannten Form eines konvexen geometrischen Programms überführen.

Um PFR einsetzen zu können müssen in jeder Zelle alle Netzteilnehmer einer von zwei disjunkten Gruppen zugeordnet werden – dies ist einerseits die Gruppe der Netzteilnehmer im Kerngebiet der Zelle, und andererseits die Gruppe der Netzteilnehmer nahe der Zellgrenze. In dieser Arbeit untersuchen wir zwei Methoden um die Netzteilnehmer zu klassifizieren. Das erste Verfahren nimmt die Zuordnung der Nutzer basierend auf deren geschätzter Distanz zur Basisstation vor. Das zweite Verfahren verwendet statt der Distanz die großräumige Streckendämpfung (engl. large-scale path-loss attenuation (LSPLA)). Der Vergleich beider Verfahren zeigt, dass das zweite Verfahren zu höheren erzielbaren Übertragungsraten führt. Außerdem zeigen wir, dass die LSPLA-basierte Klassifizierungsmethode in allen betrachteten Problemfällen eingesetzt werden kann. Wir kommen zu dem Schluss, dass es diese Klassifizierungsmethode ermöglicht spektral effiziente RRA Algorithmen anzugeben, die sich mit verhältnismäßig geringer numerischer Komplexität implementieren lassen.

# Acknowledgments

---

First and foremost, I wish to express my deepest gratitude to my supervisor Christoph Mecklenbräuker. It was really a great experience to work with him during my PhD studies. He was always motivating me with his enthusiasm. He actively contributed to my research with new ideas and guidance. It was my pleasure to participate with him in various events at several Cost Meetings (COST Action 2100 and IC1004). Additionally, I would like to express my gratitude to my second examiner Erik Ström for his patience in awaiting the final version of this thesis. I also appreciate the fruitful discussions that we had in Miami during the IEEE GLOBECOM 2010 conference and at some Cost Meetings (COST Action 2100 and IC1004).

I would like to express my gratitude to Joachim Wehinger for his support and advise during the time that I was as visiting researcher at Telecommunications Research Center Vienna. Furthermore I would like to thank my colleges and co-authors Martin Wrulich, Martin Wolkerstorfer, Christian Mehlführer, and Markus Rupp for their strong support which often brought me to new insights. This thank extends to Robert Dallinger, Aamir Habib, Markus Laner, Jesús Gutiérrez Terán, Stefan Schwarz and Martin Mayer who carefully proofread chapters of my thesis. I also would like to thank all the other colleagues from our institute with whom I shared the time during my PhD studies.

Special thanks go to Driton Statovci for his guidance, continuous support and useful suggestions as well as motivating me to keep the work ongoing. I would like to thank also Nysret Musliu who recommended to do my PhD studies at Vienna University of Technology. I am grateful to Myzafer Limani and Enver Hamiti from University of Prishtina who gave a contribution in this aspect.

Especially, I would like to thank my wife Luljeta and my daughter Laura who encouraged and supported me during writing this thesis. Their patience during the last months was an inspiration and gave me energy for finishing this work in time.

Finally, I would like to thank my parents, my father Ismet and my mother Elmije who always motivated me to do the PhD, as well as my brothers Behar and Besnik who encouraged me during all this time.



# Contents

---

1	Introduction	1
2	Radio Resource Management — an Overview	5
2.1	Radio Resource Management / Long Term Evolution . . . . .	6
3	Optimization Techniques for RRM in Wireless Communications	9
3.1	Dual Decomposition Techniques for Wireless Communications . . . . .	10
3.1.1	The Lagrangian of an Optimization Problem . . . . .	10
3.1.2	KKT optimality conditions . . . . .	11
3.2	Geometric Programming for Wireless Communications . . . . .	12
3.2.1	Geometric Programming in Basic Form . . . . .	12
3.2.2	Transformation of the GGP to GP and its form in CVX . . . . .	13
4	Capacity Density Maximization for LTE	15
4.1	Geometry of Cell Cluster Model . . . . .	16
4.1.1	Path-loss Exponent Model . . . . .	17
4.1.2	Average Received SINR . . . . .	17
4.2	Frequency Reuse Schemes . . . . .	19
4.3	Capacity density for Partial Frequency Reuse . . . . .	21
5	Power Allocation in Partial Frequency Reuse	25
5.1	Geometry of Cell Cluster Model . . . . .	26
5.2	Large-scale Path-loss Attenuation . . . . .	28
5.2.1	Antenna Gain . . . . .	28
5.2.2	Penetration Loss . . . . .	29
5.2.3	Shadowing . . . . .	30
5.2.4	Small-scale Fading . . . . .	30

5.3	Variable Power and Fixed Bandwidth Allocation Scheme . . . . .	30
5.4	Power Allocation Algorithm . . . . .	31
5.4.1	Water-filling Like Power Allocation . . . . .	33
5.5	Power Allocation Algorithms in Convex Form . . . . .	37
5.5.1	Maximization of the Minimum Rate in Convex Form . . . . .	37
5.5.2	Sum-Power Minimization in Convex Form . . . . .	38
<b>6</b>	<b>Bandwidth and Power Allocation in Partial Frequency Reuse</b>	<b>41</b>
6.1	Variable Power and Variable Bandwidth Allocation Scheme . . . . .	42
6.2	Bandwidth and Power Allocation Algorithms . . . . .	43
6.2.1	Maximization of the Minimum Rate . . . . .	43
6.2.2	Efficient Algorithms for Bandwidth and Power Allocation Depending on Users Classification . . . . .	50
6.3	Bandwidth Re-allocation Scheme . . . . .	55
6.3.1	Power Allocation and Bandwidth Re-Allocation Depending on Distance from Base Station . . . . .	56
6.3.2	Power Allocation and Bandwidth Re-allocation Depending on Large- scale Path-loss Attenuations . . . . .	60
6.4	Power Allocation and Bandwidth Adaptation Algorithms . . . . .	64
6.4.1	Optimal power and adaptive bandwidth allocation depending on mean LSPLA . . . . .	65
6.4.2	Efficient power and adaptive bandwidth algorithm depending on mean LSPLA . . . . .	72
<b>7</b>	<b>Conclusions</b>	<b>77</b>
7.1	Capacity Density Maximization . . . . .	78
7.2	Power Allocation in Partial Frequency Reuse . . . . .	78
7.3	Bandwidth and Power Allocation in Partial Frequency Reuse . . . . .	78
<b>8</b>	<b>Future Directions / Outlook</b>	<b>81</b>
	List of Symbols	83
	List of Acronyms	87
	List of Figures	89
	Bibliography	91

# 1

## Introduction

---

HIGHER transmission data rate required by mobile users is a big challenge that need to be considered. Nowadays, the mobile handsets called smartphones are capable of supporting higher communication speeds as the notebooks can do. In order to address the issue of requirement for higher transmission speed, new generation of mobile communication networks are standardized like Wireless Local Area Network (WLAN), Worldwide Interoperability for Microwave Access (WiMAX), Long Term Evolution (LTE) and Long Term Evolution-Advanced (LTE-A), that offer higher transmission rate compared with Universal Mobile Telecommunications System (UMTS). Such networks use OFDMA as multiple access scheme in the downlink that offers flexibility in bandwidth allocation. However, because of the use of OFDMA the ICI becomes a limiting factor in achieving higher capacity [1]. In order to deal with ICI issue, the development of more advanced frequency allocation schemes is necessary. Considering the fact that bandwidth resources are limited, it is necessary formulating the efficient optimization algorithms suitable for optimization the resource allocation. This would allow the mobile operators to use the bandwidth resources efficiently while satisfying the user's demands.

Until now several frequency allocation schemes have been proposed for LTE that try to reduce the ICI and increase the transmission rate. One of those schemes which seems to be most promising technique is PFR. A number of publication associated with numerical and simulation results about PFR are shown by authors in [2], [3], [4], [5], [6]. The PFR splits the bandwidth allocation into two parts: the Full Reuse (FR) part and the Partial Reuse (PR) part. For the cell center users the PFR allocates the FR part of the bandwidth, while for the cell edge users it allocates the PR part of the bandwidth. Other investigations like PFR scheme in combination with Soft Handover (SH) is done by Chiu et al. [3], where a significant improvement in the throughput for the PR region

is achieved. At the same time a decrease in the throughput of the FR region is noticed, because the resources in FR region are shared with the users in the PR region. A solution for the frequency partitioning radius in PFR through the optimization of the capacity density is done by Alsawah et al. [6], where he has found an improvement in capacity density applying PFR compared with applying reuse-1 or reuse-3. Xiang et al. [4] and Chiu et al. [3] have mentioned that cell edge bandwidth can be re-used by cell center users whenever the cell edge users are idle. Cell Capacity density maximization together with frequency bandwidth re-allocation for PFR is studied by Krasniqi et al. [7].

The cellular network users are willing to pay for the transmission rate that mobile operators are going to offer. So to satisfy the user's requirements for transmission rate with the resources that mobile operators have, further investigations differently from the definition of cell capacity density are carried out. Those investigations are focused on the optimization algorithms for power and bandwidth allocation. Such algorithms are in general non-convex because of the interference term in the Signal-to-Interference-and-Noise-Ratio (SINR) definition. During the last years many optimization algorithms have been developed for mobile networks that use frequency reuse-1. One of them is the optimal power allocation for two base station, employing the scheduling schemes under frequency reuse-1 that is studied by Gjendemsjo et al. [8]. Additionally to the power control in sum-rate maximization for reuse-1 network, the maximization of the minimum rate for two users is studied by Charafeddine et al. [9]. The optimal power allocation together with the minimum rate constraints per cell is studied by Chen et al. [10]. The sum-rate maximization under variable power control for two users, using sequential geometric programming is studied by Charafeddine et al. [11]. Differently from frequency reuse-1 the sum-rate maximization problem for power and bandwidth allocation in PFR is investigated by Krasniqi et al. [12]. Using the Dual Decomposition Techniques (DDT) analytical expressions for optimal power allocation within cell regions are derived. Further study of sum-rate maximization together with bandwidth re-allocation is done by Krasniqi et al. [13]. Under the assumption of the equal power allocation over all cells in the cluster, it was shown that the non-convex sum-rate maximization problem can be converted into convex one. For more than two users this optimization problem was found to be intractable for analytical solutions.

Differently from the sum-rate maximization problems in the study made by Chiang et al. [14], the two problems for single carrier power control: maximization the minimum rate and the sum-power minimization over multiple users within multiple cells for Code Division Multiple Access (CDMA) networks, was found to be transformable into Geometric Programming (GP) optimization problems in the high-SINR regime. The maximization of the minimum rate and the sum-power minimization for multiple users over multiple cells in PFR are investigated in [12] where without making any high-SINR approximation



is proved that those optimization problems can be converted into GP convex ones.

A frequency reuse technique as combination of power allocation and interference aware for achieving better coverage and higher spectral efficiency is investigated by Xie et al. [15]. A differentiable spectrum partitioning where the reuse distance is used to find the frequency reuse-factors is studied by Fu et al. [16]. Differently from [16] the efficient optimization algorithms based on maximization of the minimum rate are developed, that jointly optimizes the power and bandwidth allocation. Using the efficient algorithms developed by Krasniqi et al. [17], it is proven that considering the mean LSPLA as threshold for user's classification in the cell regions, the PFR becomes more efficient in power allocation than reuse-1 and reuse-3 for the same minimum rate constraints. Furthermore, using the LSPLA as threshold to classify the users, two other algorithms for power allocation and bandwidth adaption are developed. Those algorithms adapts the bandwidth allocation in the cell regions based on the amount of users classified by LSPLA threshold, and optimize the power allocation.

During my research work I published several papers as the first author and as co-author. Most of the content from the papers that I am as first author is included in my thesis. In [7] a novel frequency bandwidth re-allocation is presented and capacity density maximization is formulated for that scheme. In [12] an optimization problem for RRA is formulated where for fixed bandwidth allocation, analytical expressions are derived for power allocation. The analytical expressions are applied with the bandwidth re-allocation [13], [18]. Also in [19] a significant gain in the sum-rate is achieved applying the optimal power allocations algorithm when LSPLA threshold is used compared with use of distance threshold. The efficient power allocation and optimal bandwidth allocation problem formulated by maximization of the minimum rate is shown in [17]. Considering the maximization of the minimum rate as the optimization problem for power and bandwidth allocation in [20] the efficient algorithms for user's classification and radio resource allocation are developed.

The following chapters after introduction are organized as follows. In Chapter 2 a detailed description of RRA and Radio Resource Management (RRM) techniques for LTE are explained. Also a detailed description of the radio interface architecture implemented in LTE is shown in this chapter. In Chapter 3 two optimization techniques necessary to formulate and solve optimization problems for RRA are explained. Those include the DDT and the GP applicable to wireless communication systems. In Chapter 4 cell capacity density maximization is shown. Also the novel frequency bandwidth re-allocation is presented in this chapter where an application of this scheme to improve the capacity density is presented. In Chapter 5, the optimal power allocation algorithms are derived. Two models for cell clusters that contains all the parameters which characterize the wireless channel in the downlink (from the base station to the mobile station) are presented in this

chapter. Furthermore, in this chapter the non-convex GP optimization problems of radio resource allocation are transformed into GP convex optimization problems. In Chapter 6, efficient algorithms are presented to classify the users in the cell regions. Moreover, in this chapter efficient power and adaptive bandwidth allocation and also optimal power and adaptive bandwidth allocation algorithms are developed. The main conclusions of the thesis are presented in Chapter 7. The thesis ends with Chapter 8 where the future directions of the research and an outlook is given.

# 2

## Radio Resource Management — an Overview

---

THE difficult work for engineers is not how provide the wireless network, but how to manage with such network. The wireless era starts with the Marconi who was able to communicate with his wireless device across the Atlantic Ocean in 1901. After that other wireless systems were developed like broadcasting TV, short-wave communication etc. However the wireless communication began to have the most perspective as future communication after introducing the first cellular communication system by Nordic Mobile Telephone (NMT) in 1981 in the Nordic countries.

One of the key problems in operating for a wireless communication is still the limited spectrum [21]. In order to have a solution for this issue, the International Telecommunication Union (ITU) organization was formed in 1947 which is the main authority in specifying the bounds for spectrum allocation in wireless technologies. However, the telecommunication authorities decide for spectrum license to the wireless providers. After the mobile operators are equipped with licenses, they decide on the frequency allocation to the users such that interference is limited.

Nowadays, since the number of mobile operators is increasing and also the mobile operators need to support different technologies, because the migration from one technology to the next one takes time, it is important to have a coordination not only between the mobile operators of the same country in spectrum allocation but also between mobile operators of the neighboring countries. A study about the co-existence of mobile communication systems in cross border scenario for 2.6 GHz can be found in [22].

The 2nd generation technology named Global System for Mobile Communications (GSM) was quite successful in decreasing the interference by applying the frequency reuse

technique. However the drawback of this technique was in the limited GSM capacity. To improve the capacity of the cellular networks, other mobile systems have been developed like UMTS. The UMTS has improved the capacity by implementing the frequency reuse-1, however the limited number of channelization codes available due to the modulation scheme CDMA, makes this system still limited in offering higher capacity. Later other techniques based on CDMA like High-Speed Downlink Packet Access (HSDPA) and High-Speed Packet Access (HSPA) have been developed to improve the network capacity. Differently from the CDMA based networks, the 3rd Generation Partnership Project (3GPP) community in the year 2007 made the first standard work for LTE which is based on OFDM. A system level performance evaluation and testbed measurement for HSDPA and LTE can be found in [23].

In all cellular networks allocating the resources in a fixed way without considering the user's capacity requirements is just a waste of resources. That's why the RRM are necessary to be applied in all mobile technologies. The RRM are applied by GSM [24], UMTS [21], [25] where the network capacity is improved, while the cost for network deployment is reduced. The RRM techniques are necessary to be applied also in LTE for improving the capacity. The RRM techniques are in application also in other wireless systems like WiMAX [26] and WLAN [27]. Overall, the RRM techniques in wireless communication networks have a high impact in reducing the power consumption by base stations, the battery consumption by mobile stations, reducing the deployment cost etc.

## 2.1 Radio Resource Management / Long Term Evolution

The LTE which sometimes is called the 4th Generation (4G) provides a flat architecture that is flexible in operating with different frequency bands from 1.2 to 20 MHz. The theoretical transmission rate in the downlink is 100 Mbit/s while in the uplink is 50 Mbit/s. Compared to UMTS network where the communication between base stations is centralized in the Radio Network Controller (RNC), LTE base stations can communicate to each other directly through the interface between two eNodeBs (X2) [28]. The radio interface architecture scheme for LTE is shown in Figure 2.1. As it is shown in Figure 2.1, the LTE architecture contains two parts: the Evolved Packet Core (EPC) part and the Evolved-Universal Terrestrial Radio Access Network (E-UTRAN) part. The EPC part is responsible for functionalities like: authentication setup and end of connection [29] not so related to the interfaces. The E-UTRAN part is responsible for all functionalities that are related with RRA, communication through interfaces X2 and S1. The communication between the EPC and E-UTRAN is realized through S1 interface, which connects the Mobility Management Entity/Service-Gateway (MME/S-GW) with the base stations. One MME/S-GW can be connected to two base stations and has a key role in the mobility of

the mobile user. Also one base station can be connected to multiple MME/S-GWs.

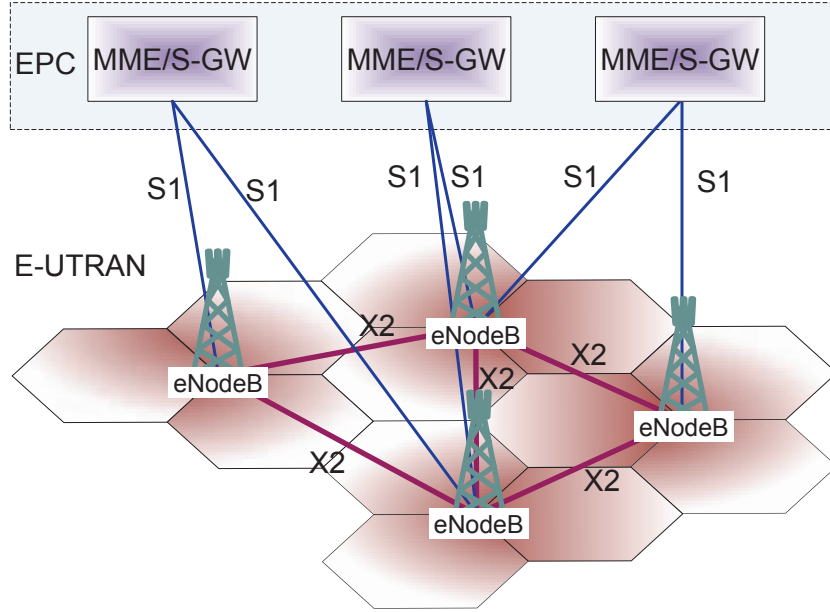


**Figure 2.1:** LTE radio interface architecture

The X2 interface connects two neighboring base stations with each other and is used for exchanging the load informations. In this case the neighboring base station take some users from the overloaded neighboring cell in order to help it to decrease the load. X2 supports the ICI mitigation by transmitting the informations about interference level to the neighboring base station. The LTE in its standard definition is planned to operate in frequency reuse-1. However, as we have mentioned before because of the OFDMA used as multiple access scheme the cell edge users receive low SINR, as result achieve low transmission rate due to the ICI. Even by exchanging the ICI information through X2 interface would not be possible to mitigate the ICI when higher number of mobile users are located at the edges of neighboring cells. To improve the received SINR by cell edge users the PFR scheme is proposed to be used for LTE. However the PFR in its proposed form is just a waste of resources. That's why applying RRA techniques based on optimization of the power and bandwidth allocation in PFR are necessary to satisfy the user's requirements and mitigate the ICI.



# 3

## Optimization Techniques for RRM in Wireless Communications

---

FROM the Shanon capacity formula it is well known that requirement for higher transmission rate by communication system depends on the available spectrum and transmit power. The spectrum resources are limited due to very high cost for spectrum license, as well as power increase is limited due to interference. Furthermore, the number of users is increasing together with the requirements for higher transmission data rate. So the question is how we can satisfy the user's requirements with radio resources that we have already. The response is using optimization techniques to optimize the spectrum allocation as well as power allocation. This makes the wireless communication systems more efficient and capable for satisfying the user's requirements. There are many optimization techniques that offers flexible ways to formulate the optimization problems for RRA in wireless communication. In this chapter we are discussing only two of them since in the most of our work throughout the thesis we use such techniques to formulate and solve the optimization problems for RRA. The used techniques are dual decomposition and geometric programming. In Section 3.1 some of the theories behind DDT is discussed. For a simple optimization problem in standard form, the formulation of the Lagrangian is shown. Furthermore, in this section some of the Karush-Kuhn-Tucker (KKT) conditions for optimality are presented which are quite useful to derive the analytical solutions for resource allocations. In Section 3.2 the GP for wireless communication is discussed. In this section the standard form of GP is presented. Another extended form of GP named the

maximization of the minimum polynomials that has found many applications in solving the interference mitigation problems for wireless communication is presented also. At the end of this chapter the way of converting the Generalized Geometric Programming (GGP) into GP and their form in Matlab Software for Disciplined Convex Programming (CVX) is presented also.

### 3.1 Dual Decomposition Techniques for Wireless Communications

Applying DDT for solving the RRM optimization problems in wireless communication is efficient and fast. Throughout DDT we decompose the optimization problem into two problems: the primal problem is the optimization problem formulated and the dual problem that is the problem defined from the Lagrangian of the primal optimization problem. By formulating the primal and the dual optimization problems we find distributed solutions that are fundamental for large wireless networks [30] and cross-layer optimization over different layers of communication [31].

#### 3.1.1 The Lagrangian of an Optimization Problem

Following [32] an optimization problem is any maximization or minimization form of an objective function followed by some inequality and equality constraints. In general form a minimization optimization problem is written as follows

$$\underset{\mathbf{x}}{\text{minimize}} \quad g_0(\mathbf{x}) \quad (3.1a)$$

subject to

$$g_i(\mathbf{x}) \leq 1, \quad i = 1, \dots, q \quad (3.1b)$$

$$h_j(\mathbf{x}) = 1, \quad i = 1, \dots, q \quad (3.1c)$$

where  $g_0 : \mathcal{R}^n \rightarrow \mathcal{R}$  is the objective (cost) function,  $g_i : \mathcal{R}^n \rightarrow \mathcal{R}$  are the inequality function and  $h_j : \mathcal{R}^n \rightarrow \mathcal{R}$  are the equality functions. Any optimization problem of form (3.1) is said to be convex if the objective (3.1a) and the constraints (3.1b)-(3.1c) are convex. More details about convex functions can be found in [32].

The Lagrangian for the optimization problem (3.1) is written as follows

$$L(\mathbf{x}, \boldsymbol{\lambda}, \boldsymbol{\mu}) = g_0(\mathbf{x}) + \boldsymbol{\lambda}^T g(\mathbf{x}) + \boldsymbol{\mu}^T h(\mathbf{x}) \quad (3.2)$$

where  $\boldsymbol{\lambda}$  is the vector elements of Lagrange multiplier that weights the functions  $g(\mathbf{x})$  defined by  $g_i(\mathbf{x})$  in the inequalities and  $\boldsymbol{\mu}$  is the vector elements of Lagrange multiplier that weights the functions  $h(\mathbf{x})$  defined by  $h_j(\mathbf{x})$  in the equalities.



The Lagrangian is important for solving optimization problems in wireless communication because during formulation of the optimization problem we won't wonder if it is convex or non-convex, since its dual optimization problem is always convex. The dual Lagrange problem is as follows

$$\text{maximize} \quad \mathcal{G}(\boldsymbol{\lambda}, \boldsymbol{\mu}) \quad (3.3a)$$

subject to

$$\boldsymbol{\lambda} \succeq \mathbf{0} \quad (3.3b)$$

where  $\mathcal{G}(\boldsymbol{\lambda}, \boldsymbol{\mu})$  denotes the dual objective. The Lagrangian and its dual function have found a large application in solving the network utility and cross-layer optimization problems for wireless communications networks [31], [33], [30], [34], [35]. Even the primal optimization problem (3.1) is non-convex the weak duality holds [32] such that optimal solution for the dual problem (3.3) is smaller or equal to the optimal solution for the primal optimization problem (3.1).

### 3.1.2 KKT optimality conditions

To derive analytical equations for optimization problem (3.1) under the assumptions that all functions in the objective, equalities and inequalities are differentiable even without knowing about the convexity, we use the KKT conditions [32]. Some of the KKT conditions that are important for solving convex or concave power allocation problems in Chapter 5 are shown in the following

$$\mathbf{x} \succeq \mathbf{0}, \quad (3.4a)$$

$$\boldsymbol{\lambda}^T g(\mathbf{x}) \leq 0, \quad (3.4b)$$

$$\boldsymbol{\mu}^T h(\mathbf{x}) = 0, \quad (3.4c)$$

$$\boldsymbol{\lambda} \succeq \mathbf{0}, \quad (3.4d)$$

$$\boldsymbol{\lambda}^T \mathbf{x} = 0, \quad (3.4e)$$

$$\nabla L \mathbf{x} = \mathbf{0}, \quad (3.4f)$$

where  $\succeq$  denotes the component-wise inequality. The first condition (3.4a) shows the positivity for optimization variables. The conditions (3.4b) and (3.4c) show the equations for the inequality and equality functions weighted by respective Lagrange multipliers. The positivity of Lagrange multiplier  $\boldsymbol{\lambda}$  is defined by Equation (3.4d). The Slater condition is defined by Equation (3.4e). The last equation (3.4f) defines the first derivative of Lagrangian with respect to the optimization variable.

## 3.2 Geometric Programming for Wireless Communications

Geometric programming is nonlinear and non-convex optimization technique that is widely used in solving RRA problems in wireless networks. Even though GPs are non-convex, there are existing methods to convert them into forms, which are suitable to finding solution. In the high-SINR regime [14] the problems of maximizing the sum-rate can be converted into GP and solved efficiently. However in most of the wireless communication technologies, the interference is the limiting factor for the performance of them. So the GP offers flexibility in formulation the RRA problems that mitigate the interference and improve the throughput, minimize the transmission energy, minimize the delay etc.

### 3.2.1 Geometric Programming in Basic Form

The GP in its basic form [36], [37] is a constrained optimization problem formulated by the objective and inequality or equality or both constraints. The objective in general is a posynomial or a monomial. However, every monomial is also a posynomial. The equalities can be also posynomials except monomials, while the inequalities can be only monomials. The GP in its basic form is given as follows

$$\underset{\mathbf{x}}{\text{minimize}} \quad g_0(\mathbf{x}) \quad (3.5a)$$

subject to

$$g_i(\mathbf{x}) \leq 1, \quad i = 1, \dots, q \quad (3.5b)$$

$$h_j(\mathbf{x}) = 1, \quad j = 1, \dots, q \quad (3.5c)$$

where the posynomials  $g_i(\mathbf{x})$  in the objective (3.5a) or in the inequality constraints (3.5b) are defined in the following form

$$g(\mathbf{x}) = \sum_{k=1}^K w_k x_1^{\delta_{1k}} x_2^{\delta_{2k}} \dots x_q^{\delta_{qk}} \quad (3.6)$$

such that  $w > 0$  and  $\delta_{qk} \in \mathcal{R}$ . The monomials in the objective (3.5a) or any of the constraints (3.5b)-(3.5c) are defined in the following form

$$g(\mathbf{x}) = w x_1^{\delta_1} x_2^{\delta_2} \dots x_q^{\delta_q}. \quad (3.7)$$

For example:  $\pi x_1^{0.7} + x_1^{10} x_2^3 x_3^{-2}$  is a posynomial and  $x_1^{-10} x_2^3 x_3^{-2} x_4$  is a monomial.

The RRA problems in wireless communication is not trivial to be formulated directly into GP forms as given by Equation (3.5). However for specific extended forms of GPs exist different methods of transforming them into GP. In the next section we explain one of the extended forms of GPs called GGP, which under a simple transformation becomes GP. After such forms are converted into GP form like in Equation (3.5), their solution be found easily by interior-point methods [38] or matlab based tool called CVX [39].

### Maximum of Minimum Posynomials

For the RRA problems in wireless communication one of the most GGP form used is the maximization of the minimum posynomials. So in this subsection we are explaining this form taking a simple example. A simple example is the maximization of the two posynomials that in GGP form is written as in the following

$$\underset{\mathbf{x}}{\text{maximize}} \quad \min\{g_1(\mathbf{x}), g_2(\mathbf{x})\} \quad (3.8a)$$

subject to

$$g_3(\mathbf{x}) \leq 1, \quad (3.8b)$$

$$h_1(\mathbf{x}) = 1 \quad (3.8c)$$

Such optimization problems are in use by UMTS for load balancing. Similar to UMTS also in LTE the maximization of the minimum SINR and the maximization of the minimum rate belongs to the maximization of the minimum posynomials.

#### 3.2.2 Transformation of the GGP to GP and its form in CVX

As we mentioned earlier the optimization problems similar to the one given by Equation (3.8) can not be solved directly. However, there are methods explained in [32], [36] and [37] where under the log transformation of the variables such problems can be converted into convex GP ones. In the following we show how the optimization problem given by Equation (3.8) can be transformed into GP. So we introduce an auxiliary variable  $z$  that lower bounds the functions in the objective (3.8a) and places them as constraints. The optimization problem (3.8) in GP form becomes

$$\underset{\mathbf{x}, z}{\text{minimize}} \quad \frac{1}{z} \quad (3.9a)$$

subject to

$$g_1(\mathbf{x}) \geq z, \quad (3.9b)$$

$$g_2(\mathbf{x}) \geq z, \quad (3.9c)$$

$$g_3(\mathbf{x}) \leq 1, \quad (3.9d)$$

$$h_1(\mathbf{x}) = 1 \quad (3.9e)$$

The GP optimization problem given by Equation (3.9) in CVX will have the following structure

```
cvx_begin gp
    variables     $\mathbf{x}, z$ 
    minimize     $1/z$ 
    subject to   $g_1(\mathbf{x}) \geq z$ 
                $g_2(\mathbf{x}) \geq z$ 
```

$$g_3(\mathbf{x}) \leq 1$$

$$h_1(\mathbf{x}) = 1$$

*cvx\_end*

# 4

## Capacity Density Maximization for LTE

---

THE high interference at the cell edge for mobile communication systems that use the OFDMA is an issue that should be mitigated. To mitigate the ICI many frequency re-use schemes have been proposed. One of the promising scheme is the PFR, which is a combination of frequency reuse-1 and the frequency reuse-3 such that frequency reuse-1 is assigned for cell center users and frequency reuse-3 is assigned for cell edge users. In this chapter, I show the results on how the cell edge bandwidth is re-used for the cell center users in order to improve the cell capacity density assuming that cell edge users are idle. In Section 4.1 the geometry of the cell cluster model is shown with all its parameters that characterize the user's channel and the received power and interference. To calculate the average received SINR for a user located at the cell center or at the cell edge, we used the geometry of the cell cluster model and path-loss model. In Section 4.2, is shown the bandwidth re-allocation scheme for PFR that represents the frequency bands allocation per sub-carrier basis and per frequency band basis. In Section 4.3, are presented the mathematical derivations for cell capacity density. To make such derivations the cell cluster model and frequency reuse pattern are taken into account. Furthermore, in this section the optimization problem for maximizing the cell capacity density under the bandwidth re-allocation scheme is formulated. At the end of this chapter simulation results are drawn to illustrate the gain in capacity density when cell edge bandwidth is re-allocated to the inner users.

## 4.1 Geometry of Cell Cluster Model

To calculate the cell capacity density the basic principle is to design a cell cluster model. In the following a cell cluster model similar to the model in [6] is shown, which contains a base station  $BS_0$  in the center of the cluster and six neighboring base stations  $BS_k$ , with  $k = 1, \dots, 6$ . Each base station is considered to offer coverage over a regular hexagon area. The cluster model is shown in Figure 4.1.

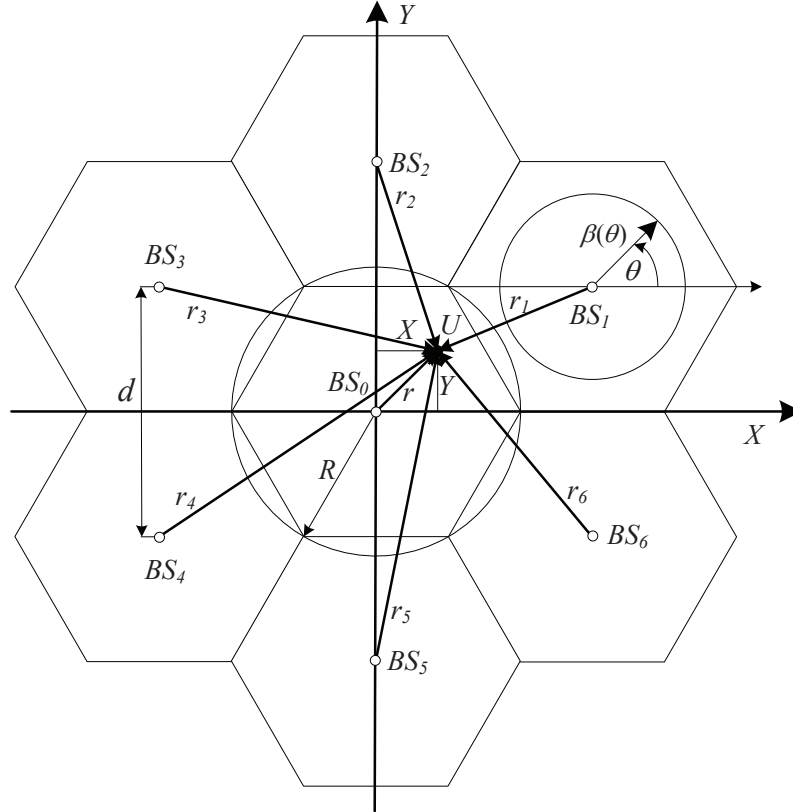


**Figure 4.1:** Cell cluster with radius classification criteria

In the cell cluster shown in Figure 4.1, each base station is equipped with three sectorized antennas, where each antenna radiates over an angle  $120^\circ$ . As it is shown in Figure 4.1 the user  $U$  that is located at cartesian coordinates  $(X, Y)$  is far from the serving base station for a distance  $r$ . The SINR received by user  $U$  is given by the following equation

$$\text{SINR} = \frac{P_r}{P_{\text{intra-cell}} + P_{\text{inter-cell}} + N_0}, \quad (4.1)$$

where  $P_r$  is the received power,  $P_{\text{intra-cell}}$  is the interference that comes from the users within the same cell and  $P_{\text{inter-cell}}$  is the interference that comes from the users located in the neighboring cells. The noise spectral density is denoted by  $N_0$ . Since LTE use OFDMA as multiple access scheme in the downlink [40], there is no intra-cell interference.

As result in Equation 4.1 from all interference terms, only the ICI remains. The received power density from the user can be described as in [6]

$$P_r = p L(r), \quad (4.2)$$

where  $p$  is the power spectral density which is given as the ratio of the total power and the total bandwidth  $p = P_{tot}/B_{tot}$ . In Equation (4.2),  $L(r)$  denotes the loss indicated by path-loss model. The path-loss model is used here is explained in the Subsection 4.1.1.

#### 4.1.1 Path-loss Exponent Model

The propagation properties for a wireless channel are determined mostly by the underlying propagation model. In our case we use the path-loss model [41], [6] which is a Free Space Path-Loss (FSPL) model given by following equation

$$L_r = \frac{L_0}{r^\alpha}, \quad (4.3)$$

where  $\alpha$  is the path-loss exponent and  $L_0$  is given by the following expression

$$L_0 = \left( \frac{v}{4\pi f} \right)^2, \quad (4.4)$$

where  $v$  is the velocity of light in the free space and  $f$  is the center carrier frequency. The path-loss exponent values varies between 2 and 4 depending on the environment: rural or urban. In the rural environments when the cell sizes are larger and the frequency reuse distance is larger, the path-loss exponent  $\alpha$  takes the values between 2 and 3. In the urban environments when the cell size is smaller and the reuse distance is smaller, the path-loss exponent takes the values between 3 and 4. More results on path-loss model depending on cell size and reuse distance can be found in [42]. Since in our study we consider the urban environment so we use the values of the path-loss exponent between 3 and 4.

#### 4.1.2 Average Received SINR

In the cell cluster model shown in Figure 4.1 only one user  $U$  is considered, so the average SINR is used as measurement metric, also according to [6] is calculated by the following equation

$$\Gamma(X, Y) = \frac{pL_0/r^\alpha}{N_0 + \sum_{i=1}^n pL_0/r_k^\alpha}, \quad (4.5)$$

where  $r_k, k = 1, \dots, 6$  are the distances of user  $U$  from the neighboring cells. For simplicity of calculations in the following, the cartesian coordinates  $(X, Y)$  are normalized to the radius of the cell  $R$ , which are denoted by  $(x, y)$ . So the average SINR in normalized coordinates according to [6] is given by following equation

$$\gamma(x, y) = \frac{\Gamma_e}{(x^2 + y^2)^{\alpha/2} [1 + \Gamma_e S(x, y)]}, \quad (4.6)$$

where  $\Gamma_e$  is the edge Signal-to-Noise-ratio (SNR) and is defined by

$$\Gamma_e = \frac{pL}{N_0 R^\alpha}. \quad (4.7)$$

The sum of all path-loss distances  $r_k$  is denoted by  $S(x, y)$  and given by following equation

$$S(x, y) = \sum_{k=1}^n [(x - x_k)^2 + (y - y_k)^2]^{-\alpha/2}, \quad (4.8)$$

where the normalized coordinates for the first tier of the interferer base stations are calculated using equations

$$x_k = \sqrt{3} \cos(k-1) \frac{\pi}{3}, \quad 1 \leq k \leq 6, \quad (4.9)$$

$$y_k = \sqrt{3} \sin(k-1) \frac{\pi}{3}, \quad 1 \leq k \leq 6. \quad (4.10)$$

Similarly to the equations for normalized coordinates of the first tier of interferer base stations, we define the equations for the normalized coordinates of the second tier interferer base stations as follows

$$x_k = 2\sqrt{3} \cos(k-1) \frac{\pi}{3}, \quad 7 \leq k \leq 18, \quad (4.11)$$

$$y_k = 2\sqrt{3} \sin(k-1) \frac{\pi}{3}, \quad 7 \leq k \leq 18. \quad (4.12)$$

The ICI is usually critical for cell edge users because the neighboring cells may use the same sub-carriers in a single frequency reuse-1 network. Also the users in the center of the cell use the same carriers, but they are more isolated from ICI because of the macro-scale path-loss. In order to minimize the ICI, a common approach is to split the cells into two regions: in a so-called FR-region and a PR-region. The FR-region is located around the base station, while the PR-region is located at the cell edge. All three sectors in FR-region use the same frequency bands like in reuse-1. In PR-region the three neighboring sectors use different frequency bands. Implying this frequency planning for the PR frequency bands, the PR-region can be considered ICI-free because the frequencies which are allocated for users in this region are different from the frequencies which are allocated to the users in neighboring cells. The classification for a user in cell is determined based on its received SINR. Depending on the value for the threshold on received SINR, we classify the users to the corresponding cell regions. If the received SINR from a user is higher than SINR threshold, that user is classified as inner user otherwise as outer user. After classifying the user, the scheduler decides which Physical Resource Block (PRB) to allocate to the user. One PRB contains 12 subcarriers where each subcarrier is 15 kHz in frequency domain [43]. The boundary between these two regions in polar coordinates is denoted as  $\beta(\theta)$ , with  $\theta$  specifying the azimuth angle. Furthermore, under the assumption of a circular boundary



$\rho = \beta(\theta)$  between the cell center region and the cell edge region, the average SINR for those regions in polar coordinates is formulated as follows

$$\gamma_\rho(r) = \begin{cases} \frac{\Gamma_e}{r^\alpha[1+\Gamma_e S(r)]}, & 0 < r \leq \rho, \\ \frac{\Gamma_e}{r^\alpha}, & \rho < r \leq 1. \end{cases} \quad (4.13)$$

## 4.2 Frequency Reuse Schemes

An exemplary frequency reuse pattern model for bandwidth allocation in PFR is presented in Figure 4.2.

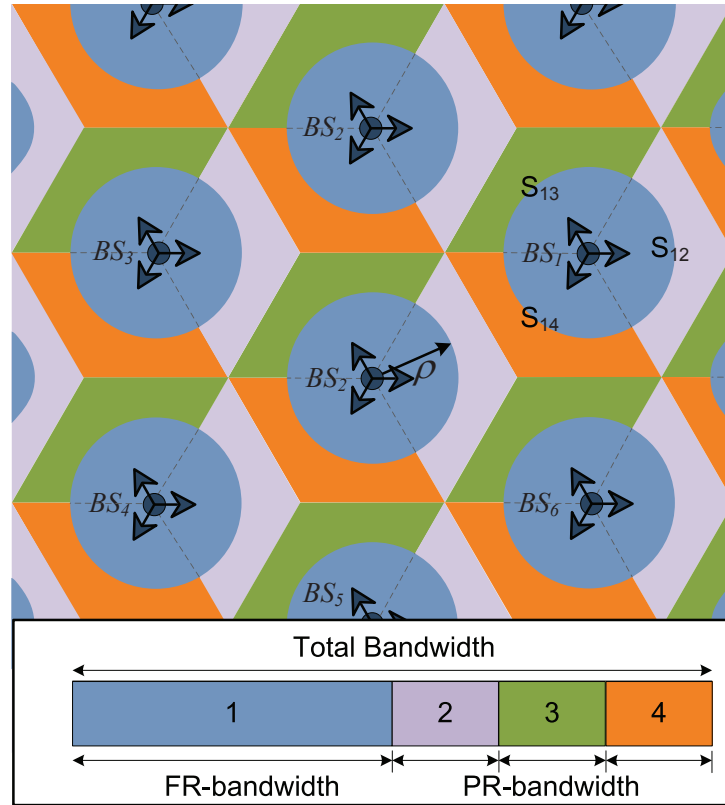


**Figure 4.2:** Frequency reuse pattern and bandwidth partitioning

In the frequency reuse pattern shown in Figure 4.2 the sectors are denoted by  $S_{12}$ ,  $S_{13}$  and  $S_{14}$  where the first subscript denotes the FR-band and the second subscript denotes the PR-bands. The equation for the total bandwidth used, compliant to the model shown in Figure 4.2 is given by following equation

$$B_{tot} = B_{FR} + 3B_{PR}, \quad (4.14)$$

where  $B_{FR}$  denotes the bandwidth allocated in FR-region and  $B_{PR}$  denotes the bandwidth allocated in PR-region. A fixed bandwidth allocation scheme is assumed here with ratio between bandwidths as  $B_{FR}/B_{PR} = 3$ .

Let us now assume all cells to be populated homogeneously with users over their area and in average all cells utilize the same transmit power. As result all subcarriers in all regions for the cells in PFR experience the same transmit power in downlink. The bandwidth allocation per subcarrier where all subcarriers have the same transmit power in the downlink as it is shown in Figure 4.3.

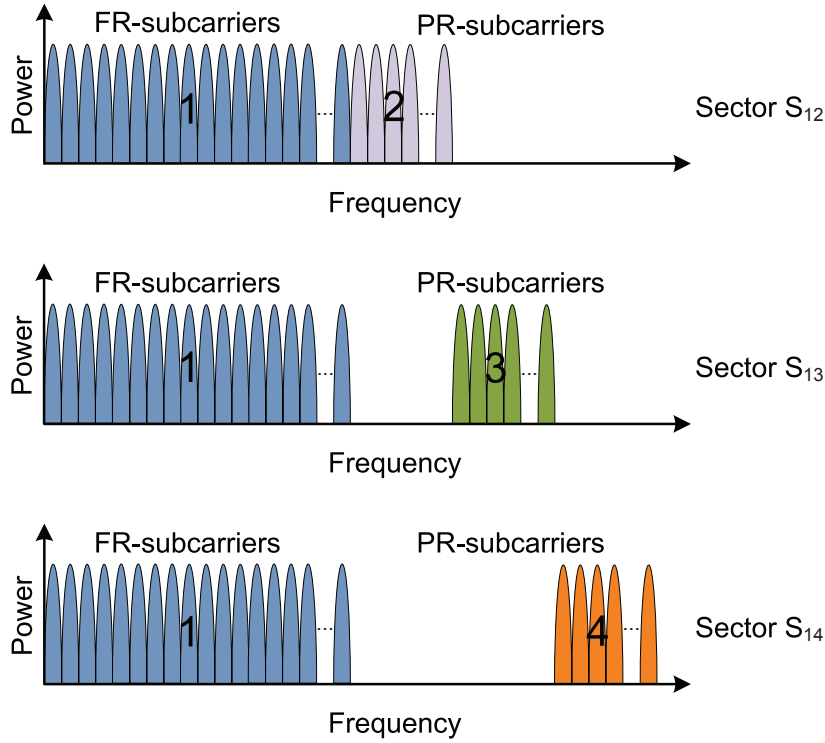


**Figure 4.3:** Downlink subcarrier allocation

In practical systems over the area of cells the users are not distributed uniformly, which means that more users can be concentrated in the area of FR-region (near the base station) than in the area of PR-region. In such case we say that cell is not loaded homogeneously over its area. To decrease the cell load in the FR region, it is necessary to re-allocate the bandwidth from PR-region to the FR-region. In make such re-allocation we introduce the parameter  $t$  which splits the PR-bandwidth in two parts. The way of allocating the bandwidth from PR-region in FR-region is shown by the bandwidth re-allocation scheme presented in Figure 4.4. The bandwidth which is re-allocated from the PR-region to the FR-region is considered to be ICI-free due to the assumption made earlier for

PR-bandwidth. From the graphical representation of the bandwidth re-allocation scheme shown in Figure 4.4 it is clear that parameter  $t$  describes the amount of the PR-bandwidth to be re-used for the FR-bandwidth. Increasing the parameter  $t$  increases the re-allocated bandwidth, but reduces the PR-band.

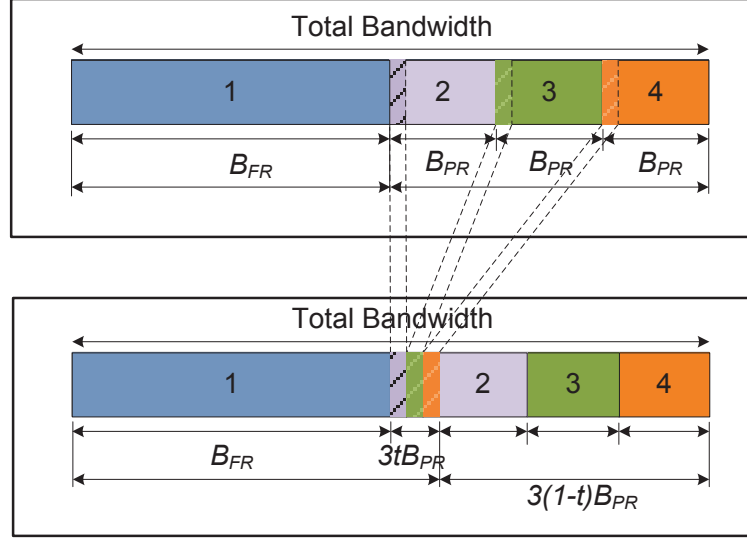


**Figure 4.4:** Partial bandwidth re-allocation scheme

### 4.3 Capacity density for Partial Frequency Reuse

In this section the capacity density taking into account the PR-band reallocation is analyzed. The capacity density achieved by a user located at polar coordinates  $(r, \theta)$  as shown in Figure 4.1, according to [6] is given by following equation

$$c_\rho(r) = b(r) \log_2[1 + \gamma_\rho(r)]. \quad (4.15)$$

where the normalized average SINR depending on the users classification is given by Equation (4.13).

The cell capacity density is defined as sum of the capacity densities in the two regions for the considered cell

$$C = C_{FR} + C_{PR}, \quad (4.16)$$

where  $C_{FR}$  denotes the capacity density in the FR-region and  $C_{PR}$  denotes the capacity density in the PR-region for the considered cell. The expressions for capacity densities can be calculated by integrating the capacity density given by Equation (4.15) over the corresponding region area. A constant bandwidth density allocation is assumed in each

region such that for given  $\rho$ , the  $b(r)$  becomes  $B_{FR}$  in the FR-region and  $B_{PR}$  in the PR-region. So the expressions for  $C_{FR}$  becomes

$$C_{FR} = 2\pi \int_0^\rho B_{FR} \log_2 \left( 1 + \frac{\Gamma_e}{r^\alpha [1 + \Gamma_e S(r)]} \right) r dr, \quad (4.17)$$

and the expression for and  $C_{PR}$

$$C_{PR} = 2\pi \int_\rho^1 B_{PR} \log_2 \left( 1 + \frac{\Gamma_e}{r^\alpha} \right) r dr. \quad (4.18)$$

To account for the PR-bandwidth re-allocation to the FR-region, we go through three steps. In the first, step we include the parameter  $t$  in Equation (4.18) and split it into two parts as shown by following equation

$$\begin{aligned} C_{PR} &= 2\pi \int_\rho^1 t B_{PR} \log_2 \left( 1 + \frac{\Gamma_e}{r^\alpha} \right) r dr \\ &\quad + 2\pi \int_\rho^1 (1-t) B_{PR} \log_2 \left( 1 + \frac{\Gamma_e}{r^\alpha} \right) r dr. \end{aligned} \quad (4.19)$$

In the second step, we replace the lower bound  $\rho$  by 0 and the upper bound 1 by  $\rho$  in the first integral of Equation (4.19). Now the modified expression for capacity in PR-region becomes

$$\begin{aligned} C_{PR}(t) &= 2\pi \int_0^\rho t B_{PR} \log_2 \left( 1 + \frac{\Gamma_e}{r^\alpha} \right) r dr \\ &\quad + 2\pi \int_\rho^1 (1-t) B_{PR} \log_2 \left( 1 + \frac{\Gamma_e}{r^\alpha} \right) r dr. \end{aligned} \quad (4.20)$$

Looking Equation (4.20) it is clear that the first integral accounts for capacity density of FR-region. And in the final step, we place the Equation (4.17) and Equation (4.20) into Equation (4.16) to form the expression for cell capacity density that takes into account the PR-bandwidth re-allocation. The equations for cell capacity density is formulated as in the following

$$\begin{aligned} C(t, \rho) &= 2\pi \int_0^\rho B_{FR} \log_2 \left( 1 + \frac{\Gamma_e}{r^\alpha [1 + \Gamma_e S(r)]} \right) r dr \\ &\quad + 2\pi \int_0^\rho t B_{PR} \log_2 \left( 1 + \frac{\Gamma_e}{r^\alpha} \right) r dr \\ &\quad + 2\pi \int_\rho^1 (1-t) B_{PR} \log_2 \left( 1 + \frac{\Gamma_e}{r^\alpha} \right) r dr. \end{aligned} \quad (4.21)$$

By increasing the parameter  $t$  we re-allocate more bandwidth from PR-region in FR-region. To maximize the cell capacity density constrained by frequency partitioning  $\rho$  and

bandwidth re-allocation  $t$  we formulate the following optimization problem

$$\underset{\rho, t}{\text{maximize}} \quad C \quad (4.22a)$$

subject to

$$0 \leq \rho \leq 1 \quad (4.22b)$$

$$0 \leq t \leq 1. \quad (4.22c)$$

### Numerical Simulations: Capacity density and frequency partitioning radius

In this section, the simulation results for capacity density and frequency partitioning radius taking into account the PR-bandwidth re-allocation are shown. The simulation parameters used for simulations are shown in Table 4.1.

**Table 4.1:** Simulation parameters

parameters	value
Total bandwidth $B_{tot}$	20 MHz
Total power $P_{tot}$	1 W
Noise spectral density $N_0$	-174 dBm/Hz
Center frequency $f$	2 GHz
Path-loss exponent $\alpha$	3.6
Cell radius $R$	100 m

To get the simulation results for the cell capacity density we use the simulation parameters given in Table 4.1 and Equation (4.21). The simulation results for cell capacity density are shown in Figure 4.5. From the simulation results shown in Figure 4.5, we see that when  $\rho = 0$  and  $t = 0$ , all the bandwidth is used only for the PR-region in the three sectors and the cell capacity has a certain value. Increasing  $\rho$  we start to share some bandwidth with the FR-region as result the cell capacity increases also. Such increase in cell capacity density continues until the frequency reuse partitioning achieves its optimal value, which in this case is  $\rho = 0.65$ . After such value by increasing the frequency reuse partitioning, we increase the FR-bandwidth as result we increase the ICI also. So cell capacity density is decreased. Such decrease in cell capacity density is compensated by PR-bandwidth re-allocation through increasing the parameter  $t$ . This happens because we are re-allocating the PR-bandwidth to the FR-region, which is considered to be ICI free. Also looking at the simulation results shown in Figure 4.5, we conclude that optimization problem given by Equation (4.22) is quasiconcave [32]. This can be verified from the graphical representation such that  $C(t, \rho) > \delta$ , where  $\delta$  is the sub level set of  $C(t, \rho)$ .

The results for maximum capacity density depending on parameter  $t$  are shown in Figure 4.6. From the simulation results shown in Figure 4.6, we notice that up to  $t = 0.17$

the maximum cell capacity density decreases, because only a few of PR-bandwidth is re-allocated to the FR-region. Increasing the bandwidth re-allocation to the FR-region, after  $t = 0.17$  the cell capacity density increases also because the increase in ICI is compensated by re-allocating the PR-bandwidth.

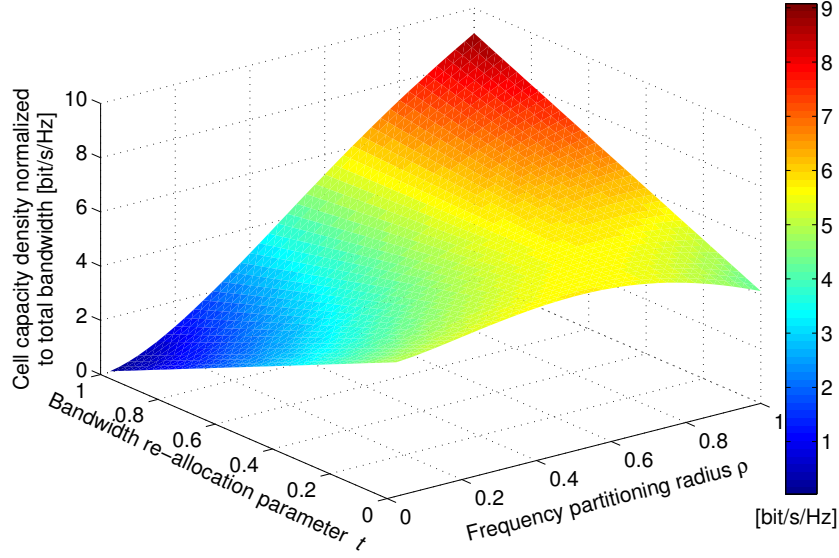


**Figure 4.5:** Cell capacity versus frequency-reuse partitioning radius for different values of parameter  $t$

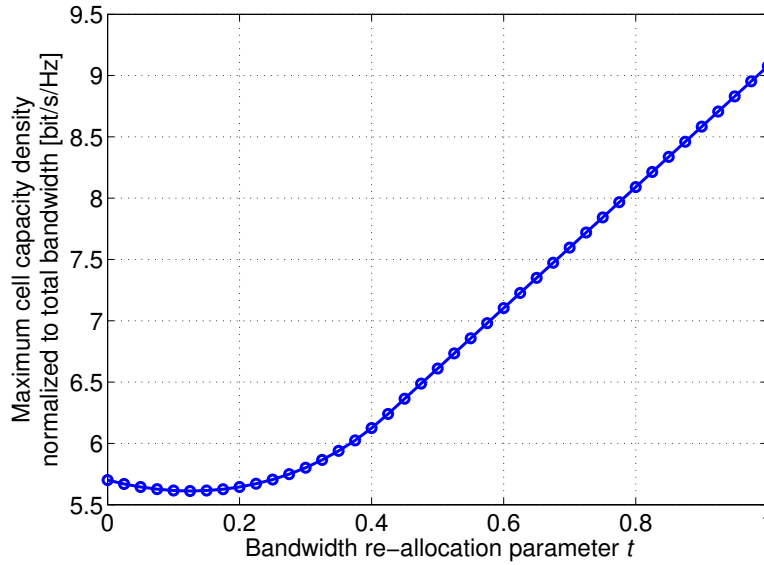


**Figure 4.6:** Maximum cell capacity versus parameter  $t$  for optimal frequency partitioning radius

# Power Allocation in Partial Frequency Reuse

---

IN this chapter, I show the sum-rate maximization by power allocation. Under the assumption for uniform power allocation to the inner (cell center) users and to the outer (cell edge) users, we transform the non-convex optimization problem for sum-rate maximization into a convex optimization problem.

In Section 5.1, the geometries of two cell cluster models for users classification are introduced. One is based on the distance threshold, where the users are classified in the cell regions based on their distance to the serving base station. The second cell cluster model uses the LSPLA threshold for users classification in the cell regions. To characterize the time variant properties of the wireless channel the LSPLA with its parameters including path-loss exponent, antenna gain, penetration loss, small-scale fading and shadowing is explained in Section 5.2. In Section 5.3, we show the frequency reuse pattern for variable power and fixed bandwidth allocation, that is applicable with both cell cluster models. Furthermore, in this section, based on the frequency reuse pattern for PFR, we formulated the optimization problems which are solvable in a water-filling like power allocation. Even more to show the importance of the optimal power allocation algorithm in reducing the ICI and increasing the sum-rate, the simulation are carried out. At the end of this chapter we show the methods to convert non-convex optimization problems of maximizing the minimum rate and the sum-power minimization for PFR into convex ones without making any assumption on power allocation or high-SINR approximation.

## 5.1 Geometry of Cell Cluster Model

In this section, the two cell clusters models with their geometric representation are shown. Each cluster contains base stations equipped with three sector antennas, where each antenna is characterized with its horizontal radiation pattern. Employing PFR in the cell clusters, each sector (cell) is considered to serve the inner and the outer users. The inner users are located near the sector antenna, while the outer users are located at the cell edge. To classify a user as an inner user or as an outer user, the definition of a threshold criterion is necessary. The first cell cluster model is shown in Figure 5.1.

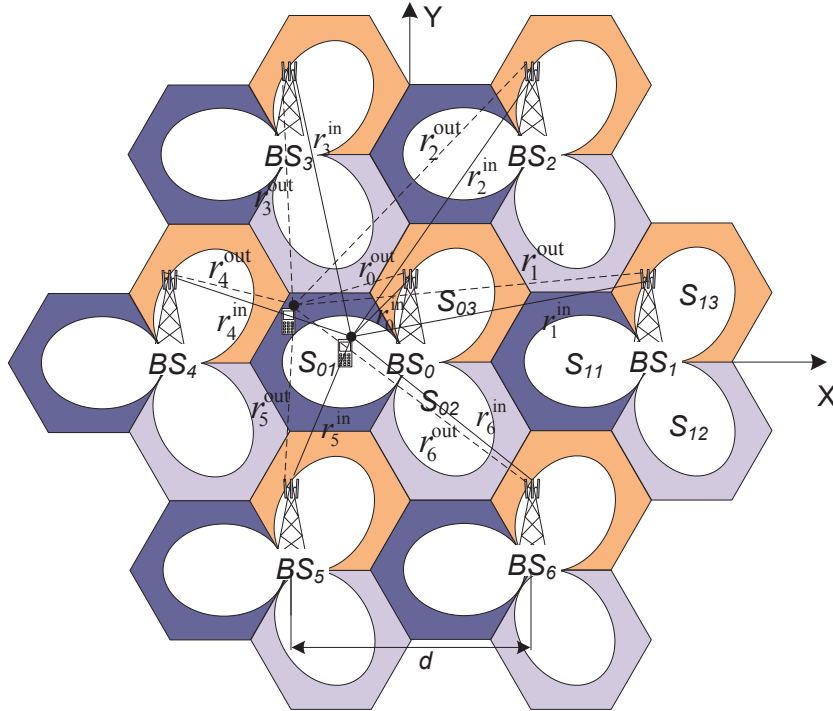


**Figure 5.1:** Cell cluster model with distance threshold criteria

The cell cluster shown in Figure 5.1, use the distance criteria to define if a user is an inner user or an outer user. Depending on the defined distance threshold a user is classified as inner user if its distance from the serving base station is smaller than distance threshold, otherwise it is classified as outer user.

The second cell cluster model is shown in Figure 5.2. In the second cell cluster shown in Figure 5.2 as threshold criteria for classifying the users in the cell regions, we use the LSPLA threshold. If the users LSPLA is greater than LSPLA threshold than a user is considered to be an inner user otherwise an outer user. In both cell cluster models depending on the threshold criteria, we consider  $N^{\text{in}}$  users located in the inner region and  $M^{\text{out}}$  users located in the outer regions.



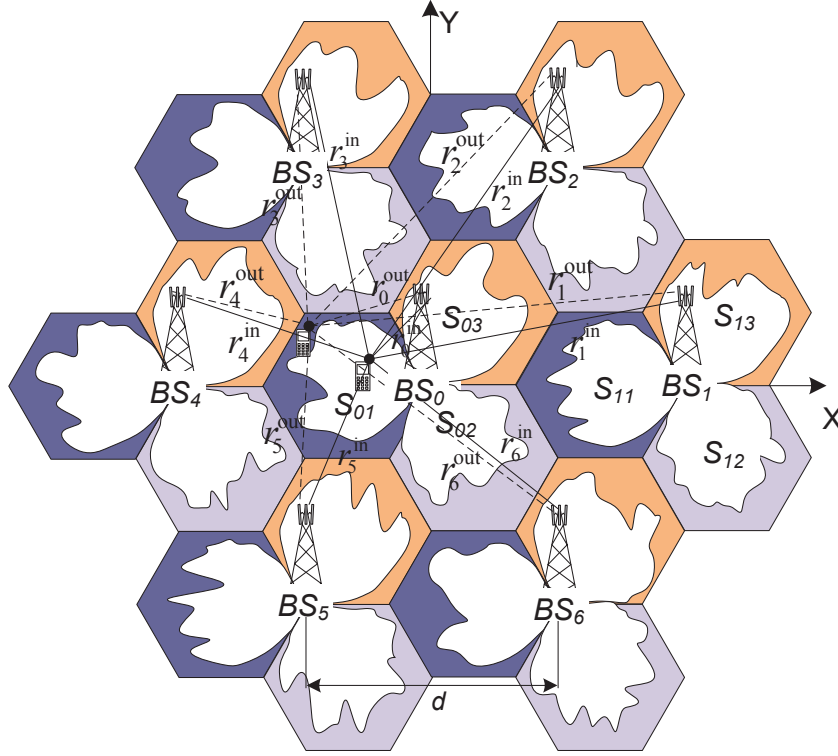


**Figure 5.2:** Cell cluster model with large-scale path-loss attenuation threshold criteria

Let's consider the base station  $BS_0$  that is located in the center of clusters. The base station has three sectorized antennas which offer coverage over three sectors denoted by  $S_{01}$ ,  $S_{02}$  and  $S_{03}$ , where the first subscript denotes the base station and the second subscript denotes the sector antenna. The users which belong to the inner region of sector  $S_{01}$ , receive power from their own sector antenna and all neighboring and non-neighboring sector antennas of base station  $BS_k$  with  $k = 0, \dots, 6$ . The transmission rate achieved by an inner user  $n$  located in the inner region of sector  $S_{01}$  is defined by following equation

$$R_n^{\text{in}} = B_n^{\text{in}} \log_2 \left( 1 + \frac{G_{0n}^{\text{in}} p_0^{\text{in}}}{N_0 B_n^{\text{in}} + \sum_{k=1}^6 G_{kn}^{\text{in}} p_k^{\text{in}}} \right). \quad (5.1)$$

In Equation (5.1) the bandwidth assigned to the inner user  $n$  is denoted by  $B_n^{\text{in}}$  and the noise spectral density by  $N_0$ . The LSPLA for the direct channel is denoted by  $G_{0n}$ , while the LSPLA of the interference channels are denoted by  $G_{kn}^{\text{in}}$ . The LSPLA for the direct and the interference channels are defined by Equation (5.3). The users which are located in the outer region of sector  $S_{01}$ , receive power from their own sector antenna and interference only from non-neighboring sectors of base stations  $BS_k$  with  $k = 1, \dots, 6$  that use the same frequency bands. The transmission rate achieved by an outer user  $m$  is defined by following equation

$$R_m^{\text{out}} = B_m^{\text{out}} \log_2 \left( 1 + \frac{G_{0m}^{\text{out}} p_0^{\text{out}}}{N_0 B_m^{\text{out}} + \sum_{k=1}^6 G_{km}^{\text{out}} p_k^{\text{out}}} \right) \quad (5.2)$$

The bandwidth allocated to the outer user  $m$  is denoted by  $B_m^{\text{out}}$ . The LSPLA for the direct channel to the outer user  $m$  is denoted by  $G_{0m}^{\text{out}}$ , while the interference channels to the outer user  $m$  are denoted by  $G_{km}^{\text{out}}$ . The direct and the interference channels similarly to the inner user, are defined by Equation (5.3). The position of the users within the cell is determined by their polar coordinates  $(r, \theta)$  converted from the cartesian coordinates  $(x, y)$ . More distant base stations are not considered in the cluster models shown in Figure 5.1 and Figure 5.2, due to increased complexity, however all the results can be extended to consider more distant base station as well.

## 5.2 Large-scale Path-loss Attenuation

The wireless channel is time variant not only because of the movement of the Receiver (Rx), but also because of the movement of the surrounding objects. Even when a mobile is not moving, due to the movement of the surrounding objects the signal can experience small-scale fading [44]. To consider most of the effects which determine the time variant properties of the wireless channels, in the following an extended version of LSPLA [45] is analyzed. The LSPLA of a direct channel or an interference channel including antenna gain, penetration loss, log-normal shadowing and small-scale fading (fast fading) is defined by following equation

$$G_{ki}^s = - [128.1 + 10\alpha \log_{10}(r_k/1000 \text{ m}) - A_k + L_p + X_\sigma + F]. \quad (5.3)$$

The  $G_{ki}^s$  is in dB, the superscript  $s \in \{\text{in}, \text{out}\}$  denotes the inner or the outer users, the subscript  $i \in \{n, m\}$  denotes the users index. The number 128.1 used in Equation (5.3) depends on the center frequency, where for the frequency 2 GHz that number is recommended by 3GPP standardization [46]. The path-loss exponent similar for the path-loss exponent model is denoted by  $\alpha$ , the distance between the mobile station and the base station is denoted by  $r$  in m, the sum of the mobile antenna gain and the base station antenna gain is denoted by  $A_k$  in dBi, the penetration loss by  $L_p$  in dB, the log-normal shadowing by  $X_\sigma$  in dB. The small-scale fading denoted by  $F$  is in dB.

### 5.2.1 Antenna Gain

In our cell cluster models, we use hexagonal cells where each hexagonal area is served by signals transmitted from directive antennas. The directive antenna is characterized by its gain, which depends on the antenna radiation pattern. We consider the horizontal antenna gain [46], [47] defined by the horizontal antenna pattern given by following equation

$$A(\theta) = - \min \left[ 12 \left( \frac{\theta}{\theta_{3dB}} \right)^2, A_m \right] \quad (5.4)$$

In Equation (5.4), the angle to the main direction of the radiation is denoted by  $\theta$ . The antenna beamwidth in degree is denoted by  $\theta_{3dB}$ . The angle of the antenna beamwidth below the horizontal plane defines the antenna tilt [48]. A study about the effects of the antenna beamwidth in the cell coverage and capacity can be found in [48], [49]. The maximum antenna attenuation is denoted by  $A_m$ .

Considering the antenna beamwidth  $\theta_{3dB} = 70^\circ$  and the antenna attenuation  $A_m = 20$  dB we have simulated the horizontal antenna gain to the direction of radiation versus the angle to the main direction. That is shown in Figure 5.3.

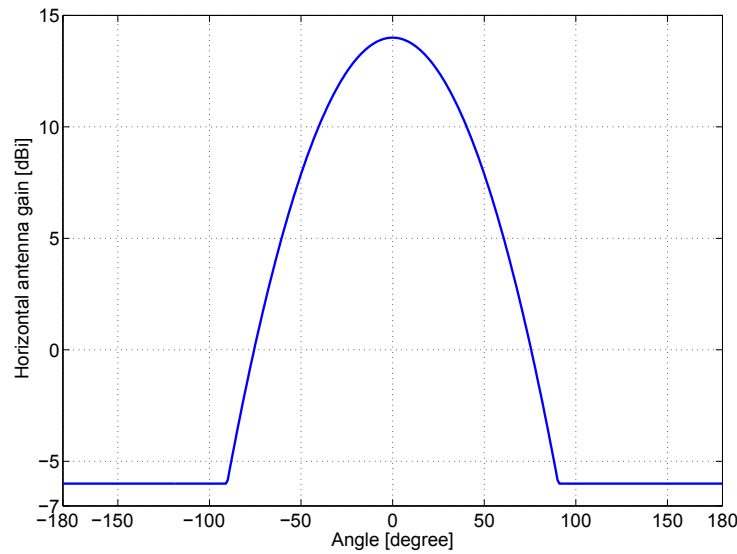


**Figure 5.3:** Horizontal antenna gain for horizontal antenna pattern

The directional antenna has been characterized by its own antenna gain of 14 dBi. The antenna pattern plays an important role in the penetration loss [44].

### 5.2.2 Penetration Loss

In the mobile communication community, it is known that indoor coverage is very important, since most of the time mobile users are inside the buildings. The received field strength from a mobile inside the buildings is different for different levels of height of the buildings and is determined by the penetration loss. The penetration loss is higher in the lower levels of the buildings than in the higher levels of the buildings [44], because in the higher levels of the buildings a direct Line-of-Sight (LOS) component could exist. Also by measurements it is proved that in higher frequencies the penetration loss is smaller than in lower frequencies [44]. In our work we use the penetration loss values recommended by 3GPP in [47].

### 5.2.3 Shadowing

The communication between mobile and base station is realized through the wireless channel which is sometimes LOS, but in most of the cases is Non-Line-of-Sight (NLOS), with many paths generated by reflection from the objects, diffraction etc. Sometimes the mobile station is near the base station, but because of the movement of the mobile station behind a building or a hill, the received signal is decreased. The effect of decrease in the received signal amplitude for a mobile station because the mobile is in shadow of the transmitted paths from the base station is called shadowing [50]. The shadowing is characterized by a log-normal distribution [51] defined by  $X_\sigma \sim \mathcal{N}(0, \sigma)$

### 5.2.4 Small-scale Fading

As result of reflections, multiple signals arrive from Transmitter (Tx) to Rx with different phases and amplitudes such that at Rx those signals are combined. Combining the signals at Rx, could increase the interference which results in change of amplitude for the received signal. Such effect is called small-scale fading.

At the operating frequency of LTE, even a small movement by 10 cm for the mobile station could have a positive or a negative effect on the received signal amplitude of the mobile station, due to small-scale fading [50]. In our study we consider the small-scale fading as chi-square distribution  $\chi_2^2$  with two degrees of freedom. The small-scale fading contributes in LSPLA given by Equation (5.3) only for the *directed* channels. The effect of the small-scale fading for the *interference* channels is neglected. This is because some components increase the amplitude of interference signal and some of the components decrease that amplitude, so when they combine at the receiver the effect is almost zero [51].

## 5.3 Variable Power and Fixed Bandwidth Allocation Scheme

In this section, we show the power allocation for fixed bandwidth allocation scheme in PFR. The bandwidth allocation is considered to be fixed in all regions of the cells, while the power allocation is considered to be variable such that it is optimized. The bandwidth and power allocation scheme is shown in Figure 5.4.

From the graphical representation in Figure 5.4 it is shown that half of the maximum cell bandwidth is allocated in the inner regions like in reuse-1, and the other half of the bandwidth is slitted in three equal parts like in reuse-3 and allocated in neighboring cell edge regions. By splitting the total bandwidth as the inner bandwidth and the outer bandwidth as we mentioned before, we minimize the ICI at the cell edge, where more power allocation is necessary due to the distance of the outer users from their own base station. For the fixed bandwidth and variable power allocation scheme shown in Figure 5.4

we show the power allocation algorithm in the following.

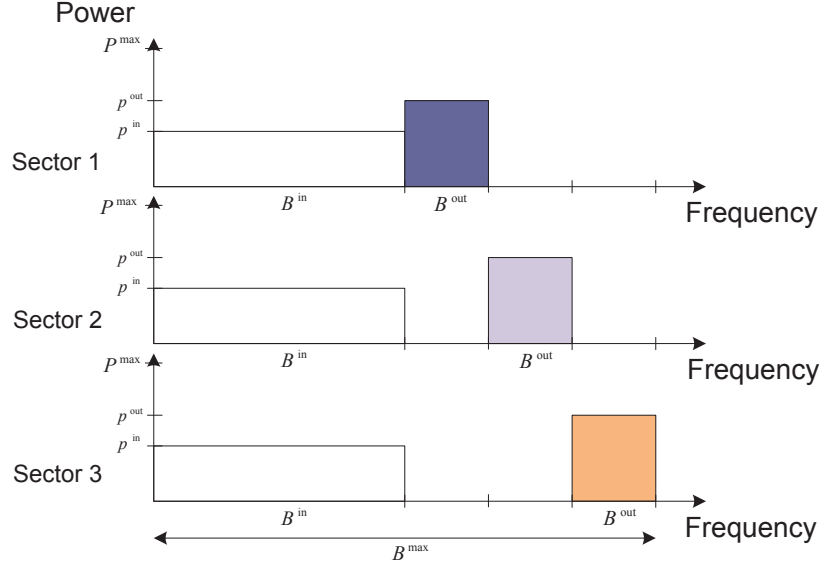


**Figure 5.4:** Frequency reuse pattern for fixed bandwidth allocation

## 5.4 Power Allocation Algorithm

In this section, we present the power allocation algorithm that classifies the users in the cell regions based on the distance threshold criteria. The power allocation algorithm is presented by Algorithm 1.

---

### Algorithm 1 Power Allocation Algorithm

---

**Require:**  $r_{\text{tgt}}, (\mathbf{r}, \theta)$

- 1: **if**  $r < r_{\text{tgt}}$  **then**
  - 2:      $(\mathbf{r}^{\text{in}}, \theta^{\text{in}}) \leftarrow (\mathbf{r}, \theta)$
  - 3: **else**
  - 4:      $(\mathbf{r}^{\text{in}}, \theta^{\text{in}}) \leftarrow (\mathbf{r}, \theta)$
  - 5: **end if**
  - 6: *Calculate the values of:*  
 $p_0^{\text{in}}, p_k^{\text{in}}, p_0^{\text{out}}, p_k^{\text{out}},$   
using power allocation given by Equation (5.5).
- 

The Algorithm 1, during classification saves the positions of the inner users at polar coordinates  $(\mathbf{r}^{\text{in}}, \theta^{\text{in}})$  and the outer users at polar coordinates  $(\mathbf{r}^{\text{out}}, \theta^{\text{out}})$ . At the last step it applies the power allocation problem to optimally allocate the power in the cell regions.

Using a vector-matrix notation the power and bandwidth allocation optimization problem is compactly written by Equation (5.5).

$$\underset{\mathbf{p}, \mathbf{b}}{\text{maximize}} \quad \mathbf{1}^T \mathbf{R}^{\text{in}} + \mathbf{1}^T \mathbf{R}^{\text{out}} \quad (5.5a)$$

subject to

$$\mathbf{A} \cdot \begin{bmatrix} \mathbf{p} \\ \mathbf{b} \end{bmatrix} = \mathbf{c}, \quad (5.5b)$$

$$\mathbf{p} \succeq \mathbf{0}, \quad (5.5c)$$

$$\mathbf{b} \succeq \mathbf{0}, \quad (5.5d)$$

where  $\mathbf{R}^{\text{in}}$  and  $\mathbf{R}^{\text{out}}$  denotes the vector elements of inner and outer user rates. We define

$$\begin{aligned} \mathbf{R}^{\text{in}} &= [R_1^{\text{in}}, R_2^{\text{in}}, \dots, R_{N^{\text{in}}}^{\text{in}}], \\ \mathbf{R}^{\text{out}} &= [R_1^{\text{out}}, R_2^{\text{out}}, \dots, R_{M^{\text{out}}}^{\text{out}}], \\ \mathbf{c} &= [P^{\text{max}}, B^{\text{max}}]^T, \\ \mathbf{A} &= \begin{bmatrix} 1 & 1 & 0 & 0 \\ 0 & 0 & 1 & 1 \end{bmatrix}. \end{aligned} \quad (5.6)$$

The maximum power and maximum bandwidth of the considered cell are denoted by  $P^{\text{max}}$  and  $B^{\text{max}}$ . The power vector  $\mathbf{p}$  and the bandwidth vector  $\mathbf{b}$  are defined by

$$\begin{aligned} \mathbf{p} &= [p_0^{\text{in}}, p_0^{\text{out}}]^T, \\ \mathbf{b} &= [B^{\text{in}}, B^{\text{out}}]^T. \end{aligned} \quad (5.7)$$

In the optimization problem (5.5), the constraints (5.5b), (5.5c) and (5.5d) are linear and hence convex. The sum-rate maximization problem given by Equation (5.5) is non-convex as it contains the sum-rate maximization in standard power control as a special case [14]. Under unequal allocation of interference powers  $p_k^{\text{in}}$  and  $p_k^{\text{out}}$ ,  $k = 1 \dots 6$  with the power  $p_0^{\text{in}}$  and  $p_0^{\text{out}}$ , but for a fixed bandwidth allocation  $B^{\text{in}}$  and  $B^{\text{out}}$  it can still be solved efficiently by geometric programming under a high-SINR approximation  $\log(1 + \text{SINR}) \approx \log(\text{SINR})$ , or sequentially approximated by geometric programs, *cf.* [14]. Differently, under the simplifying assumption that all cells use equal powers  $p_k^{\text{in}} = p_0^{\text{in}}$  and  $p_k^{\text{out}} = p_0^{\text{out}}$ ,  $k = 1, \dots, 6$  to serve the inner and outer users we show that the sum-rate maximization problem becomes convex and is solvable in a water-filling-like manner. For simplicity of notation we only consider users located in a single cell, however all presented problems and algorithms can be extended to the case of multiple users over multiple cells. It can be easily shown that the second derivative of  $R_n^{\text{in}}$  with respect to  $p_0^{\text{in}}$  is concave. As a consequence we find that  $\tilde{R}^{\text{in}}(B_n^{\text{in}}, p_0^{\text{in}}) = B_n^{\text{in}} R_n^{\text{in}}(p_0^{\text{in}}/B_n^{\text{in}})$  is concave as it is the perspective of a concave function [32]. Furthermore, since  $R_m^{\text{out}}$  is concave because it has a similar form as  $R_n^{\text{in}}$  and the sum of concave functions is concave as well, the optimization problem (5.5) is therefore concave.

### 5.4.1 Water-filling Like Power Allocation

Deriving an analytic solution for (5.5) was found to be intractable. However, for constant bandwidth allocation as shown in Figure 5.4, we derive a power allocation algorithm based on the Karush-Kuhn-Tucker (KKT) optimality conditions [32]. In order to simplify the written equations we are substituting  $G_{0n}^{\text{in}} = a_n$ ,  $\sum_{k=1}^6 G_{kn}^{\text{in}} = b_n$ ,  $G_{0m}^{\text{out}} = d_m$  and  $\sum_{k=1}^6 G_{km}^{\text{out}} = e_m$ . Following the definition of Lagrangian in Section 3.1.1, for the optimization problem (5.5), we write the Lagrangian as in the following

$$L(\mathbf{p}, \boldsymbol{\mu}, \boldsymbol{\lambda}) = \mathbf{1}^T \mathbf{R}^{\text{in}} + \mathbf{1}^T \mathbf{R}^{\text{out}} - \boldsymbol{\mu}^T (\mathbf{1}^T \mathbf{p} - P^{\text{max}}) + \boldsymbol{\lambda}^T \mathbf{p} \quad (5.8)$$

where  $\boldsymbol{\mu}$  and  $\boldsymbol{\lambda} = [\lambda^{\text{in}}, \lambda^{\text{out}}]$  are the Lagrange multipliers for the sum-power and positivity constraints, respectively. Applying the KKT conditions [52], [32] we have the following inequalities and equalities

$$\mathbf{p} \succeq \mathbf{0}, \quad (5.9a)$$

$$\mathbf{1}^T \mathbf{p} - P^{\text{max}} \leq 0, \quad (5.9b)$$

$$\boldsymbol{\lambda} \succeq \mathbf{0}, \quad (5.9c)$$

$$\lambda^{\text{in}} p^{\text{in}} = 0, \quad (5.9d)$$

$$\lambda^{\text{out}} p^{\text{out}} = 0, \quad (5.9e)$$

$$\begin{aligned} \frac{\partial L}{\partial p_0^{\text{in}}} &= - \sum_{n=1}^{N^{\text{in}}} \frac{B_n^{\text{in}}}{\log(2)} \frac{a_n N_0 B_n^{\text{in}}}{[N_0 B_n^{\text{in}} + (a_n + b_n) p_0^{\text{in}}]} \\ &\quad \cdot \frac{1}{(N_0 B_n^{\text{in}} + b_n p_0^{\text{in}})} + \mu - \lambda^{\text{in}} \\ &= f^{\text{in}}(p_0^{\text{in}}) - \lambda^{\text{in}} = 0, \end{aligned} \quad (5.9f)$$

$$\begin{aligned} \frac{\partial L}{\partial p_0^{\text{out}}} &= - \sum_{m=1}^{M^{\text{out}}} \frac{B_m^{\text{out}}}{\log(2)} \frac{d_m N_0 B_m^{\text{out}}}{[N_0 B_m^{\text{out}} + (d_m + e_m) p_0^{\text{out}}]} \\ &\quad \cdot \frac{1}{(N_0 B_m^{\text{out}} + e_m p_0^{\text{out}})} + \mu - \lambda^{\text{out}} \\ &= f^{\text{out}}(p_0^{\text{out}}) - \lambda^{\text{out}} = 0. \end{aligned} \quad (5.9g)$$

The last two equations (5.9f) and (5.9g) in the KKT conditions are the first derivative of the Lagrangian given by Equation (5.8) with respect to  $p_0^{\text{in}}$  and  $p_0^{\text{out}}$ , respectively. We continue to show that for a fixed variable  $\mu$ , the optimal power allocation can be computed efficiently. Combining the positivity constraints (5.9c) with (5.9f) and the complementary slackness constraints (5.9d), we find the optimum  $p_0^{\text{in}}(\mu)$  as a function of  $\mu$  after calculating the root of function  $f^{\text{in}}(p_0^{\text{in}})$ . Similarly, using (5.9c), (5.9g) and (5.9e) we find the optimum  $p_0^{\text{out}}(\mu)$  as a function of  $\mu$  by finding the root of function  $f^{\text{out}}(p_0^{\text{out}})$ . An efficient algorithm for finding these two roots in the general case is the Newton-Raphson method [53]. Using

$\bar{\mu}^{\text{out}} = \sum_{m=1}^{M^{\text{out}}} \frac{N_0 \log(2)}{d_m}$  and  $\bar{\mu}^{\text{in}} = \sum_{n=1}^{N^{\text{in}}} \frac{N_0 \log(2)}{a_n}$ , we find the optimum power allocation for the inner region and the outer region as in the following

$$p_0^{\text{in}} = \begin{cases} p_0^{\text{in}}(\mu), & \text{if } \frac{1}{\mu} \geq \bar{\mu}^{\text{in}}, \\ 0, & \text{otherwise,} \end{cases} \quad (5.10)$$

$$p_0^{\text{out}} = \begin{cases} p_0^{\text{out}}(\mu), & \text{if } \frac{1}{\mu} \geq \bar{\mu}^{\text{out}}, \\ 0, & \text{otherwise.} \end{cases} \quad (5.11)$$

In the case  $N^{\text{in}} = M^{\text{out}} = 1$ , the above roots can be computed analytically, giving the explicit solution

$$p_0^{\text{in}} = \begin{cases} \frac{-(a_1+2b_1)N_0B_1^{\text{in}}+\sqrt{\Delta^{\text{in}}}}{2(a_1+b_1)b_1}, & \text{if } \frac{1}{\mu} \geq \bar{\mu}^{\text{in}}, \\ 0, & \text{otherwise,} \end{cases} \quad (5.12)$$

where  $\Delta^{\text{in}}$  under the square root in Equation (5.12) is given by

$$\Delta^{\text{in}} = (a_1N_0B_1^{\text{in}})^2 + 4a_1b_1(a_1+b_1) \frac{N_0(B_1^{\text{in}})^2}{\mu \log(2)}.$$

The optimal assigned power to an outer user is analogously given by

$$p_0^{\text{out}} = \begin{cases} \frac{-(d_1+2e_1)N_0B_1^{\text{out}}+\sqrt{\Delta^{\text{out}}}}{2(d_1+e_1)e_1}, & \text{if } \frac{1}{\mu} \geq \bar{\mu}^{\text{out}}, \\ 0, & \text{otherwise,} \end{cases} \quad (5.13)$$

where  $\Delta^{\text{out}}$  under the square root in Equation (5.13) is given by

$$\Delta^{\text{out}} = (d_1N_0B_1^{\text{out}})^2 + 4d_1e_1(d_1+e_1) \frac{N_0(B_1^{\text{out}})^2}{\mu \log(2)}.$$

For searching the optimal water-level  $1/\mu$  we use a simple bisection search.

### Numerical Simulations: Power allocation algorithm

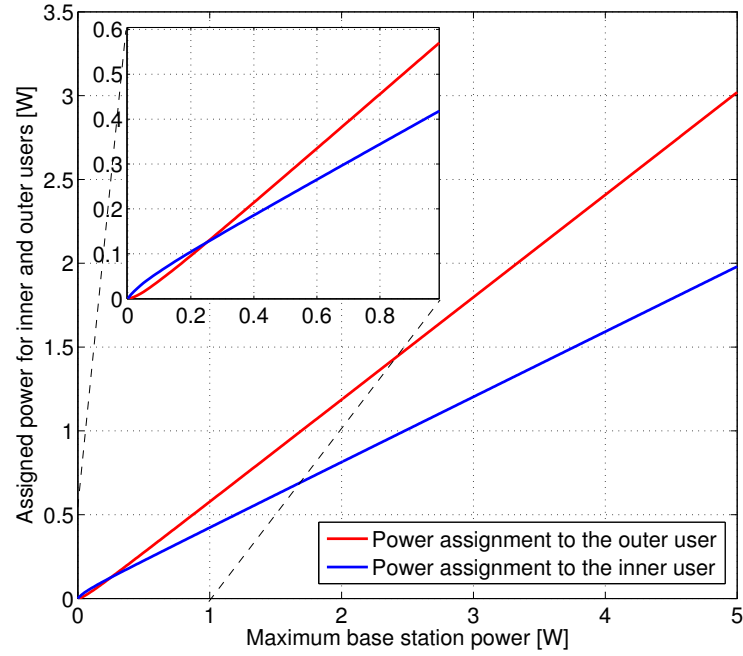
In this section, we present simulation results carried out for two users, one located in the inner region of the cell and the other one located in the outer region of the cell. During the simulations we have considered hundred channel realizations over which we have calculated the average sum-rate. The parameters used for the simulations are shown in Table 5.1.

Using Equations (5.12) and (5.13) while searching for the optimal water-level  $\frac{1}{\mu}$  through bisection search, we have simulated the optimal power allocation for the inner user and the outer user. The optimal power allocation for the inner user and the outer user is shown in Figure 5.5. When the maximum base station power is very low, all the transmit power is assigned to the inner user. Until a maximum base station power of 0.25 W, more power is assigned to the inner user than to the outer user. For maximum base station power higher than 0.25 W, more power is assigned to the outer user than to the inner user. Assigning more power to the outer user when the maximum base station power is higher, contributes in reducing the ICI and increasing the maximum sum-rate, since the outer user is interfered only from the non-neighboring sectors that use the same frequency band.



**Table 5.1:** Simulation parameters

parameters	value
Maximum base station power $P^{\max}$	5 W
Maximum base station bandwidth $B^{\max}$	20 MHz
Noise spectral density $N_0$	-174 dBm/Hz
Center frequency $f$	2.0 GHz
Pathloss exponent $\alpha$	3.75
Penetration loss $L_p$	20 dB
Shadowing $X_\sigma$	$\mathcal{N}(0, 8)$ dB
Small-scale Fading $F$	$\chi_2^2$ dB,
Inter base station distance $d$	700 m
Position of inner user in polar coordinates	(120 m, $160^\circ$ )
Position of outer user in polar coordinates	(370 m, $160^\circ$ )

**Figure 5.5:** Optimal power assignment to the inner and outer users

The maximum sum-rate achieved by the inner and the outer user as a function of the maximum base station power for optimal power allocation and fixed power allocation is shown in Figure 5.6. From the simulation results shown in Figure 5.6 we see the sum-rate gains for the optimal power allocation compared with a static power allocation. The static power allocation correspond to the optimum power allocation shown in Figure 5.5 where for  $P^{\max} = 5 \text{ W}$  around  $p_0^{\text{in}} = 40\%P^{\max}$  has been allocated to the inner user and around  $p_0^{\text{out}} = 60\%P^{\max}$  has been allocated to the outer user.

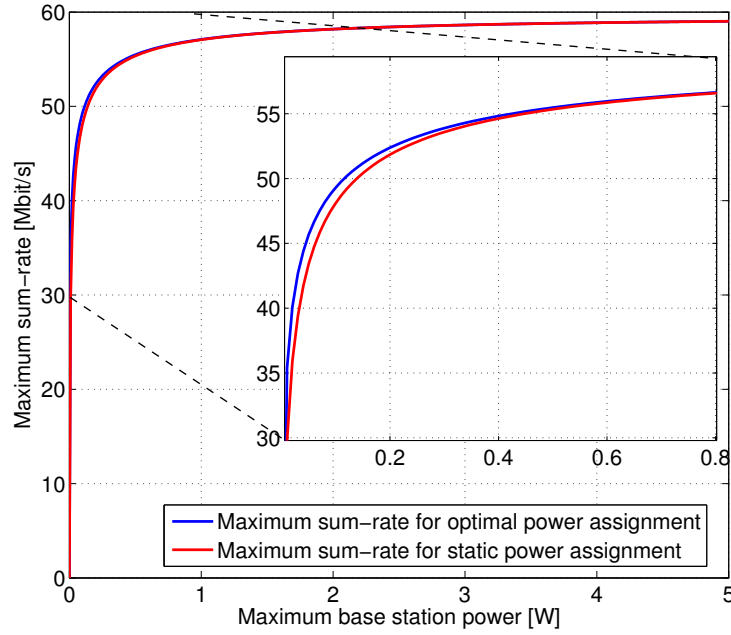


**Figure 5.6:** Maximum sum-rate for the inner and the outer users

## 5.5 Power Allocation Algorithms in Convex Form

In this section, two different types of optimization problems for systems employing the PFR and performing power and bandwidth allocation jointly are studied. Without relying on any assumptions on power allocations as in Section 5.4, we proof that these problems can be transformed into GP convex ones and hence solved efficiently using state-of-the-art convex optimization methods [32].

### 5.5.1 Maximization of the Minimum Rate in Convex Form

The problem of maximizing the minimum rate among all users in all cells in GGP form is formulated in the following:

$$\underset{\beta^{\text{in}}, \beta^{\text{out}}, t^{\text{in}}, t^{\text{out}} \in \mathcal{R}_+, \mathbf{p} \succeq \mathbf{0}}{\text{maximize}} \quad \min\{\beta^{\text{in}} t^{\text{in}} \log(2), \beta^{\text{out}} t^{\text{out}} \log(2)\} \quad (5.14a)$$

subject to

$$t^{\text{in}} \leq \log \left( 1 + \frac{p_c^{\text{in}}}{n_u^{\text{in}} \beta^{\text{in}} + \sum_{k \in \mathcal{C} \setminus c} g_{ku}^{\text{in}} p_k^{\text{in}}} \right), \quad \forall u \in \mathcal{U}_c^{\text{in}}, \quad \forall c \in \mathcal{C}, \quad (5.14b)$$

$$t^{\text{out}} \leq \log \left( 1 + \frac{p_c^{\text{out}}}{n_u^{\text{out}} \beta^{\text{out}} + \sum_{k \in \mathcal{C} \setminus c} g_{ku}^{\text{out}} p_k^{\text{out}}} \right), \quad \forall u \in \mathcal{U}_c^{\text{out}}, \quad \forall c \in \mathcal{C}, \quad (5.14c)$$

$$\beta^{\text{in}} + \beta^{\text{out}} \leq 1, \quad (5.14d)$$

$$p_c^{\text{in}} + p_c^{\text{out}} \leq P_c^{\text{max}}, \quad \forall c \in \mathcal{C}, \quad (5.14e)$$

where  $\beta^{\text{in}}$ ,  $\beta^{\text{out}}$ ,  $t^{\text{in}}$  and  $t^{\text{out}}$  are the normalized bandwidths and minimum rates allocated to inner and outer users, respectively. The subscripts  $u$  and  $c$  denote the user and cell, the calligraphies  $\mathcal{U}$  and  $\mathcal{C}$  denote the set of users and the set of cells. Furthermore,  $n_u^{\text{in}} = N_{0u}/G_u^{\text{in}}$  and  $g_{ku}^{\text{in}} = G_{ku}^{\text{in}}/G_u^{\text{in}}$  are the normalized noise and the normalized interference channel LSPLA for the inner users, respectively. Similar to the inner users  $n_u^{\text{out}} = N_{0u}/G_u^{\text{out}}$  and  $g_{ku}^{\text{out}} = G_{ku}^{\text{out}}/G_u^{\text{out}}$  are the normalized noise and the normalized interference channel LSPLA for the outer users.

**Proposition 1.** *The max-min-rate problem (5.14) can be transformed into a GP convex optimization problem.*

*Proof.* We begin by exchanging the objective in (5.14a) by its logarithm which notably does not change the optimal variables. Introducing several variable transformations  $\tilde{t}^{\text{in}} = \log(e^{t^{\text{in}}} - 1)$ ,  $\tilde{t}^{\text{out}} = \log(e^{t^{\text{out}}} - 1)$ ,  $\tilde{\beta}^{\text{in}} = \log(\beta^{\text{in}})$ ,  $\tilde{\beta}^{\text{out}} = \log(\beta^{\text{out}})$ ,  $\tilde{p}_c^{\text{in}} = \log(p_c^{\text{in}})$  and

$\tilde{p}_c^{\text{out}} = \log(p_c^{\text{out}})$ , the optimization problem (5.14) can be written in GP convex form

$$\begin{aligned} \underset{\tilde{\mathbf{p}}, \tilde{\beta}^{\text{in}}, \tilde{\beta}^{\text{out}}, \tilde{t}^{\text{in}}, \tilde{t}^{\text{out}}}{\text{maximize}} \quad & \min\{\log(\log(e^{\tilde{t}^{\text{in}}} + 1)) + \tilde{\beta}^{\text{in}} + \log(\log(2)), \\ & \log(\log(e^{\tilde{t}^{\text{out}}} + 1)) + \tilde{\beta}^{\text{out}} + \log(\log(2))\} \end{aligned} \quad (5.15a)$$

subject to

$$\log\left(e^{\tilde{t}^{\text{in}} + \tilde{\beta}^{\text{in}} + \log(n_u^{\text{in}}) - \tilde{p}_c^{\text{in}}} + \sum_{k \in \mathcal{C} \setminus c} e^{\tilde{t}^{\text{in}} + \log(g_{ku}^{\text{in}}) + \tilde{p}_k^{\text{in}} - \tilde{p}_c^{\text{in}}}\right) \leq 0, \quad \forall u \in \mathcal{U}_c^{\text{in}}, \forall c \in \mathcal{C}, \quad (5.15b)$$

$$\log\left(e^{\tilde{t}^{\text{out}} + \tilde{\beta}^{\text{out}} + \log(n_u^{\text{out}}) - \tilde{p}_c^{\text{out}}} + \sum_{k \in \mathcal{C} \setminus c} e^{\tilde{t}^{\text{out}} + \log(g_{ku}^{\text{out}}) + \tilde{p}_k^{\text{out}} - \tilde{p}_c^{\text{out}}}\right) \leq 0, \quad \forall u \in \mathcal{U}_c^{\text{in}}, \forall c \in \mathcal{C}, \quad (5.15c)$$

$$\log\left(e^{\tilde{\beta}^{\text{in}}} + e^{\tilde{\beta}^{\text{out}}}\right) \leq 0, \quad (5.15d)$$

$$\log\left(e^{\tilde{p}_c^{\text{in}}} + e^{\tilde{p}_c^{\text{out}}}\right) - \log(P_c^{\text{max}}) \leq 0, \quad \forall c \in \mathcal{C}, \quad (5.15e)$$

where in constraints (5.15b)-(5.15e) we additionally took the logarithm of both sides of the inequalities. Convexity of all constraints follows from the convexity of the log-sum-exp function [32, p. 74]. Concavity of the objective (5.15a) follows from  $\partial^2/\partial x^2(\log(\log(e^x + 1))) \geq 0$  and the fact that the point-wise minimum of concave functions is concave [32, p. 81].  $\square$

### 5.5.2 Sum-Power Minimization in Convex Form

The problem of minimizing the sum-power used by all cells in the cellular network that use PFR as frequency allocation scheme can be written as

$$\underset{\beta^{\text{in}}, \beta^{\text{out}}, t_u^{\text{in}}, t_u^{\text{out}} \in \mathcal{R}_+, \forall u \in \mathcal{U}^{\text{in}} \cup \mathcal{U}^{\text{out}}, c \in \mathcal{C}, \mathbf{p} \succeq \mathbf{0}}{\text{minimize}} \quad \sum_{c \in \mathcal{C}} p_c^{\text{in}} + \sum_{c \in \mathcal{C}} p_c^{\text{out}} \quad (5.16a)$$

subject to

$$t_u^{\text{in}} \geq R_u^{\text{tgt}}/(\beta^{\text{in}} \log(2)), \quad \forall u \in \mathcal{U}_c^{\text{in}}, \forall c \in \mathcal{C}, \quad (5.16b)$$

$$t_u^{\text{out}} \geq R_u^{\text{tgt}}/(\beta^{\text{out}} \log(2)), \quad \forall u \in \mathcal{U}_c^{\text{out}}, \forall c \in \mathcal{C}, \quad (5.16c)$$

$$t_u^{\text{in}} \leq \log\left(1 + \frac{p_c^{\text{in}}}{n_u^{\text{in}} \beta^{\text{in}} + \sum_{k \in \mathcal{C} \setminus c} g_{ku}^{\text{in}} p_k^{\text{in}}}\right), \quad \forall u \in \mathcal{U}_c^{\text{in}}, \quad \forall c \in \mathcal{C}, \quad (5.16d)$$

$$t_u^{\text{out}} \leq \log\left(1 + \frac{p_c^{\text{out}}}{n_u^{\text{out}} \beta^{\text{out}} + \sum_{k \in \mathcal{C} \setminus c} g_{ku}^{\text{out}} p_k^{\text{out}}}\right), \quad \forall u \in \mathcal{U}_c^{\text{out}}, \quad \forall c \in \mathcal{C}, \quad (5.16e)$$

$$\beta^{\text{in}} + \beta^{\text{out}} \leq 1, \quad (5.16f)$$

$$p_c^{\text{in}} + p_c^{\text{out}} \leq P_c^{\text{max}}, \quad \forall c \in \mathcal{C}, \quad (5.16g)$$

where  $R_u^{\text{tgt}}$  is the minimum target rate of a user.

**Proposition 2.** *The sum-power minimization problem (5.16) can be transformed into a GP convex optimization problem.*

*Proof.* Similarly to above we make the variable transformations  $\tilde{t}_u^{\text{in}} = \log(e^{t_u^{\text{in}}} - 1)$ ,  $\forall u \in \mathcal{U}^{\text{in}}$ ,  $\tilde{t}_u^{\text{out}} = \log(e^{t_u^{\text{out}}} - 1)$ ,  $\forall u \in \mathcal{U}^{\text{out}}$ ,  $\tilde{\beta}^{\text{in}} = \log(\beta^{\text{in}})$ ,  $\tilde{\beta}^{\text{out}} = \log(\beta^{\text{out}})$ ,  $\tilde{p}_c^{\text{in}} = \log(p_c^{\text{in}})$  and  $\tilde{p}_c^{\text{out}} = \log(p_c^{\text{out}})$ ,  $\forall c \in \mathcal{C}$ . After using the transformed variables and the logarithm in the objective and all the constraints of the optimization problem (5.16) we have the sum-power in GP convex form as in the following

$$\underset{\tilde{\mathbf{p}}, \tilde{\beta}^{\text{in}}, \tilde{\beta}^{\text{out}}, \tilde{t}^{\text{in}}, \tilde{t}^{\text{out}}}{\text{minimize}} \quad \log\left(\sum_{c \in \mathcal{C}} e^{\tilde{p}_c^{\text{in}}} + \sum_{c \in \mathcal{C}} e^{\tilde{p}_c^{\text{out}}}\right) \quad (5.17a)$$

subject to

$$\log(\log(e^{\tilde{t}_u^{\text{in}}} + 1)) \geq \log(R_u^{\text{tgt}}) - \tilde{\beta}^{\text{in}} - \log(2), \forall u \in \mathcal{U}_c^{\text{in}}, \forall c \in \mathcal{C}, \quad (5.17b)$$

$$\log(\log(e^{\tilde{t}_u^{\text{out}}} + 1)) \geq \log(R_u^{\text{tgt}}) - \tilde{\beta}^{\text{out}} - \log(2), \forall u \in \mathcal{U}_c^{\text{out}}, \forall c \in \mathcal{C}, \quad (5.17c)$$

$$\log\left(e^{\tilde{t}^{\text{in}} + \tilde{\beta}^{\text{in}} + \log(n_u^{\text{in}}) - \tilde{p}_c^{\text{in}}} + \sum_{k \in \mathcal{C} \setminus c} e^{\tilde{t}^{\text{in}} + \log(g_{ku}^{\text{in}}) + \tilde{p}_k^{\text{in}} - \tilde{p}_c^{\text{in}}}\right) \leq 0,$$

$$\forall u \in \mathcal{U}_c^{\text{in}}, \forall c \in \mathcal{C}, \quad (5.17d)$$

$$\log\left(e^{\tilde{t}^{\text{out}} + \tilde{\beta}^{\text{out}} + \log(n_u^{\text{out}}) - \tilde{p}_c^{\text{out}}} + \sum_{k \in \mathcal{C} \setminus c} e^{\tilde{t}^{\text{out}} + \log(g_{ku}^{\text{out}}) + \tilde{p}_k^{\text{out}} - \tilde{p}_c^{\text{out}}}\right) \leq 0,$$

$$\forall u \in \mathcal{U}_c^{\text{in}}, \forall c \in \mathcal{C}, \quad (5.17e)$$

$$\log\left(e^{\tilde{\beta}^{\text{in}}} + e^{\tilde{\beta}^{\text{out}}}\right) \leq 0, \quad (5.17f)$$

$$\log\left(e^{\tilde{p}_c^{\text{in}}} + e^{\tilde{p}_c^{\text{out}}}\right) - \log(P_c^{\text{max}}) \leq 0, \quad \forall c \in \mathcal{C}, \quad (5.17g)$$

In the optimization problem (5.17) the objective (5.17a) is convex since it is a log-sum-exp function. The constraints (5.17b)-(5.17c) are also convex since the  $\log(\log(e^x + 1))$  is a convex function. The other constraints (5.17d)-(5.17g) are all log-sum-exp functions also convex, so the whole optimization problem (5.17) is convex.  $\square$



# 6

## Bandwidth and Power Allocation in Partial Frequency Reuse

---

OPTIMIZING only the power allocation while considering the bandwidth allocation fixed is not the most efficient solution. Considering that bandwidth resources are very expensive and also limited, it is necessary to optimize such resources. In this chapter, I show the application of optimal power allocation algorithm for bandwidth re-allocation scheme. Furthermore, I present the optimization of the bandwidth allocation jointly with power allocation. Due to complexity in finding solutions for jointly bandwidth and power allocation, in this chapter we present the optimization of power allocation and bandwidth adaption in cell region based on users classification.

In Section 6.1 a variable bandwidth and variable power allocation scheme is shown. Using this scheme in Section 6.2, the bandwidth and power allocation algorithms for PFR in GP form are formulated.

In Section 6.3 the bandwidth re-allocation scheme is shown for PFR. Applying such scheme we obtain the results in power allocation and sum-rate maximization for two cases of users classification: classification by distance threshold and by LSPLA threshold. Furthermore in Section 6.4, considering the mean LSPLA as threshold for users classification, we have formulated two other algorithms for PFR. The optimal power and adaptive bandwidth algorithm, which adapts the bandwidth allocation based on the users classification, while optimizing the power allocation using the maximization of the minimum SINR. Using such algorithm, we have shown the optimality of PFR in power allocation.

The efficient power and adaptive bandwidth allocation algorithm, adapts the bandwidth allocation based on the users classification but optimizes the power allocation using sum-power minimization. By this algorithm, we show the efficiency in power allocation for PFR.

## 6.1 Variable Power and Variable Bandwidth Allocation Scheme

The variable bandwidth and variable power allocation scheme consists of a scheme in which the bandwidth allocation and the power allocation to the users is carried out by an optimization algorithm. Such a scheme is independent for each cell of an individual base station in terms of power allocation but dependent on the other cells of the other base station that use the same frequency bands. The variable bandwidth and variable power allocation scheme is shown in Figure 6.1. From the scheme shown in Figure 6.1 it can be seen that for an arbitrary base station, for each cell the bandwidth is split in the inner bandwidth and the outer bandwidth, differently.

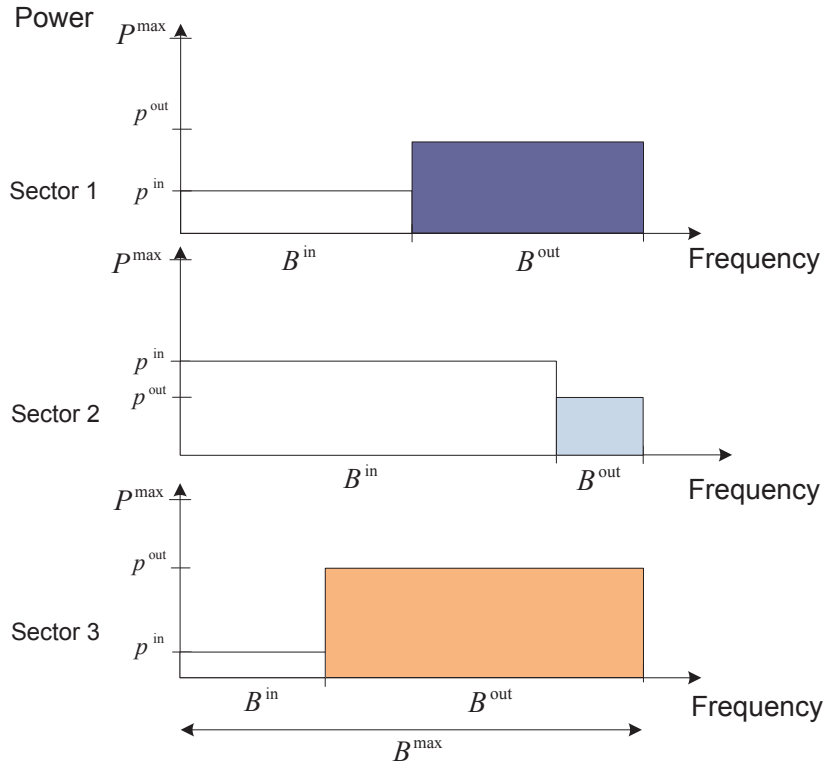


**Figure 6.1:** Variable bandwidth and power allocation scheme

Depending on the amount of the inner users and the outer users an optimization algorithm would decide for the optimal bandwidth allocation. The power allocated to the



inner users is different from the power allocated to the outer users. For each individual cell the sum of the bandwidths allocated to the inner users and to the outer users is equal to the maximum cell bandwidth. This is due to the optimality. On the other hand the sum of the power allocation is equal to the maximum base station power only in case of an optimal optimization algorithm for power allocation.

## 6.2 Bandwidth and Power Allocation Algorithms

The optimization algorithms for bandwidth and power allocation are formulated to satisfy the users requests for transmission rate with radio resource that we have. The algorithms that we show in the following use joint optimization of bandwidth and power allocation in PFR to optimally allocate the bandwidth to the users and efficiently allocate the power in the cell regions. The optimization problem which is optimal for the bandwidth allocation and sub-optimal for power allocation in PFR, is the maximization of the minimum rate. Applying such optimization problem, we formulated efficient algorithms for users classification in the cell regions.

### 6.2.1 Maximization of the Minimum Rate

In this section, the maximization of the minimum rate for systems employing PFR and performing power allocation and bandwidth allocation is studied. Without relying on any assumptions on power allocations or high-SINR approximation, we have proven that such optimization problem can be transformed into GP optimization problem and hence solved efficiently using Disciplined Convex Programming (DCP) methods. The maximization of the minimum rate offers flexibility in solving joint bandwidth and power allocation for multiple users over multiple cells. The problem of maximizing the minimum rate among all users in all cells for PFR cellular network is written in the following

$$\begin{aligned} & \underset{\beta_{cn}^{\text{in}}, \beta_{cm}^{\text{out}} \in \mathcal{R}_+, \mathbf{p} \succeq \mathbf{0}}{\text{maximize}} && \min\{\beta_{c1}^{\text{in}} t^{\text{in}} \log(2), \dots, \beta_{cN^{\text{in}}}^{\text{in}} t^{\text{in}} \log(2), \\ & && \beta_{c1}^{\text{out}} t^{\text{out}} \log(2), \dots, \beta_{cM^{\text{out}}}^{\text{out}} t^{\text{out}} \log(2)\} \end{aligned} \quad (6.1a)$$

subject to

$$t^{\text{in}} \leq \log \left( 1 + \frac{p_c^{\text{in}}}{n_1^{\text{in}} \beta_{c1}^{\text{in}} + \sum_{k \in \mathcal{C} \setminus c} g_{k1}^{\text{in}} p_k^{\text{in}}} \right), \quad \forall c \in \mathcal{C}, \quad (6.1b)$$

$$\vdots$$

$$t^{\text{in}} \leq \log \left( 1 + \frac{p_c^{\text{in}}}{n_{N^{\text{in}}}^{\text{in}} \beta_{cN^{\text{in}}}^{\text{in}} + \sum_{k \in \mathcal{C} \setminus c} g_{kN^{\text{in}}}^{\text{in}} p_k^{\text{in}}} \right), \quad \forall c \in \mathcal{C}, \quad (6.1c)$$

$$t^{\text{out}} \leq \log \left( 1 + \frac{p_c^{\text{out}}}{n_1^{\text{out}} \beta_{c1}^{\text{out}} + \sum_{k \in \mathcal{C} \setminus c} g_{k1}^{\text{out}} p_k^{\text{out}}} \right), \quad \forall c \in \mathcal{C}, \quad (6.1d)$$

$$\vdots$$

$$t^{\text{out}} \leq \log \left( 1 + \frac{p_c^{\text{out}}}{n_{M^{\text{out}}}^{\text{out}} \beta_{cM^{\text{out}}}^{\text{out}} + \sum_{k \in \mathcal{C} \setminus c} g_{kM^{\text{out}}}^{\text{out}} p_k^{\text{out}}} \right), \quad \forall c \in \mathcal{C}, \quad (6.1e)$$

$$\sum_{n=1}^{N^{\text{in}}} \beta_{cn}^{\text{in}} + \sum_{m=1}^{M^{\text{out}}} \beta_{cm}^{\text{out}} \leq 1, \quad \forall c \in \mathcal{C} \quad (6.1f)$$

$$p_c^{\text{in}} + p_c^{\text{out}} \leq P_c^{\text{max}}, \quad \forall c \in \mathcal{C}, \quad (6.1g)$$

As we have introduced in Section 3.2.1, the optimization problem of maximizing the minimum rate written by Equation (6.1) is in GGP form. In the optimization problem (6.1), the constraints (6.1b)-(6.1c) show the normalized inner user rates which are constrained by normalized minimum required inner user rate. Similarly for the outer users, the constraints (6.1d)-(6.1e) apply. The last two constraints (6.1f) and (6.1g) are the bandwidth and the power constraints.

**Proposition 3.** *The max-min-rate problem (6.1) can be transformed into GP optimization problem.*

*Proof.* Similar to the maximization of the minimum posynomials explained in Section 3.2.1, we begin by introducing a variable  $z$  which act lower bound [36] in the objective (6.1a) and by using its inverse in the objective we convert the GGP into a GP [37]. Applying exponential in both sides of constraints (6.1b)-(6.1e), which notably does not change the optimal variables, converts the optimization problem (6.1) into a GP, where CVX can be used to get the optimal bandwidth allocation and sub-optimal power allocation. Now the

optimization problem in GP form is written in the following

$$\underset{\mathbf{p} \succeq \mathbf{0}, \beta_{cn}^{\text{in}}, \beta_{cm}^{\text{out}}, z \in \mathcal{R}_+}{\text{minimize}} \quad \left\{ \frac{1}{z} \right\} \quad (6.2a)$$

subject to

$$\beta_{c1}^{\text{in}} t^{\text{in}} \log(2) \geq z \quad (6.2b)$$

$$\vdots$$

$$\beta_{cN}^{\text{in}} t^{\text{in}} \log(2) \geq z \quad (6.2c)$$

$$\beta_{c1}^{\text{out}} t^{\text{out}} \log(2) \geq z \quad (6.2d)$$

$$\vdots$$

$$\beta_{cM}^{\text{out}} t^{\text{out}} \log(2) \geq z \quad (6.2e)$$

$$\frac{n_1^{\text{in}} \beta_{c1}^{\text{in}} + \sum_{k \in \mathcal{C} \setminus c} g_{k1}^{\text{in}} p_k^{\text{in}}}{p_c^{\text{in}}} \geq e^{(t^{\text{in}}-1)}, \quad \forall c \in \mathcal{C}, \quad (6.2f)$$

$$\vdots$$

$$\frac{n_{N}^{\text{in}} \beta_{cN}^{\text{in}} + \sum_{k \in \mathcal{C} \setminus c} g_{kN}^{\text{in}} p_k^{\text{in}}}{p_c^{\text{in}}} \geq e^{(t^{\text{in}}-1)}, \quad \forall c \in \mathcal{C}, \quad (6.2g)$$

$$\frac{n_1^{\text{out}} \beta_{c1}^{\text{out}} + \sum_{k \in \mathcal{C} \setminus c} g_{k1}^{\text{out}} p_k^{\text{out}}}{p_c^{\text{out}}} \geq e^{(t^{\text{out}}-1)}, \quad \forall c \in \mathcal{C}, \quad (6.2h)$$

$$\vdots$$

$$\frac{n_{M}^{\text{out}} \beta_{cM}^{\text{out}} + \sum_{k \in \mathcal{C} \setminus c} g_{kM}^{\text{out}} p_k^{\text{out}}}{p_c^{\text{out}}} \geq e^{(t^{\text{out}}-1)}, \quad \forall c \in \mathcal{C}, \quad (6.2i)$$

$$\sum_{n=1}^{N^{\text{in}}} \beta_{cn}^{\text{in}} + \sum_{m=1}^{M^{\text{out}}} \beta_{cm}^{\text{out}} \leq 1, \quad \forall c \in \mathcal{C} \quad (6.2j)$$

$$p_c^{\text{in}} + p_c^{\text{out}} \leq P_c^{\text{max}}, \quad \forall c \in \mathcal{C}, \quad (6.2k)$$

where the constraints (6.2b)-(6.2e) are monomials [37] and posynomials as well. In the constraints (6.2f)-(6.2i), the expressions in the left side are posynomials since the ratio of posynomial by a monomial is still posynomial [37]. The last two constraints are only posynomials, so the optimization problem (6.2) is in GP form.  $\square$

### Numerical Simulations: Bandwidth and power allocation by maximization of the minimum rate

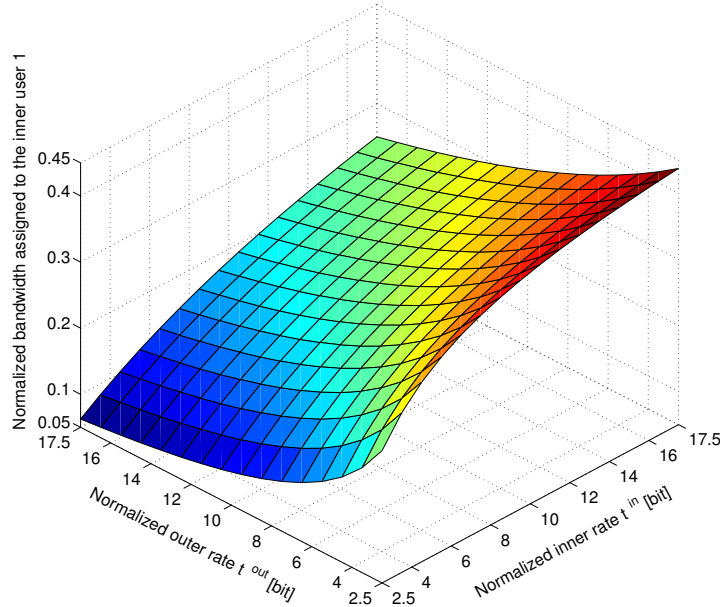
In this subsection, the simulation results for power and bandwidth allocation are shown. To get the simulation results, we use the optimization problem for maximization of the minimum rate given by Equation (6.2). For simulations we have considered two inner user located in the polar coordinates (200 m,  $160^\circ$ ), (120 m,  $160^\circ$ ) and two outer users located in polar coordinates (400 m,  $160^\circ$ ), (380 m,  $160^\circ$ ). The simulation parameters are shown in

Table 6.1.

**Table 6.1:** Simulation parameters

parameters	value
Maximum allowed base station power $P^{\max}$	40 W
Maximum base station bandwidth $B^{\max}$	20 MHz
Noise spectral density $N_0$	$-174$ dBm/Hz
Center frequency $f$	2.0 GHz
Pathloss exponent $\alpha$	3.75
Penetration loss $L_p$	20 dB
Shadowing $X_\sigma$	$\mathcal{N}(0, 8)$ dB
Small-scale Fading $F$	$\chi^2_2$ dB,
Inter base station distance $d$	700 m
Maximum cell range $r$	$(2/3)d$ m

By simulations it has been found that, the individual inner users get the same amount of bandwidth assigned as the individual outer users. This is due to the same minimum inner and the outer users requirements. Consequently, we show only the bandwidth assigned to Inner User 1 and Outer User 1 in the following. The bandwidth assigned to the Inner User 1 is shown in Figure 6.2.



**Figure 6.2:** Assigned normalized bandwidth to the inner user 1 versus normalized inner and outer rates

From the simulation results shown in Figure 6.2, we see that more bandwidth is as-

signed to the Inner User 1 when the requirement for the minimum inner user rate is increased. When the requirement for the minimum outer user rate begins to increase, the bandwidth assignment to the Inner User 1 decreases. In order to keep the inner user rate higher than the minimum requirement for the inner user rate, it is necessary that the power allocated to the inner users to be increased. The power allocation to the users in the inner region is shown in Figure 6.3.

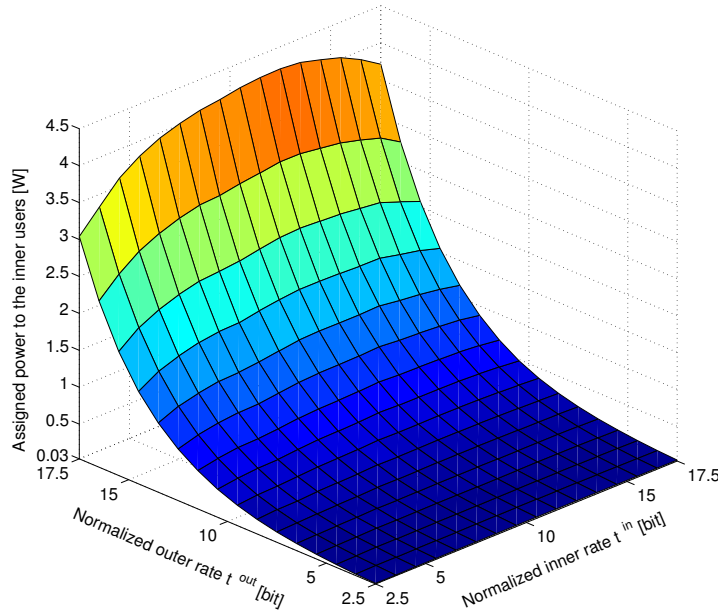


**Figure 6.3:** Assigned power to the inner users

From the simulation results for the power allocation to the inner users shown in Figure 6.3 it is clear that the power allocated to the inner users is increased in order to compensate for the minimum inner user requirement. Consequently, each inner user achieves a rate higher than the minimum requirement inner user rate.

The bandwidth allocation to the Outer User 1 is shown in Figure 6.4. Looking at the simulation results shown in Figure 6.4, we see that the bandwidth allocation to the outer user increases when the minimum required rate for the outer user increases. Because of the higher minimum required inner user rate, less bandwidth is allocated to the outer user. In this case it is necessary to allocate more power to the outer user in order to compensate for the decrease in bandwidth allocation due to the minimum inner user requirement. The power allocation to the outer users is shown in Figure 6.5. In the simulation results for the outer power allocation presented in Figure 6.5, we show how the power allocated to the outer users increases resulting from the increase of the minimum inner user required rate. Therefore, each outer user achieves a rate higher than the minimum requirement for outer users.

rate.

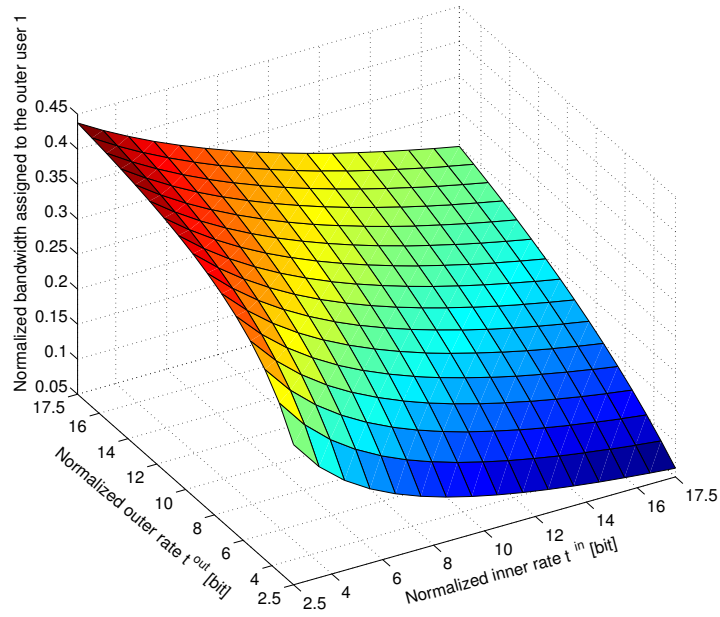


**Figure 6.4:** Assigned normalized bandwidth to the outer user 1 versus normalized inner and outer rates

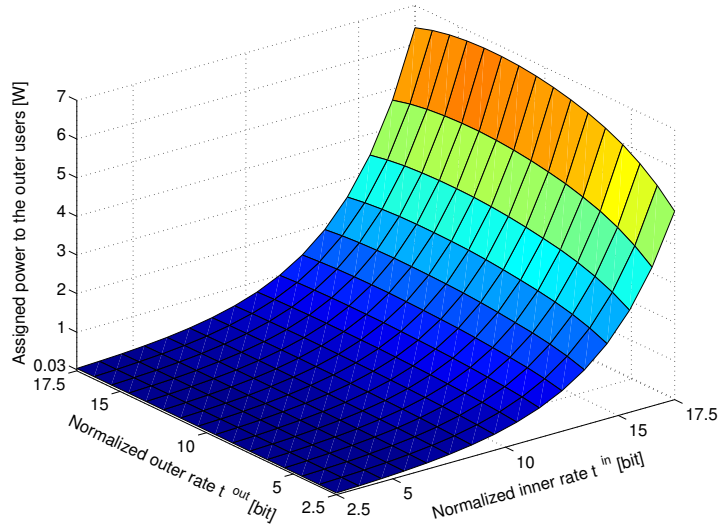


**Figure 6.5:** Assigned power to the outer users

Comparing the simulation results for the bandwidth and power assignment to the inner and the outer users, we conclude that optimization problem 6.2 offers a trade off between bandwidth allocation and power allocation to the inner and the outer users. Whenever the bandwidth allocation is decreased, the power allocation is increased in order to achieve a higher user rate than the minimum requirement rate.

Using Equation (5.1) we have simulated the transmission rates achieved by the Inner User 1 and the Inner User 2 shown in Figure 6.6 a) and Figure 6.6 b). The transmission rate achieved by the Inner User 2 is higher than transmission rate achieved by the Inner User 1, since the Inner User 2 is closer to the base station  $BS_0$ . Similarly, using Equation (5.2), we have calculated the achievable transmission rates from the Outer User 1 and the Outer User 2 shown in Figure 6.6 c) and Figure 6.6 d).

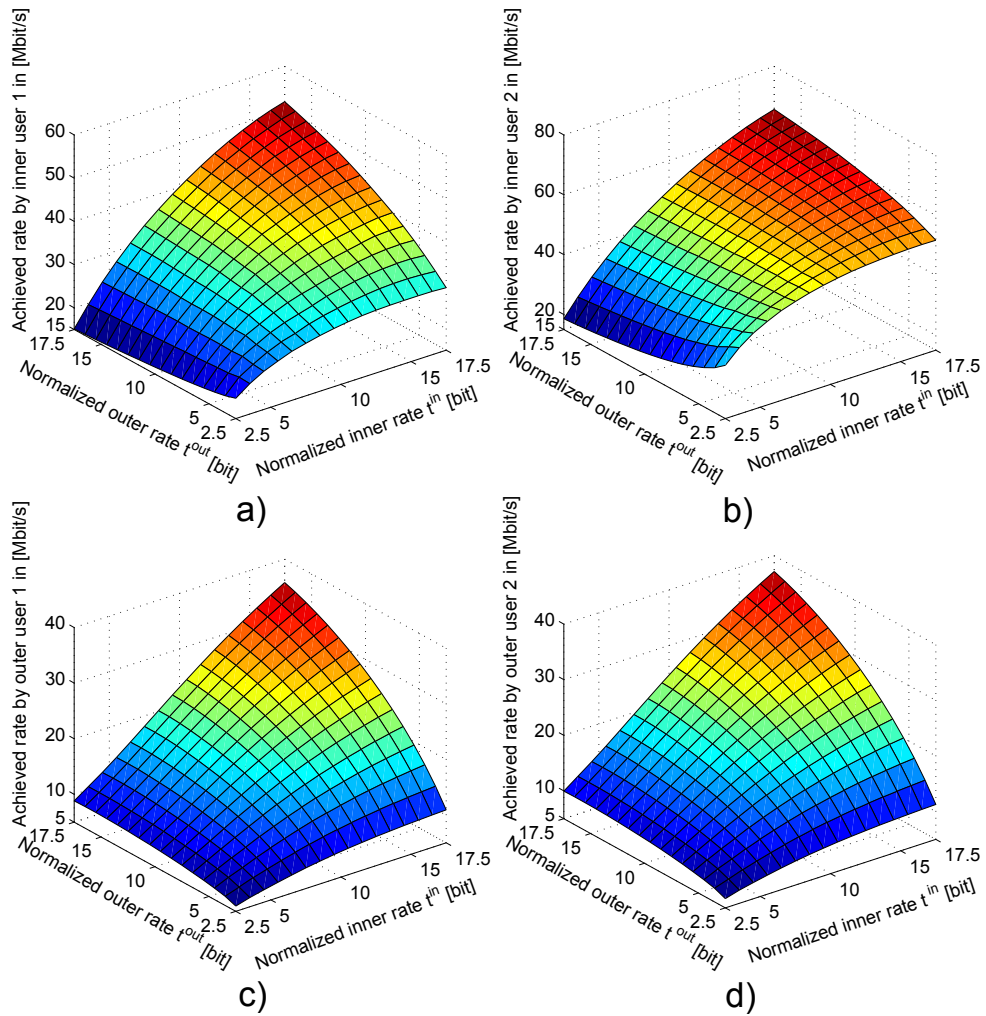


**Figure 6.6:** Transmission rate achieved by each user

Looking the achievable transmission rates for the Outer User 1 and Outer User 2, we

see that the Outer User 2 achieves higher transmission rate than Outer User 1, since it is in a closer distance to the base station  $BS_0$ . The most important result for the achievable transmission rates for the inner and the outer users shown in Figure 6.6 is that each inner user or outer user has achieved a rate higher than the minimum requirement for the inner or the outer user rate.

### 6.2.2 Efficient Algorithms for Bandwidth and Power Allocation Depending on Users Classification

In this subsection, we show the bandwidth and power allocation to the users depending on the users classification. To classify the users in which cell regions they belong, we use efficient algorithms. The algorithms are called efficient since they use the maximization of the minimum rate to efficiently allocate the power to the users. Within two cell regions, only three are the cases of use's classifications: multiple inner and multiple outer users, only inner users, only outer users. For each specific case we have formulated the algorithms which classifies the users and allocate the power and bandwidth to them.

#### Multiple users classified inner users and multiple users classified outer users

To distinguish for multiple inner and multiple outer users, we compare the users LSPLA with threshold  $G_{tgt}$  which can be any value between minimum and maximum over all LSPLA of users. If the users LSPLA is higher than threshold  $G_{tgt}$ , than those users are considered to be inner users, otherwise outer users. The classification of users as multiple inner and multiple outer users, and their bandwidth and power allocation are done by Algorithm 2.

---

**Algorithm 2** Bandwidth and Power Assignment for the Inner and the Outer Users

---

**Require:**  $G_{tgt} \in (\min(\mathbf{G}), \max(\mathbf{G})), (\mathbf{r}, \theta)$ .

---

```

1: if  $G > G_{tgt}$  then
2:    $(\mathbf{r}^{in}, \theta^{in}) \leftarrow (\mathbf{r}, \theta)$ 
3:    $\mathbf{G}^{in} \leftarrow G$ 
4: else
5:    $(\mathbf{r}^{in}, \theta^{in}) \leftarrow (\mathbf{r}, \theta)$ 
6:    $\mathbf{G}^{out} \leftarrow G$ 
7: end if
8: Calculate the values of:
    $p_0^{in}, p_k^{in}, p_0^{out}, p_k^{out}, B_n^{in}, B_m^{out}$ 
   using Equation (6.1).
```

---

In Algorithm 2, the vector  $\mathbf{G}$  denotes the vector elements of LSPLA,  $\mathbf{G}^{in}$  and  $\mathbf{G}^{out}$



denote the vector elements of LSPLA of the inner and the outer users, the  $(\mathbf{r}, \theta)$  denote the vector elements of polar coordinates of users. Similarly  $(\mathbf{r}^{\text{in}}, \theta^{\text{in}})$  denote the vector elements of polar coordinates for the inner users and  $(\mathbf{r}^{\text{out}}, \theta^{\text{out}})$  denote the vector elements of polar coordinates for the outer users. The polar coordinates are included in all algorithms since they present the locations of mobile users. Algorithm 2 requires the LSPLA threshold to be defined for any value between the minimum and the maximum over all LSPLA of users at the beginning. From the first to the sixth step, the Algorithm 2 classifies the users to the inner and the outer regions. At the eight step, it uses the maximization of the minimum rate given by Equation (6.2) to calculate the power and bandwidth allocation. The transmission rates of the inner users can be calculated using Equation (5.1) and for outer users similarly using Equation (5.2).

### All users classified as inner users

To distinguish only for inner users, we define the LSPLA threshold  $G_{\text{tgt}}$  to be smaller than all LSPLA of all users as it is shown in Algorithm 3.

---

#### **Algorithm 3** Bandwidth and Power Assignment for the Inner Users

---

**Require:**  $G_{\text{tgt}} < \min(\mathbf{G})$ .

---

- 1: **if**  $G > G_{\text{tgt}}$  **then**
  - 2:      $(\mathbf{r}^{\text{in}}, \theta^{\text{in}}) \leftarrow (\mathbf{r}, \theta)$
  - 3:      $\mathbf{G}^{\text{in}} \leftarrow G$
  - 4: **end if**
  - 5: *Calculate the values of:*  
 $p_0^{\text{in}}, p_k^{\text{in}}, B_n^{\text{in}}$   
using Equation (6.1).
- 

From the first to third step it compares all LSPLA of the users with the threshold  $G_{\text{tgt}}$  and classifies all users as inner users. In the last step runs the Equation (6.2) to calculate the power and bandwidth assignment to the inner users. The transmission rate of inner users are calculated using Equation (5.1).

### All users classified as outer users

To distinguish only for outer users, the LSPLA threshold  $G_{\text{tgt}}$  is defined to be greater than all LSPLA of users, as it is shown in Algorithm 4.

Similar to Algorithm 3, Algorithm 4 in the 1-3 step classifies all users as outer users by comparing the users LSPLA with threshold  $G_{\text{tgt}}$ . In the last step uses the maximization of the minimum rate given by Equation (6.2) to calculate the bandwidth and power assigned to the outer users. The transmission rates for the outer users are calculated using Equation (5.2).

**Algorithm 4** Bandwidth and Power Assignment for the Outer Users**Require:**  $G_{\text{tgt}} > \max(\mathbf{G})$ .

- 1: **if**  $G < G_{\text{tgt}}$  **then**
- 2:      $(\mathbf{r}^{\text{out}}, \theta^{\text{out}}) \leftarrow (\mathbf{r}, \theta)$
- 3:      $\mathbf{G}^{\text{out}} \leftarrow G$
- 4: **end if**
- 5: *Calculate the values of:*  
 $p_0^{\text{out}}, p_k^{\text{out}}, B_m^{\text{out}}$   
using Equation (6.1).

### Numerical Simulations: Efficient Algorithms for Bandwidth and Power Allocation Depending on Users Classification

In this subsection, we show the simulation results carried out using the efficient algorithms for classifying the users, and allocating the power and the bandwidth to the them. For simulation uniform distances between users are considered, such that users are distributed in a regular grid over the cell area. A realistic urban scenario is considered with its parameters shown in Table 6.2.

**Table 6.2:** Simulation parameters

parameters	value
Maximum base station power $P_c^{\text{max}}$	40 W
Maximum base station bandwidth $B_c^{\text{max}}$	20 MHz
Noise spectral density $N_0$	-174 dBm/Hz
Center frequency $f$	2.0 GHz
Path-loss exponent $\alpha$	3.75
Penetration loss $L_p$	20 dB
Shadowing $X_\sigma$	$\mathcal{N}(0, 8)$ dB
Small-scale fading $F$	$\chi_2^2$ dB,
Inter base station distance $d$	600 m
Minimum requirement inner user rate $t^{\text{in}}$	2.5 Mbit/s
Minimum requirement outer user rate $t^{\text{out}}$	2.5 Mbit/s
Number of active users within the cell	75

During simulations we have considered 100 realizations, where for each realizations all users have experienced different channels due to shadowing and small-scale fading. The efficiency of power allocation in terms of median values over those 100 realizations versus the percentage of the inner users classification  $N^{\text{in}} [\%]$  is shown in Figure 6.7. The percentage of the outer users classification is thereby equivalent to  $1 - N^{\text{in}} [\%]$ . Depending on how we classify the users comparing with LSPLA threshold  $G_{\text{tgt}}$ , we define a direct mapping of users classification to frequency reuse. Frequency reuse-1 is considered only

when the threshold  $G_{\text{tgt}}$  is chosen to be smaller than the minimum LSPLA for all users within the cell. This means 100 % of users are classified as inner users. In a such case the Algorithm 3 classifies the users and allocates the bandwidth and power to them. Similarly, we define the frequency reuse-3 when the threshold  $G_{\text{tgt}}$  is chosen to be larger than the maximum LSPLA over all users. In such case, we use the Algorithm 4 which classifies 100 % of users as outer users and allocated the bandwidth and power to them. All the other thresholds for  $G_{\text{tgt}}$  which are between the minimum and maximum of LSPLA threshold, we use to classify some users as the inner users and some users as outer users. We use the Algorithm 2 for inner and outer users classification and bandwidth and power allocation. From the simulation results shown in Figure 6.7, we see that the highest power is used from base station considering frequency reuse-1. The reason for such a high power consumption is that Algorithm 3 needs to adapt the base station power in order to serve all users classified as inner users such that users achieve rates higher than the minimum required rate. In this case the users which are located at the cell edge but classified as inner users are far from the base station hence, suffered from ICI and potentially with poor channels so they need more power. Decreasing the number of inner users classification results in the decrease of median transmit power until the classified number of inner users approach 55 %. From 55 % – 30 % of  $N^{\text{in}}/N^{\text{out}}$  there is only a small variation in median transmit power. This is the region when PFR is the most power efficient. Comparing the thresholds  $G_{\text{tgt}}$  used in this region with the mean over all LSPLA we have noticed that the threshold  $G_{\text{tgt}}$  is the same as the mean threshold. Our conclusion is that defining the threshold  $G_{\text{tgt}}$  as the mean over all LSPLA of users is a good metric for classifying the users as inner and outer users. By increasing the percentage of the outer users to more than 70 % (corresponding to the 30 % of the inner users), results in an increase of the median power as well. However, the median power used when 100 % of the users are classified as the outer users is smaller compared to the case when all users are classified as the inner users, because the users in frequency reuse-3 are interfered only by non-neighboring cells.

The uniform distribution of users within the cell and their LSPLA for one realization scenario is shown in Figure 6.8. From the simulation results shown in Figure 6.8 we see that the users experience different channels due to shadowing and small-scale fading. Some users at the cell edge have better LSPLA than some other users that are close to base stations. For the same realization in Figure 6.9 it is shown the users classification and their achieved transmission rates for the mean LSPLA of  $G_{\text{tgt}} = -110.27$  dB. For classifying the users and their power and bandwidth allocation we use the Algorithm 2. Using Algorithm 2 in this realization from 75 users uniformly distributed in cell  $S_{01}$ , 35 users are classified as inner users and 40 users are classified as outer users. From the total bandwidth allocated to cell  $S_{01}$  around 47 % is assigned to the inner users, while 53 % of bandwidth is assigned to the outer users. From the maximum possible base station power

$P_c^{\max}$ , only  $p_0^{\text{in}} = 5.04 \text{ W}$  is assigned to the inner users and  $p_0^{\text{out}} = 9.12 \text{ W}$  is assigned to the users in the outer region.

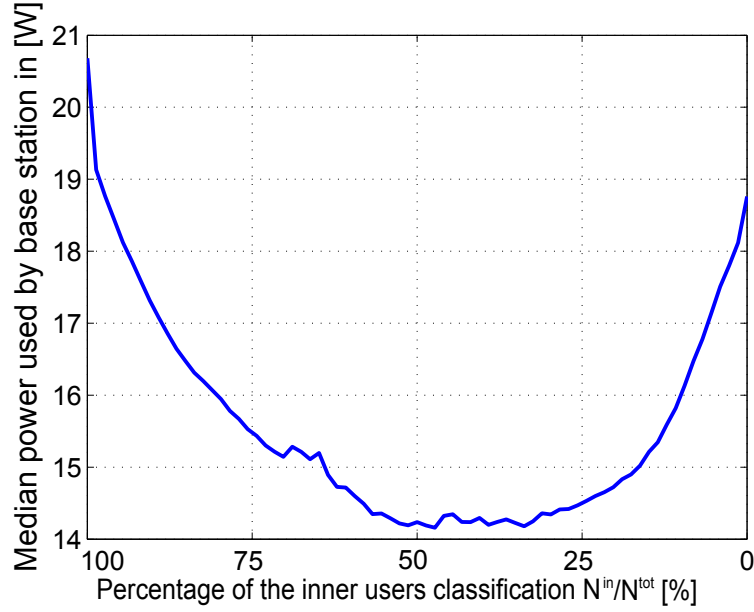


Figure 6.7: Power efficiency depending on users classification

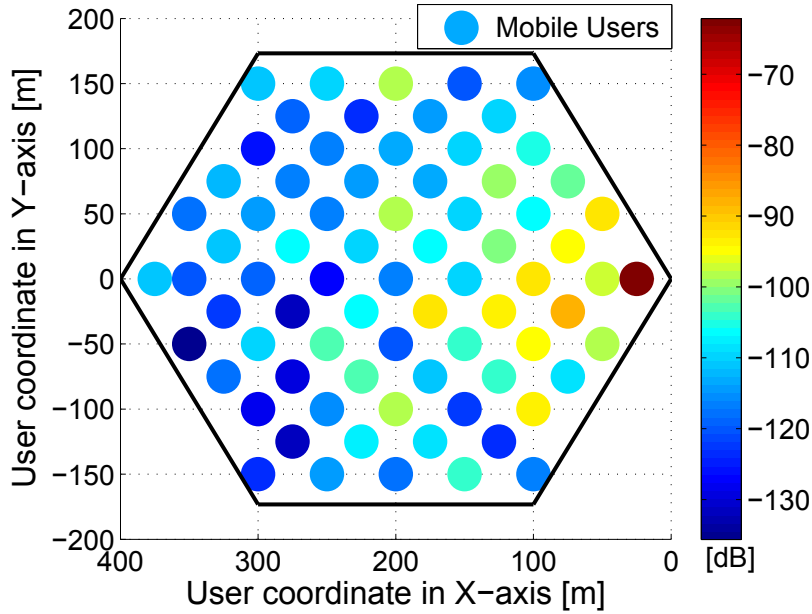
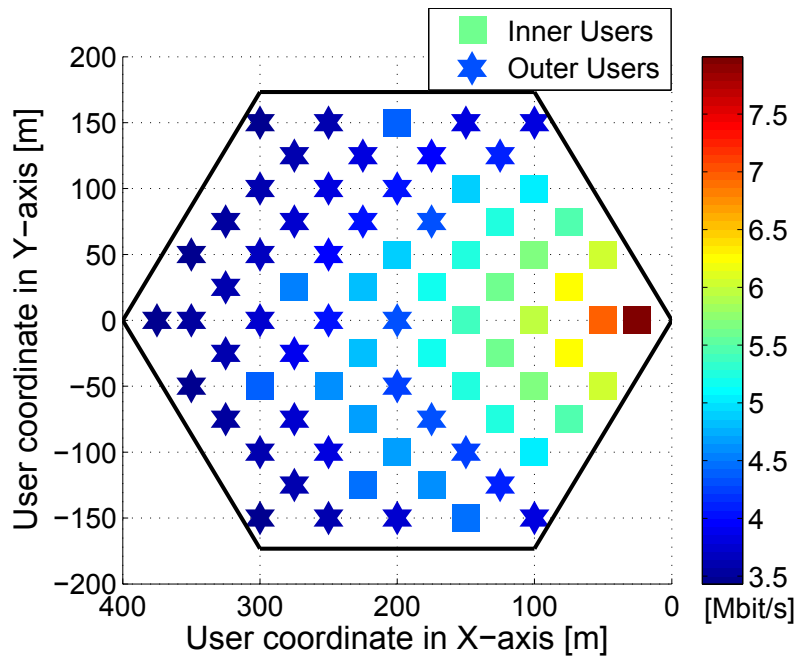


Figure 6.8: Large-scale path-loss attenuations for uniform users distribution



**Figure 6.9:** Individual users rate for large-scale path-loss attenuation mean threshold  $G_{\text{tgt}} = -110.27$  dB

### 6.3 Bandwidth Re-allocation Scheme

For cellular network planners it is more convenient to place the base station in the locations where more coverage can be offered to serve more users. In flat terrains with high density of mobile users, the base station are located in the places where more users are concentrated. Due to non-uniform distribution of users over the cell area sometimes more users are concentrated near the base stations than in the cell edge or the cell edge users are idle. So re-allocating the bandwidth reserved for the outer users to the inner users would improve the transmission rate for cell center users. A detailed study about the outer bandwidth re-allocation for improving the cell capacity density, we have shown in Section 4.3. In this section, we consider the outer bandwidth re-allocation for improving the achievable rates of the inner users. The scheme for bandwidth re-allocation is shown in Figure 6.10.

Similar to the bandwidth re-allocation investigated in Section 4.2, here we use the parameter  $t$  to account for the outer bandwidth re-allocation. As it is shown in Figure 6.10, the parameter  $t$  represents the percentage of the outer bandwidth allocated to the inner user and its values are situated within the interval  $[0,1)$ .

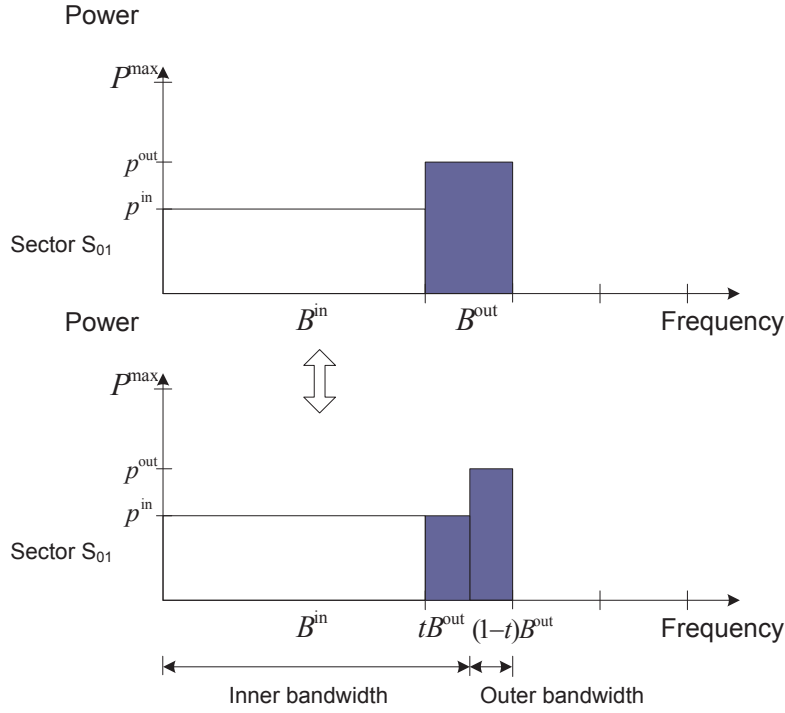


**Figure 6.10:** Bandwidth re-allocation scheme for sector  $S_{01}$

### 6.3.1 Power Allocation and Bandwidth Re-Allocation Depending on Distance from Base Station

In this section, we show the power allocation and bandwidth re-allocation by classifying users based on distance threshold. For power allocation, we use the analytical expressions for optimal power allocation derived in Section 5.4, and we apply the frequency re-use pattern shown in Figure 5.4 together with cell cluster model shown in Figure 5.1. Comparing the users distance from the base station with the pre-defined distance threshold yields three cases of users classification: one user located in the inner region and one user located in the outer region, both users located in the inner region or both users located in the outer region.

#### One user located in the inner cell region and one user located in the outer cell region

Comparing the users distances with the distance threshold one user is classified as the inner user and one user is classified as the outer user. The bandwidth assignment to users is done by using the frequency reuse pattern shown for sector  $S_{01}$  in Figure. 6.11. The optimal power assignment to the inner user is calculated by using Equation (5.12) and for the outer user by Equation (5.13). The transmission rate achieved by the inner user

is calculated by Equation (5.1), while the transmission rate achieved by the outer user is calculated by Equation (5.2).

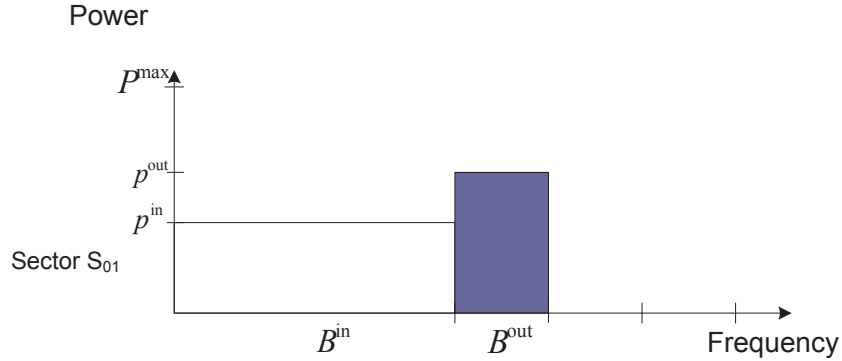


**Figure 6.11:** Frequency reuse pattern for sector  $S_{01}$

### Both users are located in the inner cell region

If both users are classified as inner users because their distances from serving base station are smaller than distance threshold, they have to share the inner bandwidth. All the available bandwidth for the inner region is assigned to both inner users such that each user gets half of the inner bandwidth. The transmission rate for inner User 1 is given as follows

$$R_1^{\text{in}} = \frac{B^{\text{in}}}{2} \log_2 \left( 1 + \frac{G_{01}^{\text{in}} P^{\text{max}}}{N_0 \frac{B^{\text{in}}}{2} + \sum_{k=1}^6 G_{k1}^{\text{in}} P^{\text{max}}} \right) \quad (6.3)$$

and the transmission rate of the inner User 2 is given as in the following

$$R_2^{\text{in}} = \frac{B^{\text{in}}}{2} \log_2 \left( 1 + \frac{G_{02}^{\text{in}} P^{\text{max}}}{N_0 \frac{B^{\text{in}}}{2} + \sum_{k=1}^6 G_{k2}^{\text{in}} P^{\text{max}}} \right) \quad (6.4)$$

From the cell cluster model it is clear that the outer bandwidth is less interfered than the inner bandwidth because it is interfered only by non-neighboring sectors. Therefore, we re-allocate that bandwidth to the inner users. The way of re-allocating the outer bandwidth and using it as inner bandwidth is shown in Figure 6.10. Changing parameter  $t$ , we know how much of the outer bandwidth is re-allocated to the inner users. To account for the bandwidth re-allocation, we modify Equation (6.3) for the inner User 1 as follows:

$$R_1^{\text{in}} = \frac{B^{\text{in}}}{2} \log_2 \left( 1 + \frac{G_{01}^{\text{in}} P^{\text{max}}}{N_0 \frac{B^{\text{in}}}{2} + \sum_{k=1}^6 G_{k1}^{\text{in}} P^{\text{max}}} \right) + t \frac{B^{\text{out}}}{2} \log_2 \left( 1 + \frac{G_{01}^{\text{out}} P^{\text{max}}}{N_0 t \frac{B^{\text{out}}}{2} + \sum_{k=1}^6 G_{k1}^{\text{out}} P^{\text{max}}} \right) \quad (6.5)$$

Equation (6.4) for the rate of the inner User 2 is modified accordingly:

$$R_2^{\text{in}} = \frac{B^{\text{in}}}{2} \log_2 \left( 1 + \frac{G_{02}^{\text{in}} P^{\text{max}}}{N_0 \frac{B^{\text{in}}}{2} + \sum_{k=1}^6 G_{k2}^{\text{in}} P^{\text{max}}} \right) + t \frac{B^{\text{out}}}{2} \log_2 \left( 1 + \frac{G_{02}^{\text{out}} P^{\text{max}}}{N_0 t \frac{B^{\text{out}}}{2} + \sum_{k=1}^6 G_{k2}^{\text{in}} P^{\text{max}}} \right) \quad (6.6)$$

### Both users located in the outer cell region

If both users are classified as outer users because their distances from the serving base station are larger than distance threshold, they have to share the outer bandwidth from the sector to which they belong. In this case, the inner bandwidth is not used due to the possibility of experiencing high interference at the cell edge. So the transmission rate of the first outer user is given by following equation

$$R_1^{\text{out}} = \frac{B^{\text{out}}}{2} \log_2 \left( 1 + \frac{G_{01}^{\text{out}} P^{\text{max}}}{N_0 \frac{B^{\text{out}}}{2} + \sum_{k=1}^6 G_{k1}^{\text{out}} P^{\text{max}}} \right) \quad (6.7)$$

The Equation for the transmission rate of the outer User 2 is defined as in the following

$$R_2^{\text{out}} = \frac{B^{\text{out}}}{2} \log_2 \left( 1 + \frac{G_{02}^{\text{out}} P^{\text{max}}}{N_0 \frac{B^{\text{out}}}{2} + \sum_{k=1}^6 G_{k2}^{\text{out}} P^{\text{max}}} \right) \quad (6.8)$$

In this case the outer users are very limited in bandwidth resources due to fixed bandwidth allocation scheme.

### Numerical Simulations: Power allocation and bandwidth re-allocation depending on distance from base station

In this section we consider uniform realization of users positions. A realistic urban scenario is considered with its parameters shown in Table 6.3.

**Table 6.3:** Simulation parameters

parameters	value
Maximum base station power $P^{\text{max}}$	5 W
Maximum base station bandwidth $B^{\text{max}}$	20 MHz
Noise spectral density $N_0$	-174 dBm/Hz
Center frequency $f$	2.0 GHz
Pathloss exponent $\alpha$	3.75
Penetration loss $L_p$	20 dB
Shadowing $X_\sigma$	$\mathcal{N}(0, 8)$ dB
Small-scale Fading $F$	$\chi_2^2$ dB,
Inter base station distance $d$	700 m
Number of user positions	100



Using the simulation parameters shown in Table 6.3 and solution for optimal power allocation taken out from optimization problem (5.5), we have shown the simulation results for two users in Figure 6.12 in terms of maximum average sum-rate depending on users random locations. We used the bandwidth reallocation scheme presented in Figure 6.10 depending on the user positions. For each specific realization of user positions we have simulated 1000 channel realizations. For the specific simulation setup considered, the case that both users are located in the inner region occurs with a probability of 59%. The case when one user is located in the inner region and the other one located in the outer region occurs with a probability of 35%. The last case when both users are located in the outer region occurs with a probability of 6%.

From the simulation results shown in Figure 6.12 we see that the highest performance is achieved when we consider the bandwidth re-allocation to the inner users. The lowest performance is achieved when both users are located in the outer region since they are located far from base stations, and they have to share a smaller portion of bandwidth compared with the inner users. Without considering the re-allocation of the outer bandwidth to the inner users, the best performance is achieved by optimal power assignment when one user is located in the inner region and one user is located in the outer region.

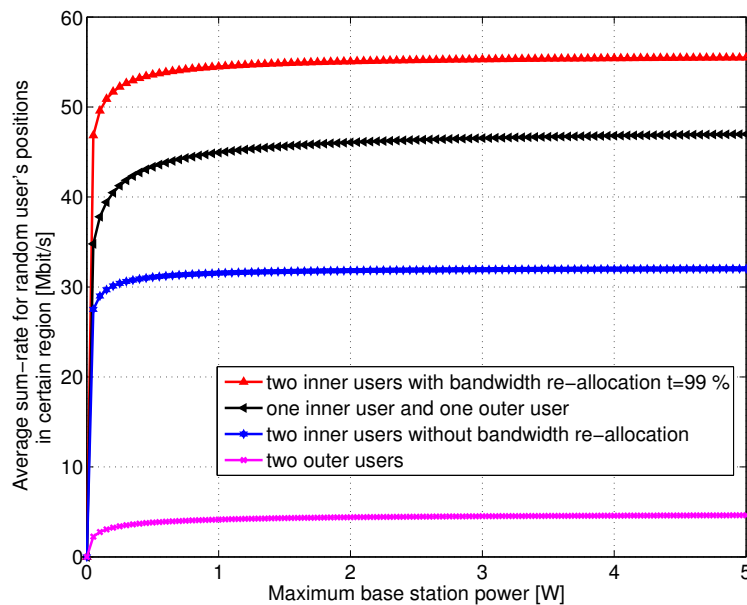


**Figure 6.12:** Maximum sum-rate for random users positions

In Figure 6.13 we show the simulation results for average sum-rate taken over random users positions in the inner and outer regions. The lower curve represents the average of all sum-rates when no re-allocation of the outer bandwidth to the inner users is carried out. A better performance in terms of average sum-rate is achieved when we consider the

re-allocation of the outer bandwidth to the inner user. This is shown by the upper curve in Figure 6.13. A performance increase of approximately 34% is achieved.

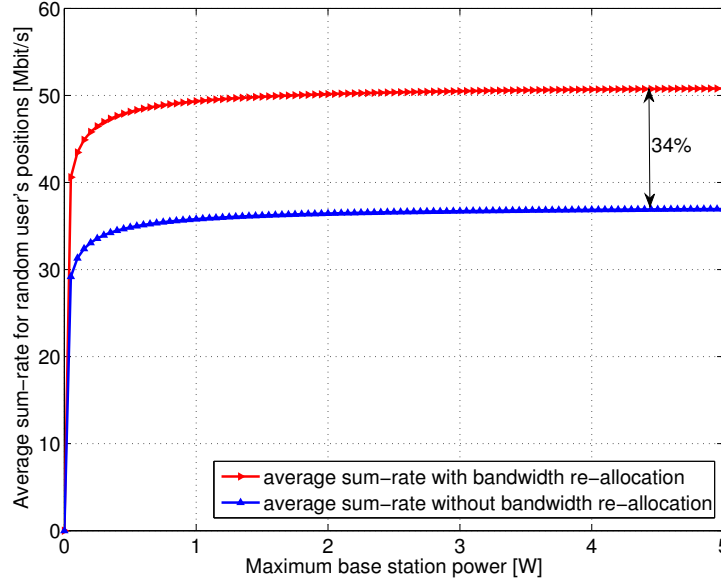


**Figure 6.13:** Maximum average sum-rate for random users positions

### 6.3.2 Power Allocation and Bandwidth Re-allocation Depending on Large-scale Path-loss Attenuations

In this subsection, differently from Subsection 6.3.1, we show the power allocation and the bandwidth re-allocation depending on mean LSPLA threshold. By comparing the LSPLA of the users with the mean LSPLA threshold denoted by  $G_{\text{tgt}}$ , for two users located in one cell, we have three cases of classifying the users. Based on the users classification, we allocate the bandwidth and power to them.

**One user located in the inner cell region and one user located in the outer cell region**

If the users LSPLA is higher than  $G_{\text{tgt}}$ , then that user is considered to be an inner user, otherwise an outer user. While during comparing the users LSPLA with  $G_{\text{tgt}}$  threshold we find that one user is classified to be the inner user and the other user to be the outer user, in a such case the amount of bandwidth assigned to them is based on the frequency reuse pattern shown for sector  $S_{01}$  in Figure 6.11. The optimal power assignment to the inner is calculated using the analytical expression given by Equation (5.12). Similarly, we calculate the power allocation to the outer user using Equation (5.13). The transmission

rate achieved by the inner user, we calculate by using Equation (5.1), and the transmission rate achieved by the outer user by Equation (5.2)

### Both users are located in the inner cell region

If the LSPLA of both considered users are higher than  $G_{\text{tgt}}$ , in such case both users are considered to be the inner users. Since, we have classified only inner users, they have to share the inner bandwidth. The maximum base station power is assigned to both inner users. The transmission rate for User 1 is calculated using Equation (6.3) and similarly we calculate the transmission rate for the inner User 2 using Equation (6.4). The LSPLA of direct channels  $G_{01}^{\text{in}}$ ,  $G_{02}^{\text{in}}$  are defined by Equation (5.3). The LSPLA of the interference channels  $G_{k1}^{\text{in}}$ ,  $G_{k2}^{\text{in}}$  are defined also by Equation (5.3) with  $F = 0\text{dB}$ . As we have mentioned previously the outer bandwidth is less interfered than the inner bandwidth since it is interfered only by non-neighboring sectors. We therefore re-allocate the outer bandwidth to the inner users. The way of re-allocating the outer bandwidth and using it as inner bandwidth is shown in the bandwidth re-allocation by Figure 6.10. To account for the bandwidth re-allocation while calculating the transmission rate of the inner User 1, we use Equation (6.3). Similarly to the inner User 1, we use Equation (6.4) to account for the bandwidth re-allocation during calculating the transmission rate.

### Both users located in the outer cell region

Both users are considered as outer users if their LSPLA is lower than threshold  $G_{\text{tgt}}$ . In this case, the inner bandwidth is not used at all due to the increase of ICI, since such bandwidth experiences high interference at the cell edge. After we have only outer users, the outer bandwidth is shared among them while the whole base station transmit power is assigned to them. The LSPLA of direct channels  $G_{01}^{\text{out}}$ ,  $G_{02}^{\text{out}}$  are defined by Equation (5.3). The LSPLA of interference channels  $G_{k1}^{\text{out}}$ ,  $G_{k2}^{\text{out}}$  are defined also by Equation (5.3). The transmission rate of the outer User 1 is calculated using Equation (6.7) and similarly the transmission rate for the outer User 2 is calculated using Equation (6.8).

### Numerical Simulations: Power allocation and bandwidth re-allocation depending on LSPLA

In this simulation we consider uniform users positions. A realistic urban scenario is considered with its parameters shown in Table 6.4. The LSPLA results for two users depending on the distance of each user to the base station are shown in Figure 6.14. To show the values of LSPLA depending on the random distances of users from the base station, we used the Equation (5.3) and the simulation parameters shown in Table 6.4. For simulation setup, we have considered 100 uniform user positions, where per each position users have experienced different channels. For each specific channel realization of random user

positions, we have compared the LSPLA of users with the mean threshold  $G_{\text{tgt}}$ , and based on that we have decided for users power allocation and bandwidth allocation. During simulations we have noticed that the case that both users are located in the inner region occurs with a probability of 16 %. The case when one user is located in the inner region and the other one located in the outer region occurs with a probability of 48 %. The last case when both users are located in the outer region occurs with a probability of 36 %. From the simulation results shown in Figure 6.14 we see that because of small-scale fading and shadowing, sometimes the user which is located far from the base station has a better LSPLA (better channel) than a user which is located near the base station. By classifying the users as inner user and outer user depending on the LSPLA threshold, we are able to assign the power and bandwidth resources in the optimal way, increase the sum-rate gain and decrease the inter-cell interference.

**Table 6.4:** Simulation parameters

parameters	value
Maximum base station power $P^{\max}$	5 W
Maximum base station bandwidth $B^{\max}$	20 MHz
Noise spectral density $N_0$	-174 dBm/Hz
Center frequency $f$	2.0 GHz
Pathloss exponent $\alpha$	3.75
Penetration loss $L_p$	20 dB
Shadowing $X_\sigma$	$\mathcal{N}(0, 8)$ dB
Small-scale Fading $F$	$\chi_2^2$ dB,
Inter base station distance $d$	700 m
Maximum cell range $r$	$(2/3)d$ m
Large-scale path-loss threshold $G_{\text{tgt}}$	-106.4 dB,
Number of channel realizations	100
Number of uniform users positions	100

In Figure 6.15, the sum-rate gain for dynamic method (classification of users is based on distance threshold) compared with a static method (classification of users is based on LSPLA threshold) is shown. For our simulation setup the static method defines a user as inner user if its distance from its serving base station is in the range  $0 < r_0^{\text{in}} \leq 0.70 \cdot r$ . Analogously an outer user has a distance in the range  $0.70 \cdot r < r_0^{\text{out}} \leq r$ . Looking at the simulation results shown in Figure 6.15, one can see that in some cases the dynamic method outperforms the static method (the sum-rate gain is positive), while in some cases both methods perform similar (the sum-rate gain is zero). This happens because the dynamic method classifies a user with bad channel to be as outer user such that experience less ICI, while the static method, for the same user with the same channel classifies as inner user because the distance criteria. In this case the user classification by

static method experience higher ICI. In all other cases when those methods perform the same, means that they have done the same user classification. For all distance thresholds from  $0.70 \cdot r$  to  $r$ , the dynamic method outperforms the static method at all positions.

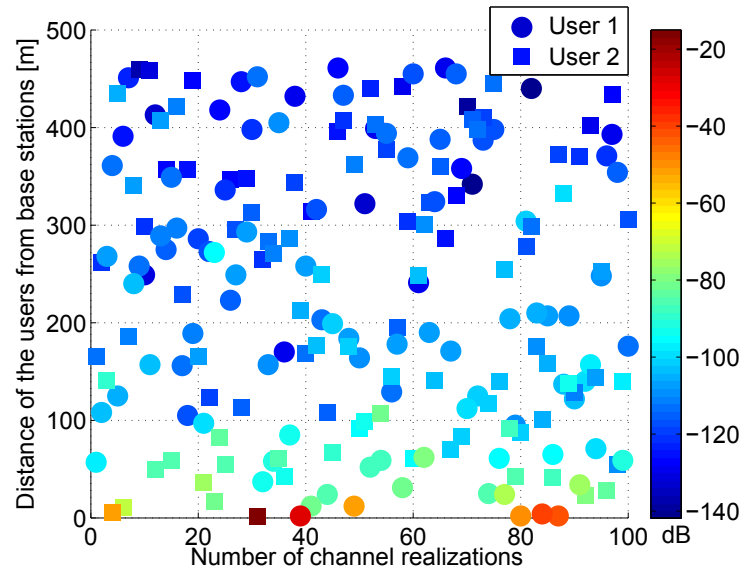


**Figure 6.14:** Large-scale path-loss attenuations for uniform users positions

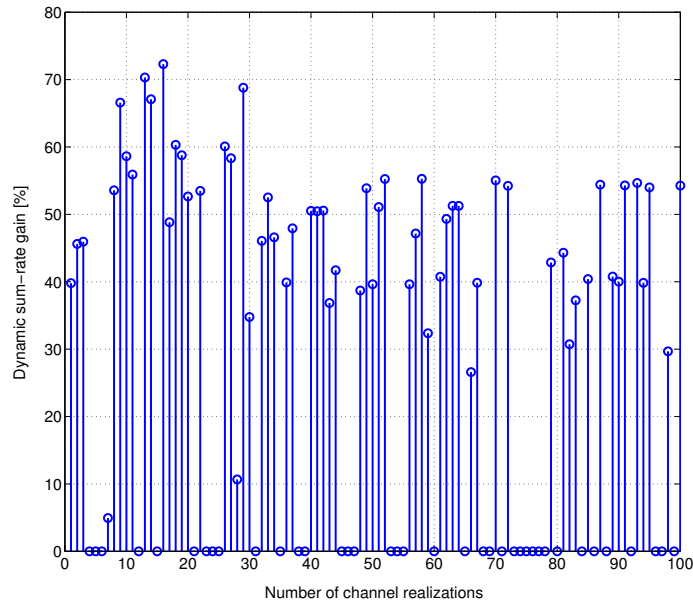


**Figure 6.15:** Sum-rate gain for dynamic method compared with static method

In Figure 6.16, the simulation results for average sum-rate taken over uniform users positions in the inner and outer regions versus maximum base station power are shown. The lower curve represents the average of all sum-rates when no re-allocation of the outer bandwidth to the inner users is carried out for the static method used. A better performance in terms of average sum-rate is achieved by the dynamic method. It is shown by simulation results that a performance increase of approximately 16.4 Mbit/s is achieved by deploying the dynamic method. Considering also outer bandwidth re-allocation to the inner users a performance increase of 3.1 Mbit/s of the dynamic method compared to the static method is achieved.

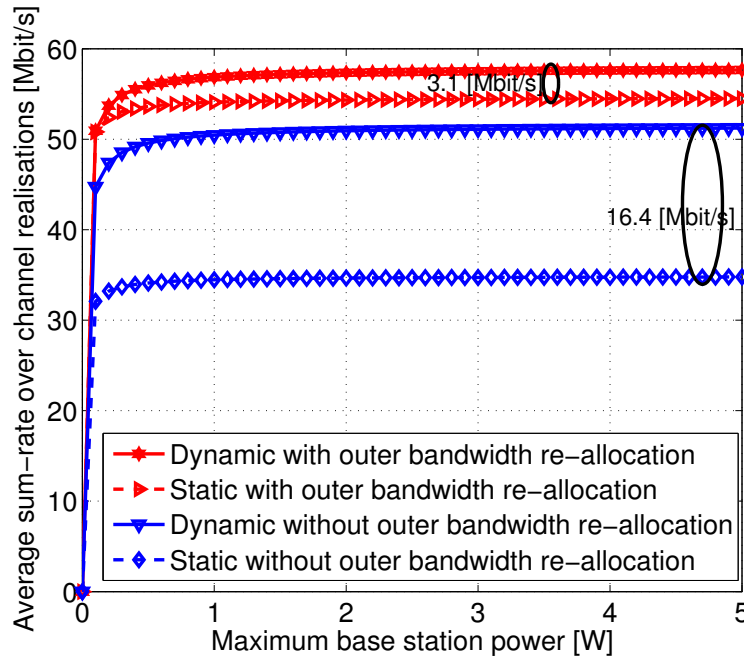


Figure 6.16: Maximum average sum-rate for uniform users positions

## 6.4 Power Allocation and Bandwidth Adaptation Algorithms

In this Section, we consider two optimization algorithms which are formulated for PFR: the optimal power and adaptive bandwidth allocation, and the efficient power and adaptive bandwidth allocation. The optimal power and adaptive bandwidth allocation algorithm works in the principle of allocating the bandwidth to the users based on their classification by the mean LSPLA threshold, while the power is allocated optimally in the cell regions. The efficient power and adaptive bandwidth allocation algorithm works in the same principle for power allocation as previous algorithm, while the power is allocated to the cell regions efficiently.

### 6.4.1 Optimal power and adaptive bandwidth allocation depending on mean LSPLA

In this subsection an optimal power and adaptive bandwidth allocation algorithm for PFR cellular networks is formulated as shown by Algorithm 5. In Subsection 6.2.2, we found that classifying the users to the respective inner and outer cell regions by using the mean LSPLA threshold gives the best performance in terms of sum-rate gain. Algorithm 5, firstly defines the LSPLA threshold  $G_{\text{tgt}}$  as the mean over all LSPLA of all users within a cell. In the next steps, it compares the LSPLA of users with mean threshold  $G_{\text{tgt}}$ , and classifies the users as the inner users and the outer users within considered cell. From the numerical simulations results in Section 6.2.1 for bandwidth allocation, we found that under the constrained of equal minimum required rate, the same amount of bandwidth is allocated to each user. Using that result for bandwidth allocation under the assumption that the minimum required received SINR is equal for all users, we adapt the bandwidth allocation to the inner region and the outer region based on the number of the inner and the outer users classified as shown by Algorithm 5. After the bandwidth adaptation, the last step in Algorithm 5 is to calculate the optimal power allocation to inner and outer cell regions.

---

**Algorithm 5** Optimal Power and Adaptive Bandwidth Algorithm

---

**Require:**  $G_{\text{tgt}} = \bar{G}$ ,  $(\mathbf{r}, \theta)$ ,  $\beta^{\text{in}} = 1/N_c$ ,  $\beta^{\text{out}} = 1/N_c$

- 1: **if**  $G > G_{\text{tgt}}$  **then**
  - 2:      $(\mathbf{r}^{\text{in}}, \theta^{\text{in}}) \leftarrow (\mathbf{r}, \theta)$
  - 3:      $\mathbf{G}^{\text{in}} \leftarrow G$
  - 4:      $N^{\text{in}} \leftarrow N^{\text{in}} + 1$
  - 5: **else**
  - 6:      $(\mathbf{r}^{\text{in}}, \theta^{\text{in}}) \leftarrow (\mathbf{r}, \theta)$
  - 7:      $\mathbf{G}^{\text{out}} \leftarrow G$
  - 8:      $M^{\text{out}} \leftarrow M^{\text{out}} + 1$
  - 9: **end if**
  - 10:  $\beta_{\text{tot}}^{\text{in}} = \beta^{\text{in}} \cdot N^{\text{in}}$ ,  $\beta_{\text{tot}}^{\text{out}} = \beta^{\text{out}} \cdot M^{\text{out}}$
  - 11: **Calculate the values of:**  
 $p_0^{\text{in}}, p_k^{\text{in}}, p_0^{\text{out}}, p_k^{\text{out}}$ ,  
using Equation (6.9).
- 

The optimal power allocation is calculated using the maximization of the minimum

SINR formulated by Equation (6.9) under sum-power constraints.

$$\underset{\beta_{cn}^{\text{in}}, \beta_{cm}^{\text{out}} \in \mathcal{R}_+, \mathbf{p} \succeq \mathbf{0}}{\text{maximize}} \quad \min\{\text{SINR}_{c1}^{\text{in}}, \dots, \text{SINR}_{cN^{\text{in}}}^{\text{in}}, \text{SINR}_{c1}^{\text{out}}, \dots, \text{SINR}_{cM^{\text{out}}}^{\text{out}}\} \quad (6.9a)$$

subject to

$$p_c^{\text{in}} + p_c^{\text{out}} \leq P_c^{\text{max}}, \quad \forall c \in \mathcal{C}, \quad (6.9b)$$

The bandwidth adaptation carried out by Algorithm 5 has result in a simplified optimization problem given by Equation (6.9), since it contains only the sum-power constraints (6.9b). The maximization of the minimum SINR formulated by Equation (6.9) is a GGP optimization problem that maximizes the minimum SINR constrained by optimal power allocation in PFR. Finding the direct solution is not easy due to formulation of the problem in GGP form. Similarly to the previous problems in GGP form, without making any assumption on high-SINR approximation [14], we convert the formulated optimization problem (6.9) into a GP optimization problem and solve it efficiently using CVX. The SINR in the general form for user  $s$  within cell  $c$  is given by the following equation:

$$\text{SINR}_{cs}^I = \frac{p_c^I}{n_s^{\text{in}} \beta_{cs}^{\text{in}} + \sum_{k \in \mathcal{C} \setminus c} g_{ks}^{\text{in}} p_k^{\text{in}}}. \quad (6.10)$$

In Equation (6.10), the superscript  $I \in \{\text{in}, \text{out}\}$  denotes the superscript for the inner users or superscript for the outer users. Further, the subscript  $s \in \{n, m\}$  denotes the indexes for inner user  $n$  or the outer user  $m$ .

**Proposition 4.** *The maximization of the minimum SINR formulated by Equation (6.9) can be transformed into GP optimization problem.*

*Proof.* Similarly to the transformation of the maximization of the minimum rate shown in Subsection 6.2.1, by introducing the auxiliary variable  $z$  such that received SINRs by users is lower bounded by  $z$ , the functions in the objective are converted into SINR constraints. Since the left side of those constraints are not posynomials, the inversion of nominator with the denominator in both sides of the SINR constraints is used to convert them into posynomials. The power constraint remains the same since they are posynomials. So the



maximization of the minimum SINR in GP form is shown by Equation (6.11).

$$\underset{\mathbf{p} \succeq \mathbf{0}, \beta_{cn}^{\text{in}}, \beta_{cm}^{\text{out}}, z \in \mathcal{R}_+}{\text{minimize}} \quad \frac{1}{z} \quad (6.11a)$$

subject to

$$\frac{n_1^{\text{in}} \beta_{c1}^{\text{in}} + \sum_{k \in \mathcal{C} \setminus c} g_{k1}^{\text{in}} p_k^{\text{in}}}{p_c^{\text{in}}} \geq \frac{1}{z}, \quad \forall c \in \mathcal{C}, \quad (6.11b)$$

$$\vdots$$

$$\frac{n_{N^{\text{in}}}^{\text{in}} \beta_{cN^{\text{in}}}^{\text{in}} + \sum_{k \in \mathcal{C} \setminus c} g_{kN^{\text{in}}}^{\text{in}} p_k^{\text{in}}}{p_c^{\text{in}}} \geq \frac{1}{z}, \quad \forall c \in \mathcal{C}, \quad (6.11c)$$

$$\frac{n_1^{\text{out}} \beta_{c1}^{\text{out}} + \sum_{k \in \mathcal{C} \setminus c} g_{k1}^{\text{out}} p_k^{\text{out}}}{p_c^{\text{out}}} \geq \frac{1}{z}, \quad \forall c \in \mathcal{C}, \quad (6.11d)$$

$$\vdots$$

$$\frac{n_{M^{\text{out}}}^{\text{out}} \beta_{cM^{\text{out}}}^{\text{out}} + \sum_{k \in \mathcal{C} \setminus c} g_{kM^{\text{out}}}^{\text{out}} p_k^{\text{out}}}{p_c^{\text{out}}} \geq \frac{1}{z}, \quad \forall c \in \mathcal{C}, \quad (6.11e)$$

$$p_c^{\text{in}} + p_c^{\text{out}} \leq P_c^{\text{max}}, \quad \forall c \in \mathcal{C}, \quad (6.11f)$$

□

The objective in optimization problem (6.11) is a monomial and the constraints (6.11b)-(6.11f) are posynomials.

### Numerical Simulations: Optimal power and adaptive bandwidth allocation

In this section are shown the simulation results for optimal power and adaptive bandwidth allocation using the Algorithm 5. The simulation parameters are shown in Table 6.5.

**Table 6.5:** Simulation parameters

parameters	value
Maximum base station power $P_c^{\text{max}}$	5 W
Maximum base station bandwidth $B_c^{\text{max}}$	20 MHz
Noise spectral density $N_0$	-174 dBm/Hz
Center frequency $f$	2.0 GHz
Path-loss exponent $\alpha$	3.75
Penetration loss $L_p$	20 dB
Shadowing $X_\sigma$	$\mathcal{N}(0, 8)$ dB
Small-scale fading $F$	$\chi_2^2$ dB,
Inter base station distance $d$	600 m
Maximum cell range $r$	$(2/3)d$ m
Number of active users within the cell	75

The main reason for using the optimal power and adaptive bandwidth allocation algorithm is to show the optimality in power allocation during different channel realization.

In the following we show the power allocation to the inner users and to the outer users only for the first 10 realizations. The optimal power allocation to the inner users for the first 10 realization versus the maximum base station power is shown in Figure 6.17. From the simulation results shown in Figure 6.17 one can see that at the first realization most of the maximum transmit base station power  $P^{\max} = 5\text{ W}$  is allocated to the inner users. To understand the reason for such a power allocation, in the following we show the simulation results for the LSPLA and the achievable rate. The LSPLA during realization 1 for the users located uniformly over the distance within cell area is shown in Figure 6.18. Using the mean LSPLA as threshold  $G_{\text{tgt}} = -108.96$  for realization 1, Algorithm 5 has classified around 33 users as inner users and around 42 users as outer users. The user classification and their achievable rates for the maximum base station power  $P_{\max} = 5\text{ W}$  is shown in Figure 6.19. In the simulation results, shown in Figure 6.19 it can be observed that each inner and the outer user has achieved a rate higher than 2.5 Mbit/s.

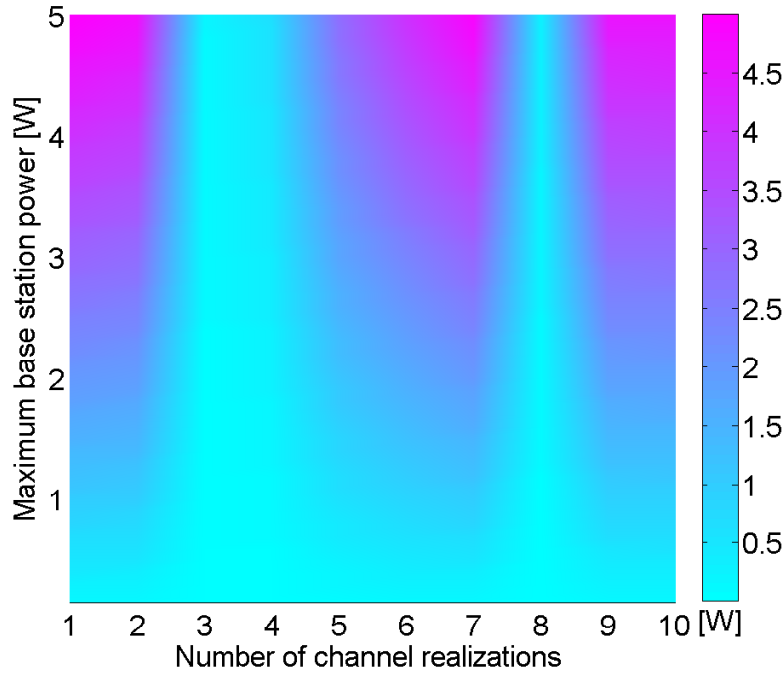


**Figure 6.17:** Optimal power allocation to the inner users

For the same realization of 10 channels, Figure 6.20 shows the optimal power allocation to the outer users. Analyzing the simulation results presented in Figure 6.20 one can see that from the first 10 realizations in the realization 3 most of the transmit base station power  $P_{max} = 5W$  is allocated to the outer users. To see the effects of such power allocation for realization 3, we analyze the LSPLA and the achievable rate for the realization 3. The LSPLA of users for realization 3 is shown in Figure 6.21. Using the mean LSPLA threshold  $G_{tgt} = -110.70$  dB for the maximum base station transmit power  $P_{max} = 5W$ , Figure 6.22 shows the user classification as the inner and the outer users and their achievable rates. From the simulation results shown in Figure 6.22 it has been found that around 31 users are classified as inner users and around 44 users are classified as outer users. Even most of the power has been allocated to the outer users for realization 3, still each inner and outer user has achieved a rate higher than  $2.5$  Mbit/s.

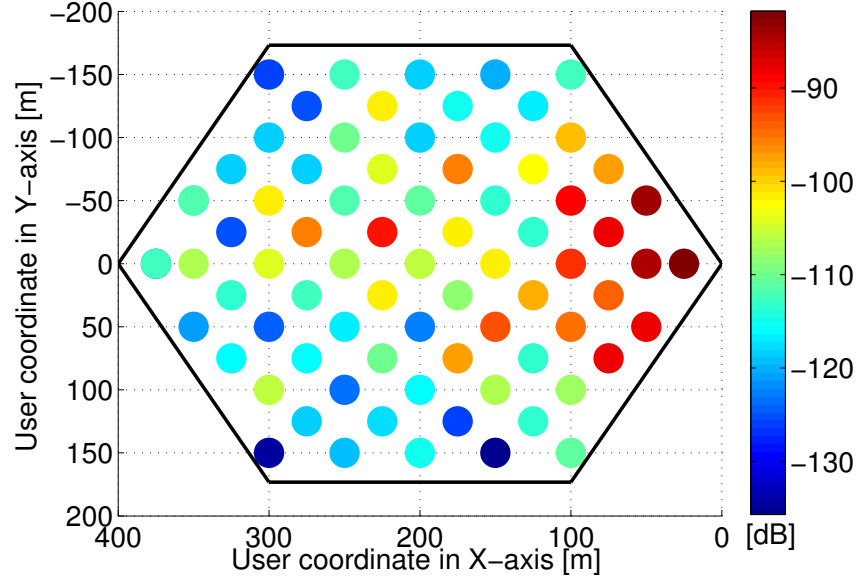


**Figure 6.18:** Large-scale path-loss attenuations for the realization 1

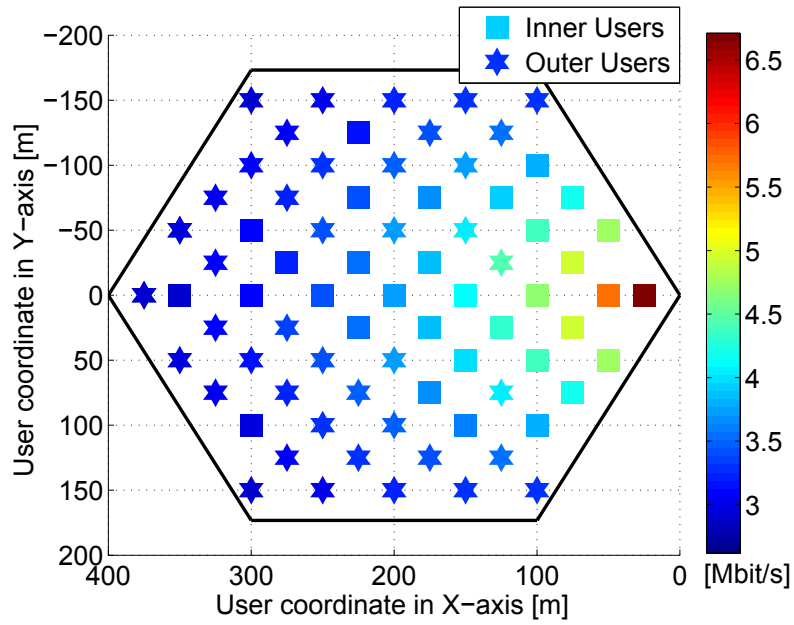


**Figure 6.19:** Achievable rate for realization 1 and maximum base station power

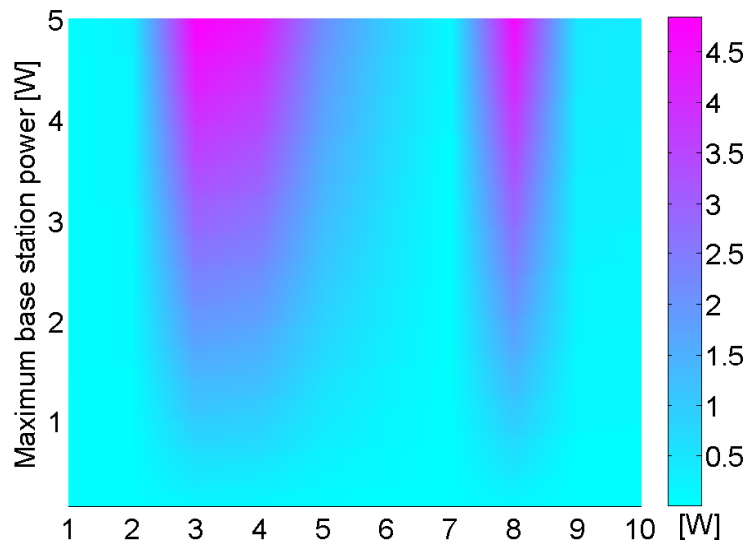


**Figure 6.20:** Optimal power allocation to the outer users

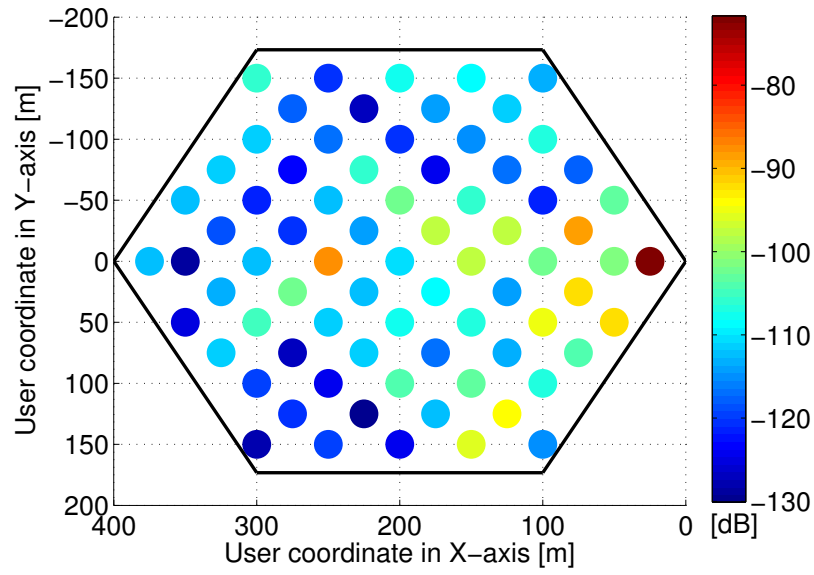


**Figure 6.21:** Large-scale path-loss attenuations for the realization 3

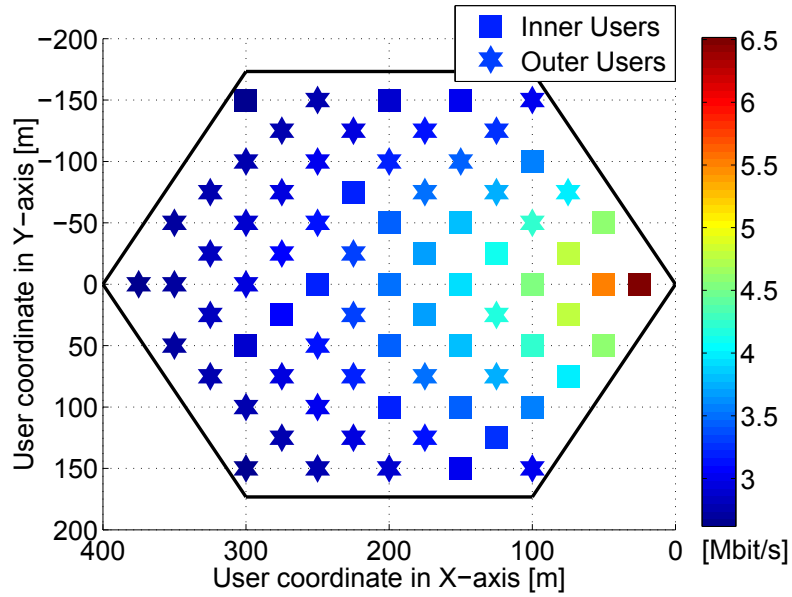


**Figure 6.22:** Achievable rate for realization 3 and maximum base station power

### 6.4.2 Efficient power and adaptive bandwidth algorithm depending on mean LSPLA

In this subsection, we show the formulation of the efficient power allocation and adaptive bandwidth allocation algorithm similar to Algorithm 5 for PFR cellular networks.

---

**Algorithm 6** Efficient Power and Adaptive Bandwidth Algorithm

---

**Require:**  $G_{\text{tgt}} = \bar{G}, (\mathbf{r}, \theta), \beta^{\text{in}} = 1/N_c, \beta^{\text{out}} = 1/N_c$

```

1: if  $G > G_{\text{tgt}}$  then
2:    $(\mathbf{r}^{\text{in}}, \theta^{\text{in}}) \leftarrow (\mathbf{r}, \theta)$ 
3:    $\mathbf{G}^{\text{in}} \leftarrow G$ 
4:    $N^{\text{in}} \leftarrow N^{\text{in}} + 1$ 
5: else
6:    $(\mathbf{r}^{\text{in}}, \theta^{\text{in}}) \leftarrow (\mathbf{r}, \theta)$ 
7:    $\mathbf{G}^{\text{out}} \leftarrow G$ 
8:    $M^{\text{out}} \leftarrow M^{\text{out}} + 1$ 
9: end if
10:  $\beta_{\text{tot}}^{\text{in}} = \beta^{\text{in}} \cdot N^{\text{in}}, \beta_{\text{tot}}^{\text{out}} = \beta^{\text{out}} \cdot M^{\text{out}}$ 
11: Calculate the values of:
     $p_0^{\text{in}}, p_k^{\text{in}}, p_0^{\text{out}}, p_k^{\text{out}},$ 
    using Equation (6.12).

```

---

The sum-power minimization problem is given by Equation (6.12).

$$\underset{\beta_{cn}^{\text{in}}, \beta_{cm}^{\text{out}} \in \mathcal{R}_+, \mathbf{p} \succeq \mathbf{0}}{\text{minimize}} \quad \sum_{n=1}^{N^{\text{in}}} p_{cn}^{\text{in}} + \sum_{m=1}^{M^{\text{out}}} p_{cm}^{\text{out}} \quad (6.12a)$$

subject to

$$\frac{p_c^{\text{in}}}{n_1^{\text{in}} \beta_{c1}^{\text{in}} + \sum_{k \in \mathcal{C} \setminus c} g_{k1}^{\text{in}} p_k^{\text{in}}} \geq \text{SINR}_{\min}^{\text{in}}, \quad \forall c \in \mathcal{C}, \quad (6.12b)$$

$$\vdots$$

$$\frac{p_c^{\text{in}}}{n_{N^{\text{in}}}^{\text{in}} \beta_{cN^{\text{in}}}^{\text{in}} + \sum_{k \in \mathcal{C} \setminus c} g_{kN^{\text{in}}}^{\text{in}} p_k^{\text{in}}} \geq \text{SINR}_{\min}^{\text{in}}, \quad \forall c \in \mathcal{C}, \quad (6.12c)$$

$$\frac{p_c^{\text{out}}}{n_1^{\text{out}} \beta_{c1}^{\text{out}} + \sum_{k \in \mathcal{C} \setminus c} g_{k1}^{\text{out}} p_k^{\text{out}}} \geq \text{SINR}_{\min}^{\text{out}}, \quad \forall c \in \mathcal{C}, \quad (6.12d)$$

$$\vdots$$

$$\frac{p_c^{\text{out}}}{n_{M^{\text{out}}}^{\text{out}} \beta_{cM^{\text{out}}}^{\text{out}} + \sum_{k \in \mathcal{C} \setminus c} g_{kM^{\text{out}}}^{\text{out}} p_k^{\text{out}}} \geq \text{SINR}_{\min}^{\text{out}}, \quad \forall c \in \mathcal{C}, \quad (6.12e)$$

$$p_c^{\text{in}} + p_c^{\text{out}} \leq P_c^{\text{max}}, \quad \forall c \in \mathcal{C}, \quad (6.12f)$$

Algorithm 6 works in principle as the Algorithm 5, except that instead of maximizing the minimum SINR deploys a sum-power minimization to efficiently allocate the power to the inner and the outer users.

The objective (6.12a) minimizes all power in all regions of the considered cells. The constraints (6.12b)-(6.12c) show that the individual inner users SINR's are lower bounded by the minimum inner user SINR. Similarly to the inner users, the constraints (6.12d)-(6.12e) show that the SINRs for outer users are lower bounded by the minimum outer user SINR. The last constraint (6.13f) shows that the sum of power allocated in the inner region and the outer region should not be higher than the maximum base station power. As it is formulated the optimization problem is not a GP or any other extended forms of GP's like GGP due to non-posynomial standard form of SINR constraints.

**Proposition 5.** *The sum-power minimization problem (6.12) can be converted into a geometric programming problem.*

*Proof.* Similarly to the optimization problem given by Equation (6.9), we begin by changing the nominator with the denominator in the constraints (6.12b)-(6.12e) in order to convert them to posynomials. This led us to the optimization problem formulated in the GP form as formulated in the following

$$\underset{\beta_{cn}^{\text{in}}, \beta_{cm}^{\text{out}} \in \mathcal{R}_+, \mathbf{p} \succeq \mathbf{0}}{\text{minimize}} \quad \sum_{n=1}^{N^{\text{in}}} p_{cn}^{\text{in}} + \sum_{m=1}^{M^{\text{out}}} p_{cm}^{\text{out}} \quad (6.13a)$$

subject to

$$\frac{n_1^{\text{in}} \beta_{c1}^{\text{in}} + \sum_{k \in \mathcal{C} \setminus c} g_{k1}^{\text{in}} p_k^{\text{in}}}{p_c^{\text{in}}} \leq \frac{1}{\text{SINR}_{\min}^{\text{in}}}, \quad \forall c \in \mathcal{C}, \quad (6.13b)$$

$\vdots$

$$\frac{n_{N^{\text{in}}}^{\text{in}} \beta_{cN^{\text{in}}}^{\text{in}} + \sum_{k \in \mathcal{C} \setminus c} g_{kN^{\text{in}}}^{\text{in}} p_k^{\text{in}}}{p_c^{\text{in}}} \leq \frac{1}{\text{SINR}_{\min}^{\text{in}}}, \quad \forall c \in \mathcal{C}, \quad (6.13c)$$

$$\frac{n_1^{\text{out}} \beta_{c1}^{\text{out}} + \sum_{k \in \mathcal{C} \setminus c} g_{k1}^{\text{out}} p_k^{\text{out}}}{p_c^{\text{out}}} \leq \frac{1}{\text{SINR}_{\min}^{\text{out}}}, \quad \forall c \in \mathcal{C}, \quad (6.13d)$$

$\vdots$

$$\frac{n_{M^{\text{out}}}^{\text{out}} \beta_{cM^{\text{out}}}^{\text{out}} + \sum_{k \in \mathcal{C} \setminus c} g_{kM^{\text{out}}}^{\text{out}} p_k^{\text{out}}}{p_c^{\text{out}}} \leq \frac{1}{\text{SINR}_{\min}^{\text{out}}}, \quad \forall c \in \mathcal{C}, \quad (6.13e)$$

$$p_c^{\text{in}} + p_c^{\text{out}} \leq P_c^{\max}, \quad \forall c \in \mathcal{C}, \quad (6.13f)$$

where the objective (6.13a) and the constraints (6.13b)-(6.13f) are posynomials.  $\square$

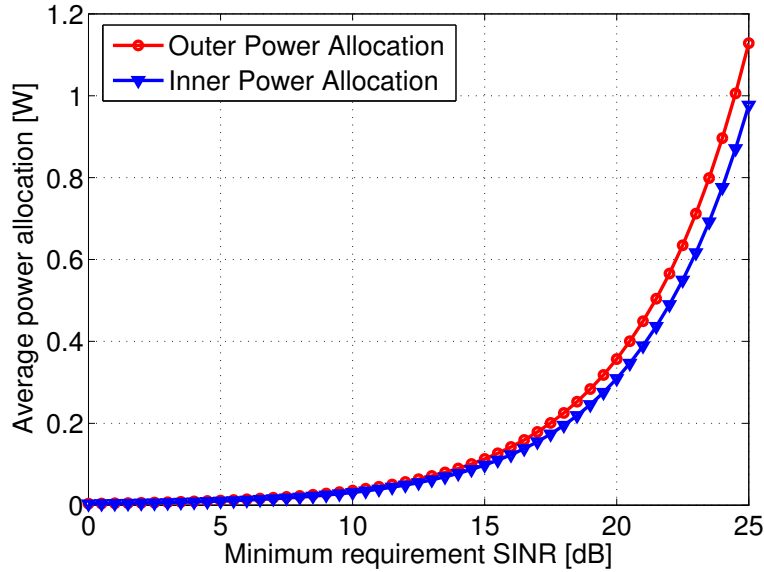
## Numerical Simulations: Efficient power and adaptive bandwidth allocation

The simulation results shown here are carried out using Algorithm 6 and the simulation parameters in Table 6.6.

**Table 6.6:** Simulation parameters

parameters	value
Maximum base station power $P_c^{\max}$	40 W
Maximum base station bandwidth $B_c^{\max}$	20 MHz
Noise spectral density $N_0$	-174 dBm/Hz
Center frequency $f$	2.0 GHz
Path-loss exponent $\alpha$	3.75
Penetration loss $L_p$	20 dB
Shadowing $X_\sigma$	$\mathcal{N}(0, 8)$ dB
Small-scale fading $F$	$\chi_2^2$ dB,
Inter base station distance $d$	600 m
Maximum cell range $r$	$(2/3)d$ m
Users requirement SINR $SINR_{min}$	[0 : 0.5 : 25] dB
Number of users within cell	75

During the simulations 100 realizations are considered, where for each realization the users have experienced different channels. The average power allocation for the inner region and the outer region versus the minimum required SINR is shown in Figure 6.23.

**Figure 6.23:** Average power allocation for the inner region and the outer region

The simulation results shown in Figure 6.23 indicate high efficiency of power allocation performed by Algorithm 6, for low minimum required SINR. Increasing the minimum SINR requirement, increases also the average power allocated to the inner and the outer regions. Even for a SINR requirement of 25 dB the average power allocated in the inner region is below 1 W and that allocated to the outer region below 1.2 W.



In order to show the LSPLA, received SINR and the achievable rate in the following is chosen one realization out of 100 realization for the minimum SINR requirement  $\text{SINR}_{\min} = 15$  dB. The LSPLA of users located in the cell for the considered realization is shown in Figure 6.24. From the LSPLA of users shown in Figure 6.24 we see that users experience different LSPLA due to shadowing and small-scale fading. Using the mean LSPLA as the threshold  $G_{\text{tgt}} = -110.58$  dB, about 35 users are classified as inner users and about 40 users are classified as the outer users.

The inner users and the outer users locations together with their received SINRs are shown in Figure 6.25. Looking at the simulation results shown in Figure 6.25, one can see that each inner and the outer user has received a higher or equal SINR than the minimum SINR requirement of 15 dB.

For the same configuration in the following the achievable rate by the inner and the outer users is shown. From Figure 6.26 it is shown that each inner and the outer user achieve a rate higher than 1 Mbit/s. Evaluating the simulation results for average power allocation shown in Figure 6.23, for the selected minimum SINR requirement of 15 dB we see that from the total power allocation around 0.097 W is allocated to the inner users, and around 0.011 W is allocated to the outer users. Such result in average power allocation confirm that Algorithm 6 is very efficient in power allocation for PFR.

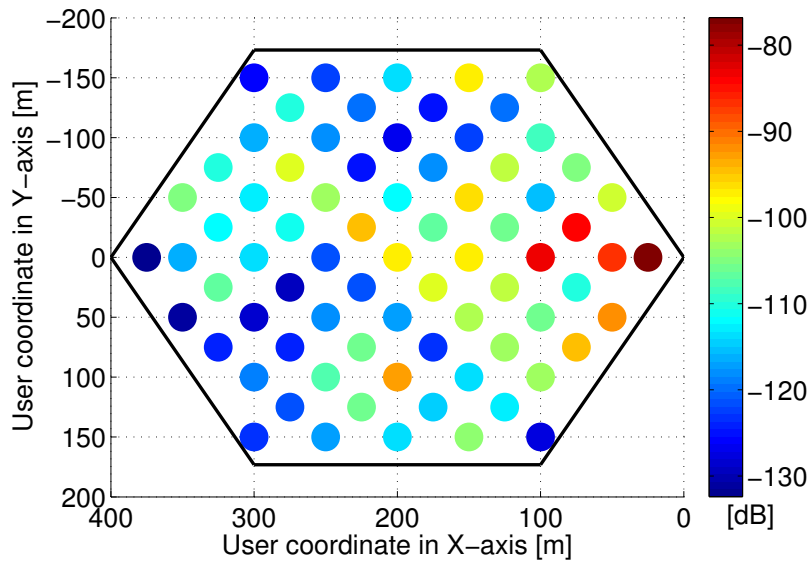


**Figure 6.24:** Large-scale path-loss attenuations for realization 7

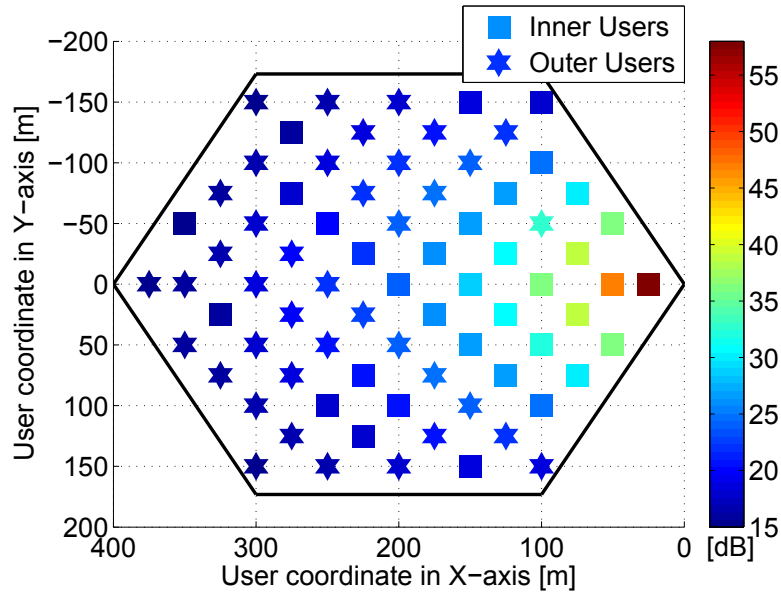


Figure 6.25: Users received SINRs

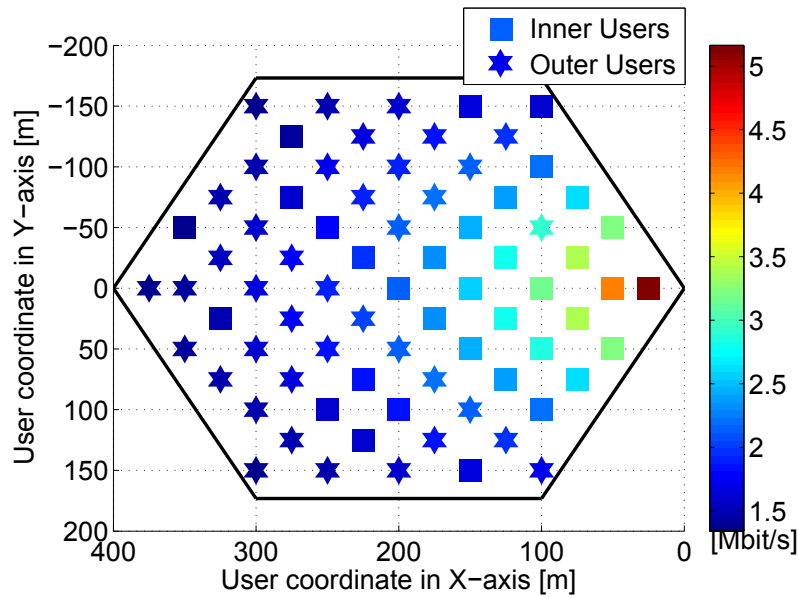


Figure 6.26: Achievable rate by the users

# Conclusions

---

IN the thesis I give an overview of the RRM techniques for PFR in LTE networks. The 3GPP, by whom LTE is standardized, proposes OFDMA as multiple access scheme in the downlink. Due to the use of OFDMA the ICI becomes critical at the cell edge. One of the many tasks of RRM is the reduction of the ICI while increasing the achievable capacity of the network. Two radio resources are considered to be of primary importance: power and bandwidth. Both radio resources are very limited and costly. The power is limited due to the associated increase of the ICI to the neighboring cells, while the bandwidth is limited due to limited spectrum license. Hence optimization of such resources is advantageous. We have formulated optimization problems for RRA which are efficient and optimal in resource allocation. These problems are formulated based on the mathematical framework of convex optimization. The mathematical methods used throughout the thesis are introduced in Chapter 3. The main part of the thesis is focused on three topics: capacity density maximization, power allocation and joint power and bandwidth allocation. Initially, we considered the maximization of the cell capacity density by applying a bandwidth re-allocation scheme with constant power allocation. Next, we developed optimization problems for power allocation. Finally, we developed optimization techniques for joint power and bandwidth allocation. Overall, we formulated efficient, optimal power allocation and adaptive bandwidth allocation algorithms.

In the following we present the most important conclusions for capacity density maximization, power allocation in PFR, as well as joint power and bandwidth allocation in PFR.

## 7.1 Capacity Density Maximization

We developed and analyzed a novel flexible bandwidth allocation scheme [7] for PFR considering the case that the cell is not always populated homogeneously over the area. We formulated the capacity density taking into account cell edge bandwidth re-allocation. Further, we formulated the optimization problem for maximizing the capacity density constrained by optimum frequency partitioning radius and the cell edge bandwidth re-allocation parameter. By solving the optimization problems for maximizing the capacity density we found an upper bound on cell edge bandwidth re-allocation.

Simulations indicated that re-allocating the cell edge bandwidth to the cell center increases the capacity density by 4.9 bit/s/Hz for frequency reuse-1 whenever the cell edge users are idling.

## 7.2 Power Allocation in Partial Frequency Reuse

In this part of thesis, we introduced the cell cluster scheme for PFR where the user's classification into cell regions is obtained based on the LSPLA threshold. We formulated the optimization problems for sum-rate maximization [12] in PFR considering the bandwidth and the power allocation. In general, such problems are non-convex and, therefore, hard to solve. However, under the additional assumption of a uniform power allocation over all cells, we are able to convexify this optimization problem.

Using dual decomposition techniques, we found the optimal power allocation in the inner and the outer cell regions for a fixed bandwidth allocation within cell regions. Such optimal allocation of power significantly reduces the ICI and simultaneously increases the sum-rate.

Simulations showed also that our optimal power allocation algorithm outperforms the static power allocation method. The gains achieved by our algorithm compared with static power allocation are shown in the maximum sum-rate.

Moreover, we formulated the optimization problem for the maximization of the minimum rate and for the minimization of the sum-power for multiple users over multiple cells in PFR. A variable transformation was able to convert these non-convex optimization problems into convex forms which are solvable efficiently using well known state-of-the-art interior-point methods.

## 7.3 Bandwidth and Power Allocation in Partial Frequency Reuse

Finally, we optimized jointly the bandwidth and power allocation by solving the maximization of the minimum rate. We found efficient solutions for power allocation and

optimal solutions for bandwidth allocation. Also by analyzing the simulation results we proved that PFR is more efficient in power allocation than frequency reuse-1 or frequency reuse-3. Such efficiency is achieved when for user's classification in cell regions the LSPLA threshold is defined as the mean LSPLA.

Further, we treated the allocation of power and re-allocation of bandwidth jointly and show that a significant increase in the sum-rate for the cell center users is achievable. Firstly, the joint power allocation and bandwidth re-allocation algorithms are proposed and applied to the cell cluster where we classify the users based on the distance threshold (static method). Later we have applied the same optimization algorithm for a cell cluster where the user's classification is based on mean LSPLA threshold (dynamic method).

By simulation it is shown that about 34% more gain is achieved in average sum rate when the bandwidth re-allocation is considered for the static method. Further we compared the dynamic method with the static method where in most of the cases a higher gain is achieved by dynamic method. There are only few cases when both methods perform similarly. Also in the case of average sum-rate we achieve a sum-rate increase by 3.1 Mbit/s with the dynamic method compared to the static method when outer bandwidth re-allocation is considered. About 16.4 Mbit/s more sum-rate is achieved for the same scenario without outer bandwidth re-allocation.

Concerning the bandwidth allocation by maximization of the minimum rate we have noticed that bandwidth allocation in the cell regions is obtained depending on the amount of the user's classified. Using this fact, we have developed two algorithms: the optimal power and adaptive bandwidth algorithm and the efficient power and adaptive bandwidth algorithm.

The optimal power and adaptive bandwidth algorithm use the maximization of the minimum SINR to optimally allocate the power in the cell regions, while the bandwidth is allocated adaptively based on the user's classification by LSPLA threshold. Applying such algorithm is shown that each user has achieved a rate higher than 2.5 Mbit/s for the maximum base station transmit power 5 W.

The efficient power and adaptive bandwidth allocation algorithm use the sum-power minimization to efficiently allocate the power in the cell regions based on the minimum received SINR criteria, while it allocates the bandwidth adaptively based on the user's classification by the LSPLA threshold. With such algorithm it is shown that each user has achieved a SINR higher than minimum requirement SINR and a transmission rate higher than 1.5 Mbit/s even for an average power allocation smaller than 1.2 W.



# Future Directions / Outlook

---

THE main contribution of this thesis is the development of optimization problems for RRA in PFR cellular networks.

In the first part we introduced a novel bandwidth re-allocation scheme for PFR and formulated the optimization problem that maximize the cell capacity density taking into account bandwidth re-allocation. The results were quite impressive and confirmed the gain from re-allocating the cell edge bandwidth to the cell center users when the cell edge users are idle.

In the second part we formulated the RRA optimization problems for power allocation. We applied the DDT to solve such optimization problems for PFR. A significant decrease in the ICI and a significant increase in the sum-rate is achieved. Such optimization techniques are proved to work well for fixed bandwidth allocation schemes. However for variable bandwidth allocation the dual decomposition methods offer intractable solutions. Implementing a scheduler together with the optimization of the power allocation is a future direction. Also using interior point algorithms based on barrier methods is the next task to solve the joint optimization of power and bandwidth allocation in PFR.

In the third part which is the last part of the thesis we formulated the optimization problems for joint optimization of power and bandwidth allocation applying GP. We achieved very good results which could be interesting for cellular network operators on how to dimension the cell. By dimensioning cells we mean that no matter where the user is, either at the cell center or cell edge, it should be able to receive a rate higher than a minimum required rate or an SINR higher than minimum required SINR. The next step will be to compare the aforementioned optimization algorithms for PFR with frequency reuse-1. Such results are expected to help the mobile operators to decide on implementation the PFR in LTE networks.

From all what I showed in the thesis one can understand that there are still many open questions for research in resource optimization for LTE. Finding solution for such problems would yield in energy saving and simultaneously, offer higher data rates to the users.



# List of Symbols

---

Lowercase symbols	Description
$\mathbf{b}$	vector elements of maximum bandwidth allocation
$\mathbf{c}$	vector elements of maximum power and bandwidth
$c$	denotes the cell
$d$	distance between two base stations
$f$	center carrier frequency
$g_0$	function in the objective
$g_i$	function in the inequality
$g_{kn}^{\text{in}}$	normalized LSPLA of inner user $n$
$g_{km}^{\text{out}}$	normalized LSPLA of outer user $m$
$h_j$	function in the equality
$k$	base station index
$m$	index for outer user
$n$	index for inner user
$p$	power spectral density
$\mathbf{p}$	vector of power allocation
$p_0^{\text{in}}$	power allocation to inner users
$p_k^{\text{in}}$	interference to inner users
$p_0^{\text{out}}$	power allocation to outer users
$p_k^{\text{out}}$	interference to outer users
$r$	distance from base station to the user
$r_{\text{tgt}}$	distance target
$\mathbf{r}^{\text{in}}$	vector elements of inner user distances
$\mathbf{r}^{\text{out}}$	vector elements of inner user distances
$s$	subscript for inner or outer user
$t$	bandwidth re-allocation parameter

$t^*$	maximum bandwidth re-allocation
$t^{\text{in}}$	normalized required inner user rate
$t^{\text{in}}$	normalized required outer user rate
$u$	user
$v$	velocity of light in free space
$\mathbf{x}$	vector of optimization variables
$x$	normalized cartesian coordinate of $X$
$y$	normalized cartesian coordinate of $Y$
$z$	auxiliary variable
<b>Uppercase symbols</b>	<b>Description</b>
$A$	normalization matrix
$A_k$	sum of BS and MS antenna gain
$A_m$	antenna attenuation
$A(\theta)$	horizontal antenna pattern
$B_{\text{tot}}$	total base station bandwidth
$B_{FR}$	bandwidth assigned to FR region
$B_{PR}$	bandwidth assigned to PR region
$B_n^{\text{in}}$	bandwidth assigned to to user $n$ in inner region
$B_m^{\text{out}}$	bandwidth assigned to to user $m$ in outer region
$B^{\text{max}}$	maximum base station bandwidth
$C$	cell capacity density
$C_{FR}$	cell capacity density in FR region
$C_{PR}$	bandwidth assigned to PR region
$\mathcal{C}$	set of cells
$F$	fast fading
$\mathcal{G}$	large-scale path-loss attenuation (LSPLA)
$G$	objective of a dual optimization problem
$G_{0n}^{\text{in}}$	LSPLA of direct channels for inner user $n$
$G_{kn}^{\text{in}}$	LSPLA of interference channels for inner user $n$
$G_{0m}^{\text{out}}$	LSPLA of direct channels for outer user $m$
$G_{km}^{\text{out}}$	LSPLA of interference channels for inner user $m$
$\mathbf{G}^{\text{in}}$	vector elements for LSPLA of inner users
$\mathbf{G}^{\text{out}}$	vector elements for LSPLA of outer users
$I$	superscript for inner or outer set of users
$L$	Lagrangian of an optimization problem
$L_r$	FSPL model

$L_0$	loss indicated by path-loss exponent model
$L_p$	penetration loss
$M^{\text{out}}$	number of outer users
$N^{\text{in}}$	number of inner users
$N_0$	noise spectral density
$P_r$	received power
$P_{\text{intra-cell}}$	intra-cell interference
$P_{\text{inter-cell}}$	inter-cell interference
$P^{\text{max}}$	maximum base station transmit power
$\mathcal{R}^n$	real $n$ -dimensional domain
$R_n^{\text{in}}$	achievable rate by inner user $n$
$R_m^{\text{out}}$	achievable rate by outer user $m$
$\mathbf{R}^{\text{in}}$	vector elements of achievable rates by inner users
$\mathbf{R}^{\text{out}}$	vector elements of achievable rates by outer users
$S$	sum of path-loss distances
$U$	user
$\mathcal{U}_c^{\text{in}}$	set of inner users in cell $c$
$\mathcal{U}_c^{\text{out}}$	set of outer users in cell $c$
$X_\sigma$	log-normal shadowing
<b>Greek symbols</b>	<b>Description</b>
$\alpha$	path-loss exponent
$\beta(\theta)$	boundary between two regions in PFR
$\beta^{\text{in}}$	normalized inner bandwidth
$\beta^{\text{out}}$	normalized outer bandwidth
$\chi$	chi square distribution
$\delta$	exponent in the monomials of GPs
$\gamma_\rho$	average SINR in polar coordinates
$\lambda$	lagrange multiplier
$\mu$	lagrange multiplier
$\rho$	frequency partitioning radius
$\hat{\rho}$	resulting frequency partitioning radius
$\theta$	azimuth angle
$\theta_{3dB}$	antenna beamwidth
$\nabla$	operator for first derivative
$\Gamma$	average SINR in Cartesian coordinates
$\Gamma_e$	average SINR in Cartesian coordinates at cell edge



# List of Acronyms

---

<b>CDMA</b>	Code Division Multiple Access
<b>CVX</b>	Matlab Software for Disciplined Convex Programming
<b>DCP</b>	Disciplined Convex Programming
<b>DDT</b>	Dual Decomposition Techniques
<b>EPC</b>	Evolved Packet Core
<b>E-UTRAN</b>	Evolved-Universal Terrestrial Radio Access Network
<b>FR</b>	Full Reuse
<b>FSPL</b>	Free Space Path-Loss
<b>GP</b>	Geometric Programming
<b>GGP</b>	Generalized Geometric Programming
<b>GSM</b>	Global System for Mobile Communications
<b>HSDPA</b>	High-Speed Downlink Packet Access
<b>HSPA</b>	High-Speed Packet Access
<b>ICI</b>	Inter Cell Interference
<b>ITU</b>	International Telecommunication Union
<b>KKT</b>	Karush-Kuhn-Tucker
<b>LTE</b>	Long Term Evolution
<b>LTE-A</b>	Long Term Evolution-Advanced

**LSPLA** Large-Scale Path-Loss Attenuation

**LOS** Line-of-Sight

**MME/S-GW** Mobility Management Entity/Service-Gateway

**NMT** Nordic Mobile Telephone

**NLOS** Non-Line-of-Sight

**OFDMA** Orthogonal Frequency Division Multiple Access

**OFDM** Orthogonal Frequency Division Multiplexing

**PRB** Physical Resource Block

**PFR** Partial Frequency Reuse

**PR** Partial Reuse

**RRM** Radio Resource Management

**RRA** Radio Resource Allocation

**RNC** Radio Network Controller

**Rx** Receiver

**SH** Soft Handover

**SINR** Signal-to-Interference-and-Noise-Ratio

**SNR** Signal-to-Noise-ratio

**Tx** Transmitter

**UMTS** Universal Mobile Telecommunications System

**WiMAX** Worldwide Interoperability for Microwave Access

**WLAN** Wireless Local Area Network

**X2** the interface between two eNodeBs

**3GPP** 3rd Generation Partnership Project

**4G** 4th Generation

# List of Figures

---

2.1	LTE radio interface architecture . . . . .	7
4.1	Cell cluster with radius classification criteria . . . . .	16
4.2	Frequency reuse pattern and bandwidth partitioning . . . . .	19
4.3	Downlink subcarrier allocation . . . . .	20
4.4	Partial bandwidth re-allocation scheme . . . . .	21
4.5	Cell capacity versus frequency-reuse partitioning radius for different values of parameter $t$ . . . . .	24
4.6	Maximum cell capacity versus parameter $t$ for optimal frequency partitioning radius . . . . .	24
5.1	Cell cluster model with distance threshold criteria . . . . .	26
5.2	Cell cluster model with large-scale path-loss attenuation threshold criteria . . .	27
5.3	Horizontal antenna gain for horizontal antenna pattern . . . . .	29
5.4	Frequency reuse pattern for fixed bandwidth allocation . . . . .	31
5.5	Optimal power assignment to the inner and outer users . . . . .	35
5.6	Maximum sum-rate for the inner and the outer users . . . . .	36
6.1	Variable bandwidth and power allocation scheme . . . . .	42
6.2	Assigned normalized bandwidth to the inner user 1 versus normalized inner and outer rates . . . . .	46
6.3	Assigned power to the inner users . . . . .	47
6.4	Assigned normalized bandwidth to the outer user 1 versus normalized inner and outer rates . . . . .	48
6.5	Assigned power to the outer users . . . . .	48
6.6	Transmission rate achieved by each user . . . . .	49
6.7	Power efficiency depending on users classification . . . . .	54
6.8	Large-scale path-loss attenuations for uniform users distribution . . . . .	54

6.9 Individual users rate for large-scale path-loss attenuation mean threshold $G_{\text{tgt}} = -110.27$ dB . . . . .	55
6.10 Bandwidth re-allocation scheme for sector $S_{01}$ . . . . .	56
6.11 Frequency reuse pattern for sector $S_{01}$ . . . . .	57
6.12 Maximum sum-rate for random users positions . . . . .	59
6.13 Maximum average sum-rate for random users positions . . . . .	60
6.14 Large-scale path-loss attenuations for uniform users positions . . . . .	63
6.15 Sum-rate gain for dynamic method compared with static method . . . . .	63
6.16 Maximum average sum-rate for uniform users positions . . . . .	64
6.17 Optimal power allocation to the inner users . . . . .	68
6.18 Large-scale path-loss attenuations for the realization 1 . . . . .	69
6.19 Achievable rate for realization 1 and maximum base station power . . . . .	70
6.20 Optimal power allocation to the outer users . . . . .	70
6.21 Large-scale path-loss attenuations for the realization 3 . . . . .	71
6.22 Achievable rate for realization 3 and maximum base station power . . . . .	71
6.23 Average power allocation for the inner region and the outer region . . . . .	74
6.24 Large-scale path-loss attenuations for realization 7 . . . . .	75
6.25 Users received SINRs . . . . .	76
6.26 Achievable rate by the users . . . . .	76



# Bibliography

---

- [1] M. Wolkerstorfer, T. Nordström, B. Krasniqi, M. Wrulich, and C. Mecklenbräuker, “OFDM/OFDMA subcarrier allocation, chapter 6,” in *Cross Layer Designs in WLAN Systems* (N. Zorba, C. Skianis, and C. Verikoukis, eds.), pp. 161–192, Leicester (UK): troubadour publishing ltd., 2011.
- [2] K. Son, S. Chong, and G. de Veciana, “Dynamic association for load balancing and interference avoidance in multi-cell networks,” in *Proc. 5th International Symposium on Modeling and Optimization in Mobile, Ad Hoc and Wireless Networks and Workshops WiOpt 2007*, pp. 1–10, Apr. 16–20, 2007.
- [3] C.-S. Chiu and C.-C. Huang, “Combined partial reuse and soft handover in OFDMA downlink transmission,” in *Proc. IEEE Vehicular Technology Conf. VTC Spring 2008*, pp. 1707–1711, 2008.
- [4] Y. Xiang, J. Luo, and C. Hartman, “Inter-cell interference mitigation through flexible resource reuse in OFDMA based communication networks,” in *Proc. European Wireless 2007*, 2007.
- [5] P. Godlewski, M. Maqbool, and M. Coupechoux, “Analytical evaluation of various frequency reuse schemes in cellular OFDMA networks,” in *perso.telecom-paristech.fr*, 2008.
- [6] A. Alsawah and I. Fialkow, “Optimal frequency-reuse partitioning for ubiquitous coverage in cellular systems,” in *16th European Signal Processing Conference - publi-etis.ensea.fr*, 2008.
- [7] B. Krasniqi, M. Wrulich, and C. Mecklenbräuker, “Network-load dependent partial frequency reuse for LTE,” in *Proc. 9th International Symposium on Communications and Information Technology, 2009. ISCIT*, pp. 672–676, Sept. 2009.
- [8] A. Gjendemsjo, D. Gesbert, G. Oien, and S. Kiani, “Optimal power allocation and scheduling for two-cell capacity maximization,” in *Proc. 4th International Symposium on Modeling and Optimization in Mobile, Ad Hoc and Wireless Networks*, pp. 1–6, april 2006.
- [9] M. Charafeddine and A. Paulraj, “2-sector interference channel communication for sum rates and minimum rate maximization,” in *Proc. 43rd Annual Conference on Information Sciences and Systems, 2009. CISS 2009.*, pp. 951–956, March 2009.
- [10] C. S. Chen and G. E. Oien, “Optimal power allocation for two-cell sum rate maximization under minimum rate constraints,” in *Proc. Wireless Communication Systems. 2008. ISWCS '08. IEEE Int. Symp*, pp. 396–400, 2008.

- [11] M. Charafeddine and A. Paulraj, "Sequential geometric programming for  $2 \times 2$  interference channel power control," in *Proc. 41st Annual Conf. Information Sciences and Systems CISS '07*, pp. 185–189, 2007.
- [12] B. Krasniqi, M. Wolkerstorfer, C. Mehlführer, and C. F. Mecklenbräuker, "Sum-rate maximization for multiple users in partial frequency reuse cellular networks," in *Proc. IEEE GLOBECOM Workshops (GC Wkshps)*, pp. 814–818, 2010.
- [13] B. Krasniqi, M. Wolkerstorfer, C. Mehlführer, and C. Mecklenbräuker, "Sum-rate maximization by bandwidth re-allocation for two users in partial frequency reuse cellular networks," in *44th Asilomar Conference on Signals, Systems and Computers*, (Pacific Grove (CA), USA), November 2010.
- [14] M. Chiang, C. W. Tan, D. Palomar, D. O'Neill, and D. Julian, "Power control by geometric programming," *IEEE Transactions on Wireless Communications*, vol. 6, pp. 2640 – 2651, July 2007.
- [15] Z. Xie and B. Walke, "Frequency reuse techniques for attaining both coverage and high spectral efficiency in OFDMA cellular systems," in *Proc. WCNC 2010*, 2010.
- [16] W. Fu, Z. Tao, J. Zhang, and D. Agrawal, "Differentiable spectrum partition for fractional frequency reuse in multi-cell OFDMA networks," in *Proc. WCNC 2010*, 2010.
- [17] B. Krasniqi and C. Mecklenbräuker, "Maximization of the minimum rate by geometric programming for multiple users in partial frequency reuse cellular networks," in *IEEE 74th Vehicular Technology Conference (VTC 2011-fall)*, (San Francisco, USA), September 2011.
- [18] B. Krasniqi, M. Wolkerstorfer, C. Mehlführer, and C. Mecklenbräuker, "Weighted sum-rate maximization for two users in partial frequency reuse cellular networks," in *11th MCM COST2100, Aalborg, Denmark*, (Aalborg, Denmark), June 2010.
- [19] B. Krasniqi, C. Mehlführer, and C. Mecklenbräuker, "Bandwidth re-allocation depending on large-scale path-loss for two users in partial frequency reuse cellular networks," in *1st Scientific Meeting COST Action IC1004*, (Lund, Sweden), June 2011.
- [20] B. Krasniqi and C. Mecklenbräuker, "Efficiency of partial frequency reuse in power used depending on users selection for cellular networks," in *22nd Annual IEEE International Symposium on Personal, Indoor and Mobile Radio Communications (PIMRC 2011)*, (Toronto, Canada), pp. 268–272, September 2011.
- [21] J. Zander and S. Kim, *Radio Resource Management for Wireless Networks*. Artech House Publishers, 2001.
- [22] A. Paier, B. Krasniqi, and C. Mecklenbräuker, "Investigation of the coexistence of communication systems in the 2.6 GHz band in cross border scenarios," tech. rep., Bundesministerium für Verkehr, Innovation und Technologie, Sektion III/Abteilung PT3, 2009.
- [23] S. Caban, C. Mehlführer, M. Rupp, and M. Wrulich, *EVALUATION OF HSDPA AND LTE From Testbed Measurements to System Level Performance*. Published by Wiley., 2011.
- [24] F. Rodrigo, P. Cavalcanti, and S. Andersson, *Optimizing Wireless Communication Systems*. Springer, 2009.
- [25] Z. Huan and K. J. R. Liu, *Resource Allocation for Wireless Networks, Basics, Techniques and Applications*. Cambridge, 2008.
- [26] G. Vivier, *Radio Resources Management in WiMAX: From Theoretical Capacity to System Simulations*. Wiley-ISTE, 2009.

- [27] A. Hills and B. Friday, "Radio resource management in wireless LANs," *IEEE Commun. Mag.*, vol. 42, no. 12, 2004.
- [28] "Evolved Universal Terrestrial Radio Access Network (E-UTRAN); X2 general aspects and principles (release 8), 3GPP Technical Specification TS 36.420 v8.1.0 December 2008 [online]. Available: [www.3gpp.org](http://www.3gpp.org)."
- [29] E. Dahlman, S. Parkvall, and J. Sköld, *4G LTE/LTE-Advanced for Mobile Broadband*. Published by Elsevier Ltd., 2011.
- [30] D. P. Palomar and M. Chiang, "A tutorial on decomposition methods for network utility maximization," *IEEE J. Sel. Areas Commun.*, vol. 24, no. 8, pp. 1439–1451, 2006.
- [31] B. Johansson, P. Soldati, and M. Johansson, "Mathematical decomposition techniques for distributed cross-layer optimization of data networks," *IEEE J. Sel. Areas Commun.*, vol. 24, no. 8, pp. 1535–1547, 2006.
- [32] S. Boyd and L. Vandenberghe, *Convex Optimization*. Cambridge University Press, 2004.
- [33] L. Xiao, M. Johansson, and S. P. Boyd, "Simultaneous routing and resource allocation via dual decomposition," *IEEE Trans. Commun.*, vol. 52, no. 7, pp. 1136–1144, 2004.
- [34] J.-W. Lee, M. Chiang, and A. R. Calderbank, "Network utility maximization and price-based distributed algorithms for rate-reliability tradeoff," in *Proc. 25th IEEE Int. Conf. Computer Communications INFOCOM 2006*, pp. 1–13, 2006.
- [35] M. Chiang, S. H. Low, A. R. Calderbank, and J. C. Doyle, "Layering as optimization decomposition: Framework and examples," in *Proc. ITW '06 Punta del Este Information Theory Workshop IEEE*, pp. 52–56, 2006.
- [36] M. Chiang, *Geometric Programming for Communication Systems*. now Publishers Inc, 2005.
- [37] S. Boyd, S.-J. Kim, L. Vandenberghe, and A. Hassibi, "A tutorial on geometric programming," *Optimization and Engineering*, vol. 8, no. 1, pp. 67–127, 2007.
- [38] Nesterov and Nemirovsky, "Interior-point polynomial algorithms in convex programming," *SIAM 1994*, 1994.
- [39] M. Grant and S. Boyd, "CVX: Matlab software for disciplined convex programming, version 1.21." <http://cvxr.com/cvx>, Apr. 2011.
- [40] E. Dahlman, S. Parkvall, J. Skold, and P. Beming, *3G Evolution, HSDPA and LTE for Mobile Broadband*. Elsevier, 2007.
- [41] V. S. Abhayawardhana, I. J. Wassell, D. Crosby, M. P. Sellars, and M. G. Brown, "Comparison of empirical propagation path loss models for fixed wireless access systems," in *Proc. VTC 2005-Spring Vehicular Technology Conf. 2005 IEEE 61st*, vol. 1, pp. 73–77, 2005.
- [42] D. Lee, X. C, U. Mayekar, and M. Mohile, "Frequency reuse factor vs. pathloss exponent and sectorization," in *1997 IEEE MTT-S Symposium on Technologies for Wireless Applications Digest*, pp. 1–6, june 1997.
- [43] S. Sesia and M. Baker, *LTE – The UMTS Long Term Evolution From Theory to Practice*. A John Wiley and Sons, Ltd, Publication, 2009.
- [44] T. S. Rappaport, *Wireless Communications: Principle and Practice*. Prentice Hall, Inc., 1996.
- [45] M. Rahman and H. Yanikomeroglu, "Inter-cell interference coordination in OFDMA networks: A novel approach based on integer programming," in *Proc. IEEE 71st Vehicular Technology Conf. (VTC 2010-Spring)*, pp. 1–5, 2010.

- [46] “*Physical Layer Aspects for Evolved Universal Terrestrial Radio Access (UTRA)* (release 7), 3GPP Technical Report TR 25.814 v7.1.0 September 2006 [online]. Available: [www.3gpp.org](http://www.3gpp.org).”
- [47] “*Further Advancements for Evolved Universal Terrestrial Radio Access (E-UTRA)* (release 9), 3GPP Technical Report TR 36.814 v0.4.1 February 2009 [online]. Available: [www.3gpp.org](http://www.3gpp.org).”
- [48] O. N. C. Yilmaz, S. Hamalainen, and J. Hamalainen, “Analysis of antenna parameter optimization space for 3GPP LTE,” in *Proc. IEEE 70th Vehicular Technology Conf. Fall (VTC 2009-Fall)*, pp. 1–5, 2009.
- [49] F. Gunnarsson, M. N. Johansson, A. Furuskar, M. Lundevall, A. Simonsson, C. Tidestav, and M. Blomgren, “Downtilted base station antennas - a simulation model proposal and impact on HSPA and LTE performance,” in *Proc. VTC 2008-Fall Vehicular Technology Conf. IEEE 68th*, pp. 1–5, 2008.
- [50] A. F. Molisch, *Wireless Communications*. John Wiley and Sons, Ltd, Publication, 2011.
- [51] J. M. Kelif and M. Coupechoux, “Joint impact of pathloss shadowing and fast fading - an outage formula for wireless networks,” *CoRR*, vol. abs/1001.1110, 2010.
- [52] S. Boyd, L. Xiao, and A. Mutapcic, “Notes on decomposition methods.” Lecture Notes for Course EE392o, October 2003. Stanford University.
- [53] S. C. Chapra and R. P. Canale, *Numerical Methods for Engineers*. McGraw-Hill, 2009.

# *Curriculum Vitae*

## Bujar Krasniqi



---

### Personal Data

Date of Birth	October 25 <sup>th</sup> , 1981
Place of Birth	Prishtinë
Citizenship	Kosovar

### Education

2007 - 2011	<b>Ph.D. Study, Vienna University of Technology</b> Thesis: " <i>Partial Frequency Reuse for Long Term Evolution</i> " Supervisor: Prof. Christoph Mecklenbräuker
2000 - 2006	<b>Dipl.-Ing. Degree studies, Telecommunication and Copmuters Department, Faculty of Electrical and Computer Engineering, University of Prishtina</b>
2004	<b>Award:</b> "Student i Dalluar" (eng. Eminent Student), from University of Prishtina
1996 - 2000	<b>Gymnasium "Sami Frashëri"</b> Prishtinë
1988-1996	<b>Primary school "Naim Frashëri"</b> , Breznicë, Obiliq

# Working Experience

2007-present

**University assistant and Research Assistant in the Flexible Wireless Communication Group**, Institute of Telecommunications, Vienna University of Technology.

- Radio Resource Management - *Joint radio resource management for UMTS long term evolution and future networks beyond 3G*
- Dynamic Spectrum Allocation
- Online Optimization of MIMO-OFDM Radio Resources
- Tight-Coupling of Radio Link Control, Medium Access Control, and the Physical Layer
- Teaching: Mobile Communications

(01-09). 2007

**System Engineer, Kosovo Energy Corporation**,  
Responsible for Digital Communication System (DCS)